Synthetic, kinetic and electrochemical aspects of betadiketonato titanium(IV) complexes

A dissertation submitted in accordance with the requirements of the degree

Magister Scientiae

in the

Department of Chemistry

Faculty of Science

at the

University of the Free State

by

Tsietsi Abram Tsotetsi

Supervisor

Dr. J Conradie

March 2007

Acknowledgements

"I will stand before you by the rock at Horeb" *– Exodus 3 verse 6 (NIV)*

The author would like to thank God father for the energy and strength He has given to me, guidance and patience in this study.

The author would like to thank Dr. J. Conradie, promoter/supervisor, for her patience, excellent leadership, and valuable discussion with her. Thanks for your valuable input, suggestions and important discussions.

Prof Jannie Swarts and Physical Chemistry group, thanks for your inputs in this study. To thank my colleagues, friends and personnel of Chemistry Department for their support during tough times. Dr K. von Eschwege and Prof Riaan Luyt for language editing. Prof Steve Basson for your advices and inputs.

The author would like to acknowledge Prof. Fay R. C. (Cornell University, U.S.A.), Prof. Comba P. (Germany), Prof Graham W. (Canada) and Prof Yamamoto A. (Japan) for their valuable inputs and discussion during the course of the project.

To my friends and family especially my mother ***Mofokeng Mphakiseng****, thanks for everything, support and showing your love.*

The author acknowledges NRF for financial assistance.

Tsotetsi Tsietsi Abram

March 2007

Contents

List of Abbreviations

A	absorbance
bipy	2,2-bipyridine
CO	carbon monoxide or carbonyl
Cp	cyclopentadienyl $(C_5H_5)^-$
CV	cyclic voltammetry
δ	chemical shift
D_O	diffusion coefficient of the oxidized species
D_R	diffusion coefficient of the reduced species
ε	molecular extinction coefficient
E	applied potential
E^{01}	formal reduction potential
E_a	energy of activation
en	ethane-1,2-diamine
E_{pa}	peak anodic potential
E_{pc}	peak cathodic potential
ΔE_p	separation of peak anodic and peak cathodic potentials
Et	ethyl
F	Faraday constant (96485.3 C mol^{-1})
Fc	ferrocene or ferrocenyl
Fc^+	ferrocenium
ΔG^*	free energy of activation
h	Planck's constant (6.626×10^{-34} J s)
ΔH^*	enthalpy of activation
Hacac	2,4-pentanedione, acetylacetone
H_2biphen	2,2'-biphenyldiol
Hba	1-phenyl-1,3-butanedione, benzoylacetone
Hbfcm	1-ferrocenyl-3-phenylpropane-1,3-dione, benzoylferrocenoylmethane
Hbnp	1-phenyl-4-nitrophenylpropane-1,3-dione (*para*-NO_2-dibenzoylmethane)
Hdbm	1,3-diphenylpropane-1,3-dione, dibenzoylmethane
Hdfcm	1,3-diferrocenylpropane-1,3-dione, diferrocenoylmethane
Hfca	1-ferrocenylbutane-1,3-dione, ferrocenoylacetone

LIST OF ABBREVIATIONS

Hfctfa	1-ferrocenyl-4,4,4-trifluorobutane-1,3-dione, ferrocenoyltrichloroacetone
Htfaa	1,1,1-trifluoro-2,4-pentanedione, trifluoroacetylacetone
Htfba	1-phenyl-3-trifluorobutanedione, trifluorobenzoylacetone
Hthba	I-phenyl-3-thenoylpropane-I,3-dione, thenoylbenzoylacetone
i_{pa}	peak anodic current
i_{pc}	peak cathodic current
IR	infrared spectroscopy
k_2	second-order rate constant
k_b	Boltzmann constant (1.381×10^{-23} J K^{-1})
K_c	Equilibrium constant
k_{obs}	observed rate constant
k_s	rate constant of solvation
L	ligand
l	path length
LDA	lithium diisopropylamide
λ_{exp}	wavelength at maximum absorbance
M	central metal atom
Me	methyl
n	number of electrons
$[NBu_4]^+[PF_6]^-$	tetrabutylammonium hexafluorophosphate
NHE	normal hydrogen electrode
NEt_3	triethylammine
^{1}H NMR	proton nuclear magnetic resonance spectroscopy
Ph	phenyl (C_6H_5)
pK_a	-log K_a, K_a = acid dissociation constant
ppm	parts per million
py	pyridine
R	gas constant (8.134 J K^{-1} mol^{-1})
RT	room temperature
S	solvent
ΔS^*	entropy of activation
SCE	saturated calomel electrode
SHE	standard hydrogen electrode
T	temperature
Tc	titanocene

LIST OF ABBREVIATIONS

THF	tetrahydrofuran
UV/Vis	ultraviolet/visible spectroscopy
$\Delta V^{\ddagger}$	volume of activation
ν(C=O)	infrared carbonyl stretching frequency
X	halogen
χ_R	group electronegativity (Gordy scale) of R group

List of structures.

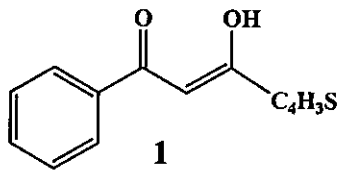

1

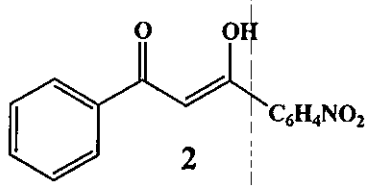

2

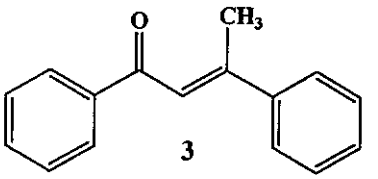

3

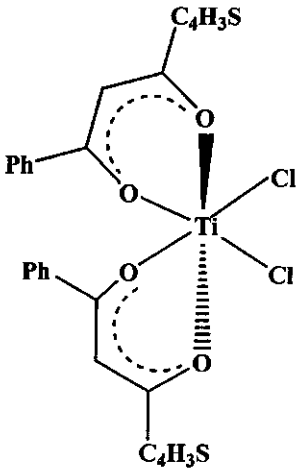

4

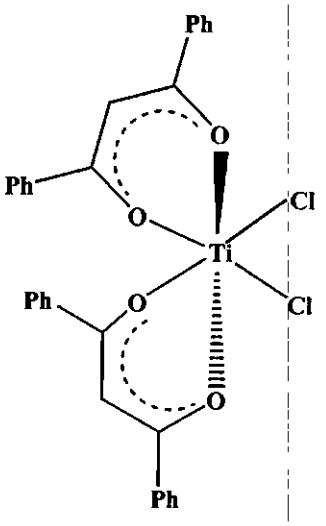

5

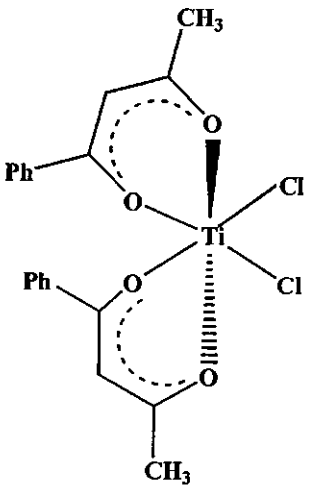

6

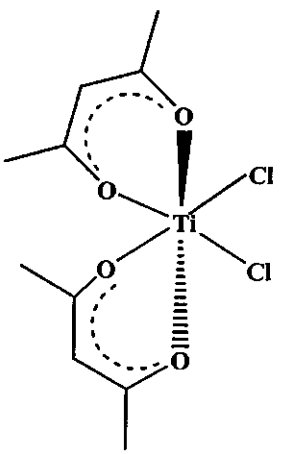

7

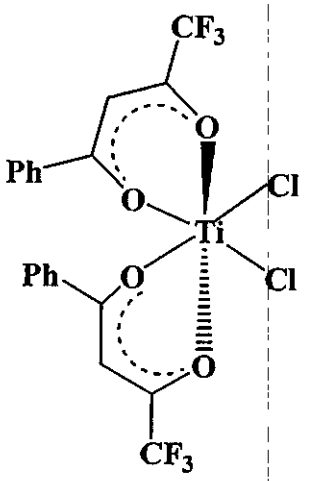

8

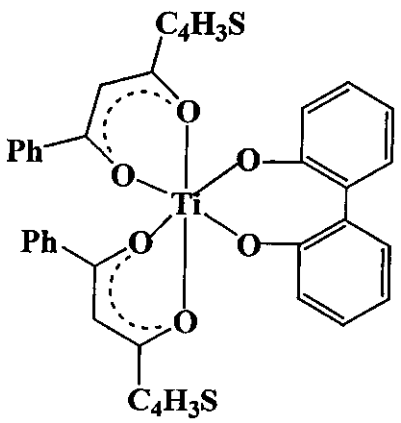

9

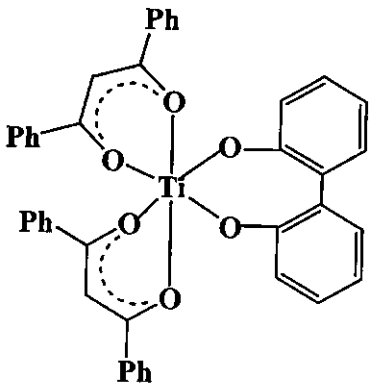

10

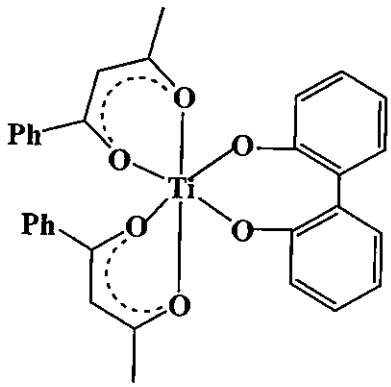

11

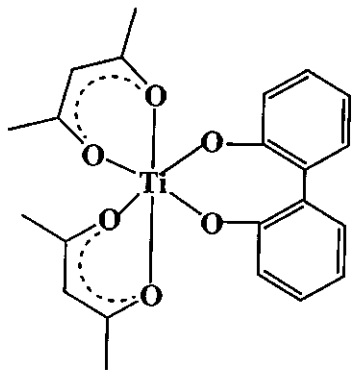

12

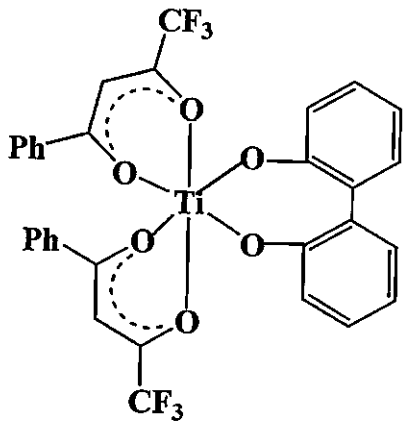

13

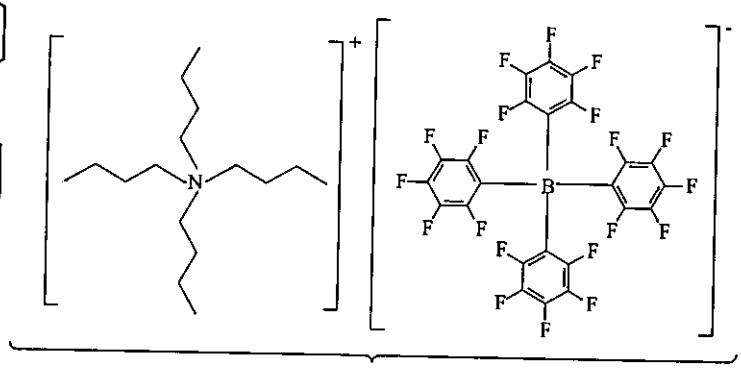

1 Introduction and Aim of Study.

1.1 Introduction

β-Diketones and metal β-diketonates have uses ranging from the synthetic,[1] metal extraction by chelation,[2] kinetic,[3] biomedical applications as used in antibacterial antibiotics,[4] structural,[5] catalysis[6] and many others.[7] β-Diketones can be usefully employed in the synthesis of natural products.[8] Titanium(IV) for example, can be extracted by pure acetylacetone in 75% yield, by benzoylacetone and dibenzoylmethane.[9]

Complexes of titanium(IV) are widely studied for a variety of purposes, mainly serving as catalysts in different organic reactions. Titanium alkoxides are excellent precursors for the deposition of metal oxides used in optoelectronics, high-T_c superconductors and ceramic materials.[10] Titanium alkoxy systems are, for example, effective catalysts in a variety of processes such as the Diels-Alder reaction,[11] C-C bond forming reactions,[12] esterification reactions including ones involved in the production of dialkyl phthalate plasticisers,[13] polymerisation of alkenes and alkynes,[14] asymmetric and enantioselective reactions[15] and many more.[16] However, since titanium alkoxides are very sensitive to hydrolysis, a problem frequently encountered when used as catalysts, is that as the catalytic reaction commences, there is some cleavage of the Ti-OR bonds due to the reaction with water that is produced as by-product in the reaction, for example in esterification reactions.[17] Studies on sol-gel systems involving $[Ti(OR)_4]$ have shown that the rate of hydrolysis of the metal alkoxide can be significantly reduced by the presence of bulky,[18] or chelating ligands as acetylacetonate and glycols.[19] Thus, producing titanium(IV) complexes exhibiting enhanced resistance to hydrolysis, is extremely valuable.

1.2 Aims and goals of the study

With this background the following goals were set for this study:

1) Synthesis and characterisation of complexes containing a titanium(IV) centre coordinated to either β-diketonato or β-diketonato and another bi-chelating ligand. These complexes will have an octahedral co-ordination sphere of the type [Ti(β-diketonato)$_2$Cl$_2$] and [Ti(β-diketonato)$_2$(biphen)], β-diketonato = acac (acetylacetonato, $CH_3COCHCOCH_3^-$), ba (benzoylacetonato, $C_6H_5COCHCOCH_3^-$), dbm (dibenzoylmethanato, $C_6H_5COCHCOC_6H_5^-$), tfba (trifluorobenzoyllacetonato, $C_6H_5COCHCOCF_3^-$) and thba (theonylbenzoylacetonato, $C_6H_5COCHCOC_4H_3S^-$); biphen = 2,2'-biphenyldiolato.
2) Testing of the hydrolytic stability of the titanium(IV) complexes synthesized.
3) The synthesis and characterisation of β-diketone ligands in terms of pK_a-values (for $PhCOCH_2COR'$ with R' = $C_6H_4NO_2$ and C_4H_3S), keto-enol equilibrium constants and the rate of conversion between keto and enol isomers.
4) A kinetic study of the substitution of Cl^- from the synthesized titanium complexes, [Ti(β-diketonato)$_2$Cl$_2$], with the bi-chelating ligand, 2,2-biphenyldiol.
5) An electrochemical study utilizing cyclic voltammetry of all the synthesized titanium(IV) complexes to determine the electrochemical reversibility and the formal reduction potentials of the redox active titanium(IV) center.

---

[1] Pedersen, C. J., Salem, N. J. and Weinmayr, V., *US Pat.*, 2 857 223 (1959); Weinmayr, V., *Naturwissenschaften*, **45**, 311 (1958).
[2] Stary, J., *The Solvent Extraction of Metal Chelates*, Macmillan, pp: 51 – 55, 1964; Marcus, Y. and Keates, A. S., *Ion Exchange and Solvent Extraction of Metal Complexes*, Wiley-Interscience, pp: 499 – 521, 1969.
[3] Leipoldt, J. G., Basson, S. S., van Zyl, G. J. and Steyn, G. J. J., *J. Organomet. Chem.*, **418**, 241 (1991); Leipoldt, J. G. and Grobler, E. C., *Transition Met. Chem. (Weinheim Ger.)*, **11**, 110 (1986); Leipoldt, J. G., Lamprecht, G. J. and Steynberg, E. C., *J. Organomet. Chem.*, **402**, 259 (1991).
[4] Bennet, I., Broom, N. J. P., Cassels, R., Elder, J. S., Masson, N. D. and O'Hanlon, P. J., *Bioorg. Med. Chem. Lett.*, **9**, 1847 (1999).
[5] Roodt, A., Leipoldt, J. G., Swarts, J. C. and Steyn, G. J. J., *Acta Cryst.*, **C48**, 547 (1992); Swarts, J. C., Vosloo, T. G., Leipoldt, J. G. and Lamprecht, G. J., *Acta Cryst.*, **C49**, 760 (1993); Lamprecht, G. J., Swarts, J. C., Conradie, J. and Leipoldt, J. G., *Acta Cryst.*, **C49**, 82 (1993); Glidewell, C. and Zakaria, C. M., *Acta Cryst.*, **C50**, 1673 (1994); Haaland, A. and Nilsson, J., *Chem. Commun.*, 88 (1968); Yogev, A. and Mazyr, Y., *J. Org. Chem.*, **32**, 2162 (1967).
[6] Cullen, W. R., Rettig, S. J. and Wickenheiser, E. B., *J. Mol. Catal.*, **66**, 251 (1991); Cullen, W. R. and Wickenheiser, E. B., *J. Organomet. Chem.*, **370**, 141 (1989).
[7] Mehrotra, R. C., Bohra, R. and Gaur, D. P., *Metal β-Diketonates and Allied Derivatives*, Academic Press, London, pp. 268–277, 1978.
[8] Pellicciari, R., Fringuelli, R., Sisani, E. and Curini, M., *J. Chem. Soc., Perkin Trans* 1, 2567 (1981).
[9] Stary, J., *The Solvent Extraction of Metal Chelates*, Macmillan, pp: 51 – 55, 1964; Marcus, Y. and Keates, A. S., *Ion Exchange and Solvent Extraction of Metal Complexes*, Wiley-Interscience, pp: 51 – 70, 1969.
[10] Bradley, D. C., *Chem. Rev.*, **89**, 1317 (1989); Braunemann, A., Hellwog, M., Varede, A., Bhakta, R. K., Winter, M., Shivashankar, S. A., Fisher, R. A. and Devi, A., *Dalton Trans.*, 3485 (2006).
[11] Chen, Y., Yekta, S. and Yudir, A. K., *Chem. Rev.*, **103**, 3155 (2003).

[12] Kitamoto, D., Imma, H. and Nakai, T., *Tetrahedron Lett.*, **36**, 1861 (1995).
[13] Hinde, N. J. and Hall, C. D., *J. Chem. Soc., Perkin Trans.* 2, 1249 (1998).
[14] Gibson, V. C. and Spitzmesser, S. K., *Chem. Rev.*, **103**, 283 (2003); Akagi, K., Mochiznki, K., Aoki, Y. and Shirakawa, H., *Bull. Chem. Soc. Jpn.*, **66**, 3444 (1993).
[15] Kocovsky, P., Vyskocil, S. and Smrcina, M., *Chem. Rev.*, **103**, 3213 (2003); van der Linden, A., Schaverien, C. J., Meijboom, N., Ganter, C. and Orpen, A. G., *J. Am. Chem. Soc.*, **117**, 3008 (1995); Balsells, J., Davis, T. J., Caroll, P. and Walsh, P. J., *J. Am. Chem. Soc.*, **124**, 10336 (2002).
[16] Balsells, J., Davis, T. J., Caroll, P. and Walsh, P. J., *J. Am. Chem. Soc.*, **124**, 10336 (2002); Keck, G. E., Tarbet, K. H. and Geraci, L. S., *J. Am. Chem. Soc.*, **115**, 8467 (1993); Faller, J. W., Sams, D. W. I. and Liu, X., *J. Am. Chem. Soc.*, **118**, 1217 (1995).
[17] Corden, J. P., Errington, W., Moore, P., Partridge, M. G. and Wallbridge, M. G. H., *Dalton Trans.*, 1846 (2004).
[18] Boyle, T. J., Pearson, A. T. and Schwartz, R. W., *Ceram. Trans.*, **43**, 79 (1993).
[19] Aizwa, M., Nosaka, Y. and Fujii, N., *J. Non-Cryst. Solids*, **128**, 77 (1991).

2 Literature Survey and Fundamental Aspects

In this study a variety of octahedral β-diketonato titanium(IV) complexes of the type [Ti(β-diketonato)$_2$Cl$_2$] and [Ti(β-diketonato)$_2$(biphen)], biphen = 2,2'-biphenyldiolato were synthesized and characterized by means of infra-red (**IR**), ultra violet (**UV/vis**), proton nuclear magnetic resonance (^{1}**H NMR**) spectroscopy and cyclic voltammetry. Selected β-diketones were synthesized, characterized and pK_a values determined. Kinetic results include the conversion of the β-diketone from the enol to the keto-isomer and the substitution kinetics of the chloride ligands from the [Ti(β-diketonato)$_2$Cl$_2$] with biphen. The literature study thus include a discussion on the chemistry of β-diketones, titanium(IV) complexes, electrochemistry and substitution kinetics.

2.1. Chemistry of β-diketones

In this study, β-diketones containing a phenyl group, were complexed to titanium. Two β-diketones were synthesized for this purpose. A discussion on the application, general properties and synthetic routes of β-diketones, is thus relevant.

2.1.1. Introduction

β-Diketones, which appear to have been investigated with virtually every metal and metalloid in the periodic table, are amongst the most widely studied coordination compounds.[1] Even though β-diketones represent one of the oldest classes of chelating ligands, its coordination chemistry continues to attract much interest, due to the industrial applications of several of its metal derivatives. Several research groups recognized the potential of β-diketones, for example, as an extracting and complexing agent of metal ions in solutions, for chromatographic separations and as NMR shift-reagents.[1] β-Diketonato complexes of transition metals have therefore been the subject for different applications and studies, ranging from synthetic,[2] kinetic[3] and structural[4] topics to catalysis[5] and others.[6]

2.1.2. Properties of β-diketones.

β-Diketones exist in solution and in vapour phase generally as an equilibrium mixture of keto and enol tautomers (see Scheme 2. 1). The enol isomer can exist as two tautomers stabilized by a hydrogen bridge.[7] Keto-enol tautomerism has been studied for many years by techniques such as bromine titration,[8] IR (infrared spectroscopy),[9] UV (ultraviolet spectroscopy),[10] HPLC (high performance liquid chromatography),[11] polarographic measurements, energy of polarization and NMR (nuclear magnetic resonance).[12] Since the rate of the keto-enol interconversion is usually slow, separate NMR signals of the protons due to the enol and keto forms may be observed. By intensity measurements the relative ratio of the two forms can be determined. Conversion from one enol form to another, however, is very fast, with a rate constant of ~10^6 s^{-1}.[13] Theoretical calculations by Moon and Kwon indicated that the equilibrium constant is highly dependent on the character of the R groups attached to the β-diketone backbone (see Scheme 2. 1).[14] Generally, the enol tautomer is more stable than the keto tautomer, due to intramolecular hydrogen bonding and simultaneous conjugation.[15] In solution, the enolic form is generally favoured by nonpolar solvents,[16] higher concentrations,[17] and lower temperatures.[17, 18]

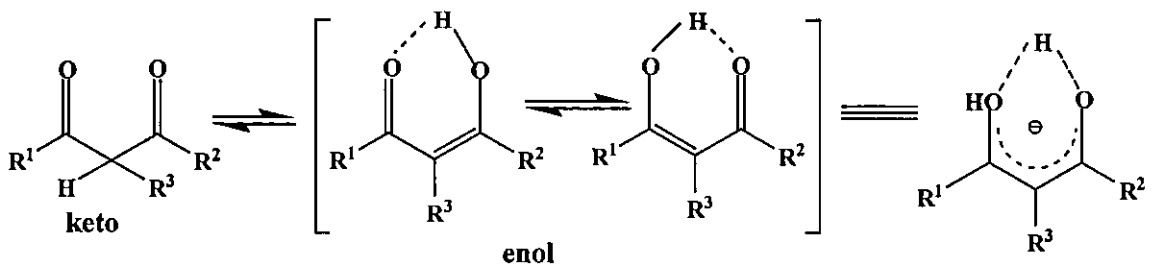

Scheme 2. 1: Schematic representation of tautomerism of β-diketones with the enol form showing pseudo-aromatic character.

The size and electronegativity of the R substituents influence the relative quantity ratios of the tautomers. The proportion of the enol tautomer generally increases when an electron-withdrawing group, *e.g.*, fluorine, is substituted for hydrogen at an α-position relative to a carbonyl group in the β-diketones.[19] Substitution of R^3 by a bulky group such as an alkyl tends to produce a steric hindrance between R^2 and R^1 in favour of the keto tautomer.[20, 21]

Two different driving forces that control the conversion of β-diketones from keto into enol isomer were postulated by du Plessis *et al.*[6] These forces, labelled electronic and resonance driving forces, determine the formation of the preferred enol isomer. The electronic driving force is controlled by the electronegativity of the R^1 and R^2 substituents on the β-diketone:

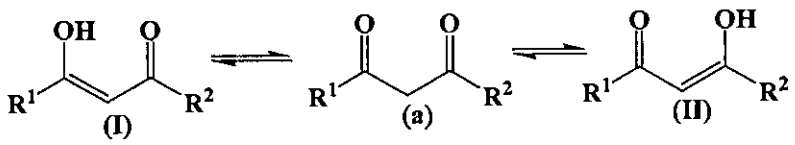

When the electronegativity of R^1 is greater than that of R^2, the carbon atom of the carbonyl group adjacent to R^2 on the β-diketone, **(a)**, will be less positive in character than the carbon atom of the other carbonyl, implying that the enol **(II)** will dominate. However, it has been shown that the electronic driving force is not always applicable in determining the dominant enol isomer when either R^1 or R^2 is an aromatic group such as ferrocenyl or phenyl. In this case, the resonance driving force leading to the formation of different canonical forms of the specific enol isomer lowers the energy of this isomer enough to allow it to dominate over the existence of other isomers, which may be favoured by electronic forces.[6, 17]

The methine proton in the keto form and hydroxyl proton in the enol form of β-diketones are acidic and its removal generates 1,3-diketonato anions, which is the source of an extremely broad class of coordination compounds referred to as diketonatos or acetylacetonatos. Diketonato anions are powerful chelating species and form complexes with virtually every transition and main group element.[1] An additional feature of keto-enol tautomerism of the β-diketone is that the enol form is more reactive.[22]

2.1.3. Synthesis of β-diketones

β-Diketones can be obtained from the acylation of ketones by esters (Claisen condensation),[6, 23] acid anhydrides or acid chlorides in the presence of a base *e.g.*, alkali-metal hydroxides, ethoxides, hydrides or amides as condensing agents, to enhance the relatively low reactivity of the ester carbonyl group.[24] The process consists of the replacement of an α-hydrogen atom of the ketone by an acyl group and the reaction involves a carbon-carbon bond formation (Scheme 2. 2).

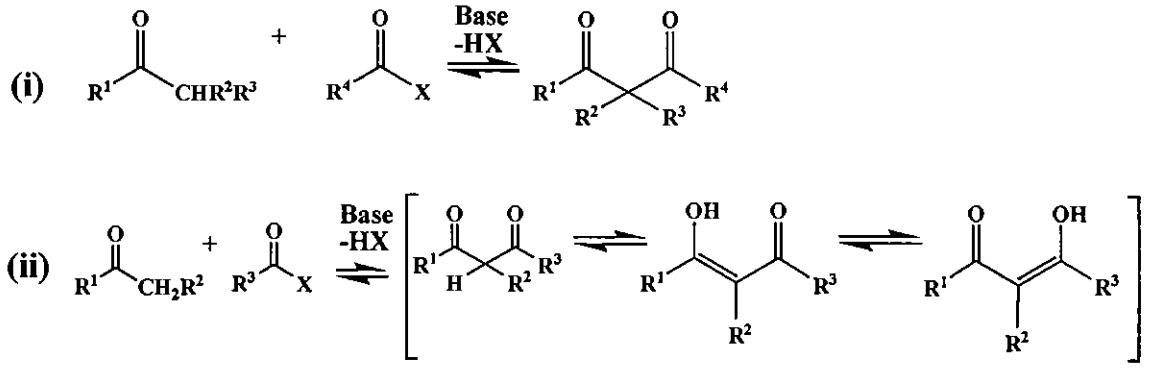

Scheme 2. 2: The synthesis of β-diketones. In (i) enolization is not structurally possible. The type, size and electronegativity of the R groups in (ii) will determine which isomer dominates.

The mechanism involves a three-step ionic mechanism,[25] to form the β-diketone anion, which by acidification yields the β-diketone, see Scheme 2. 3. For this illustration the base, lithium diisopropylamide (LDA), and the ethyl ester, R^2COOEt, is used.

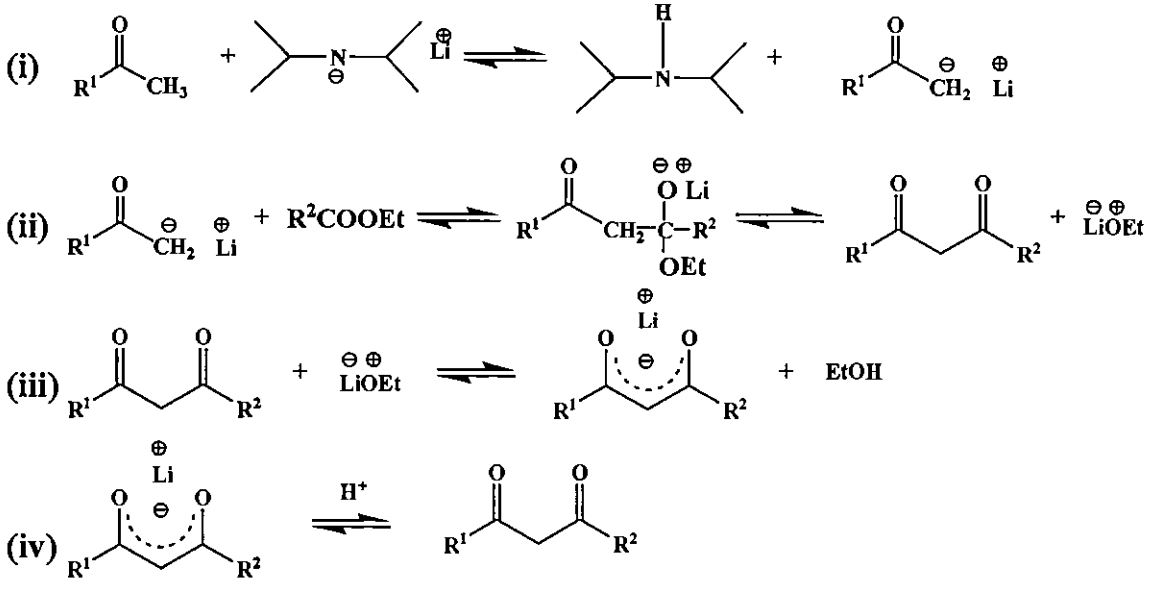

Scheme 2. 3: The mechanism for the formation of β-diketones by the acylation of a ketone R^1COCH_3 with an ester R^2COOEt by means of the basic reagent lithium diisopropylamide involves a three-step ionic mechanism to form the β-diketone anion, which by acidification yields the β-diketone.

The first step **(i)** involves the removal of an α-hydrogen on the ketone as a proton, to form a ketone anion, which is a hybrid of the resonance structures $^-CH_2COR^1$ and $CH_2{=}C(\bar{O})\ R^1$. The second step **(ii)** is formulated as the addition of the ketone anion to the carbonyl carbon of the ethyl ester, accompanied by the release of ethoxide ion to form the β-diketone. The third step **(iii)** consists of the removal of a methylenic hydrogen on the β-diketone as a proton to form the β-diketone anion, which is a resonance hybrid of structures $R^1CO\bar{C}HCOR^2$, $R^1C(\bar{O}){=}CHCOR^2$ and $R^1COCH{=}C(\bar{O})R^2$. The three steps of the mechanism are reversible. In practice, the equilibrium of the overall reaction is shifted in the direction of the

condensation product by the precipitation of the β-diketone as its lithium salt. A fourth step, involving the acidification of the β-diketone anion, yields the β-diketone.

The acylation of ketones with esters in the presence of a basic reagent may be accompanied by certain side reactions. For example, the ketone may undergo aldol condensation (see Scheme 2. 4) to form an α,β-unsaturated ketone or a more complex condensation product.[26] If the ester that is used as acylation agent contains α-hydrogen atoms, it may condense with itself to form a β-keto ester. Esters having α-hydrogen atoms may also undergo an aldol reaction with the carbonyl group of the ketone.[25] Purification of the β-diketone by flash chromatography or other methods is thus normally necessary.

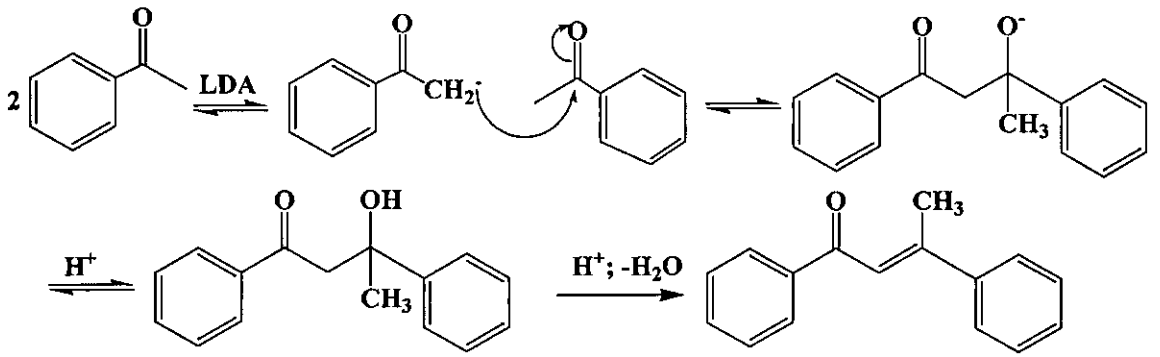

Scheme 2. 4: Reaction scheme illustrating the self aldol condensation of acetophenone.

The method for the synthesis of a β-diketone containing a *para*-NO_2-benzoyl group was described by Cravero.[27] This procedure involves an acid-catalysed condensation. The compound *para*-NO_2-benzoylacetone was obtained from the addition of *para*-NO_2-acetophenone and acetic anhydride to an acetic acid-BF_3 complex at 0°C and then at 25°C for 24 hours (see Scheme 2. 5).

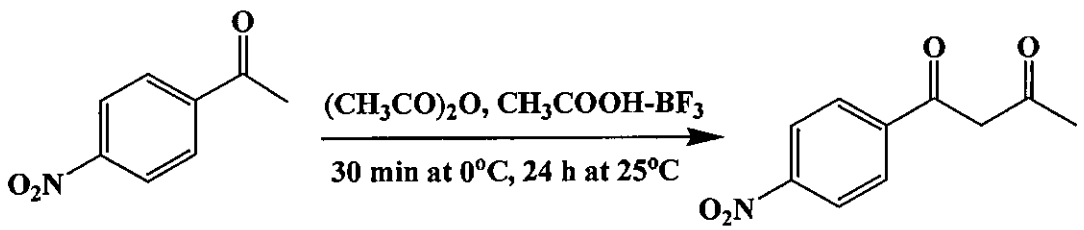

Scheme 2. 5: Synthesis of *para*-NO_2-benzoylacetone.[27]

New synthetic approaches to modify and functionalize the β-diketone in R^1, R^2 and/or R^3 positions, to increase yields and to avoid the side reactions that could be encountered with Claisen condensations have been developed.[28] One of the most important improvements has

been the successful reaction of 1-diazo-1-lithioacetone with aldehydes, followed by acid-induced transformation of the α-diazo-β-hydroxyketone thus formed, into the corresponding β-diketone with R = Pr^n, $PhCH_2$, Ph_2CH, PhCH=CH and Ph, in the presence of Rh^{II}acetate as catalyst.[29]

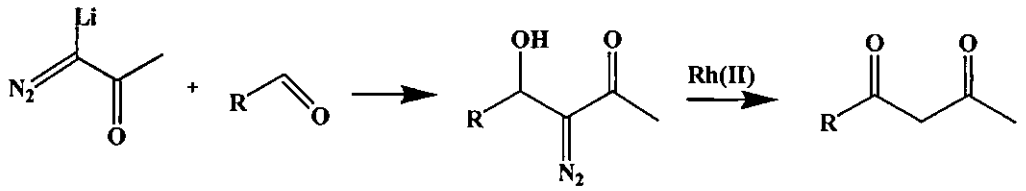

Scheme 2. 6: α–Diazo-β-hydroxyketones obtained by condensation of aldehydes with 1-diazo-1-lithioacetone, are efficiently transformed into the corresponding β-diketones by exposure to rhodium(II) acetate.

Under the appropriate conditions the enolic hydrogen atom of a β-diketonato ligand can be replaced by a metal cation to produce a six-membered pseudo-aromatic chelating ring.[1] Mono, bis, tris and even tetrakis β-diketonato metal complexes are known.[30]

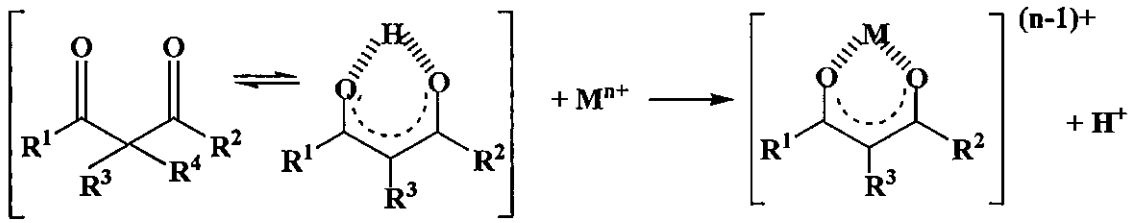

Scheme 2. 7: Formation of a six-membered pseudo-aromatic chelating ring of metal β-diketonatos.

2.2. Titanium(IV) Complexes

Titanium as first member of the *3d* transition series has four valence electrons, $3d^2 4s^2$. The most stable and common oxidation state is Ti(IV),[31] which involves loss of all four electrons. Compounds of Ti(III),[32] Ti(II),[33] Ti(0),[34] Ti(-I)[35] and Ti(-II)[36] are also known (see Table 2. 1).[37]

The best studied group of titanium(IV) complexes may be the alkoxides[37] and other titanium-oxygen-bonded compounds. The interest in alkoxides of titanium was stimulated by the use of alkoxides in heat-resistant paints.[38] After the two monomeric titanium(IV) complexes $[Ti^{IV}(ba)_2(OEt)_2]$ (budoditane, Hba = benzoylacetone) and $[Ti^{IV}Cp_2Cl_2]$ (titanocene

dichloride, Cp = C_5H_5) qualified for clinical trials as antitumor agents, there has been increased interest in the development of new antitumor metal agents.[39]

Table 2. 1: Oxidation States and Stereochemistry of a variety of titanium compounds.[37]

Oxidation State	Coordination number	Geometry	Examples
Ti^{-I}	6	octahedral	$[Ti(bipy)_3]^-$
Ti^0	6	octahedral	$[Ti(bipy)_3]$
Ti^{II}, d^2	4	distorted tetrahedral	$(\eta^5\text{-}C_5H_5)_2Ti(CO)_2$
	6	octahedral	$TiCl_2$
Ti^{III}, d^1	3	planar	$Ti\{N(SiMe_3)_2\}_3$
	5	trigonal bipyramidal	$TiBr_3(NMe_3)_2$
	6	octahedral	TiF_6^{3-}, $TiCl_3(THF)_3$
Ti^{IV}, d^0	4	Tetrahedral	$TiCl_4$
	4	Distorted tetrahedral	$(\eta^5\text{-}C_5H_5)_2TiCl_2$
	5	Distorted trigonal bipyramidal	$K_2Ti_2O_5$
	5	Square planar	TiO(porphyrin)
	6	Octahedral	TiF_6^{2-}, $Ti(acac)_2Cl_2$
	7	ZrF_7^{3-}-type	$[Ti(O_2)F_5]^{3-}$
	7	Pentagonal bipyramidal	$Ti_2(ox)_3 \cdot 10H_2O$
	8	Distorted dodecahedral	$TiCl_4(diars)_2$, $Ti(S_2CNEt_2)_4$

2.2.1.Mono-β-diketonato Titanium(IV) Complexes

In 1967 Doyle and Tobias[40] reported the synthesis of a series of mono-β-diketonato titanium(IV) complexes of the type $[Cp_2TiL]^+X^-$ where L is the conjugate base of acetylacetone (Hacac), benzoylacetone (Hba), dibenzoylmethane (Hdbm), dipivalomethane and tropolone, and X^- is ClO_4^-, BF_4^-, PF_6^-, AsF_6^-, SbF_6^- or $CF_3SO_3^-$. In all the cases, the β-diketonato ligands act as a bidentate ligand with the configuration about the titanium approximately tetrahedral.[41]

The mono-β-diketonato titanocene(IV) complexes were synthesized according to Scheme 2. 8. Titanocene dichloride dissolves in water to give various hydrolyzed cationic species (Scheme 2. 9).[42] Either one of the cationic species can react with $AgClO_4$ to form the hydrolyzed titanium(IV) perchlorate species. This reaction is driven by the precipitation of silver chloride. Addition of the β-diketonato displaces the perchlorate anion to produce the titanocene(IV)-β-diketonato complex. A base as hydrogen acceptor is not needed due to the fact that the β-diketone moiety has a keto-enol tautomer with the reactive enol form the major species in solution.[43] Even at high concentrations of the chelating ligand, it is impossible to produce the *bis* chelate.

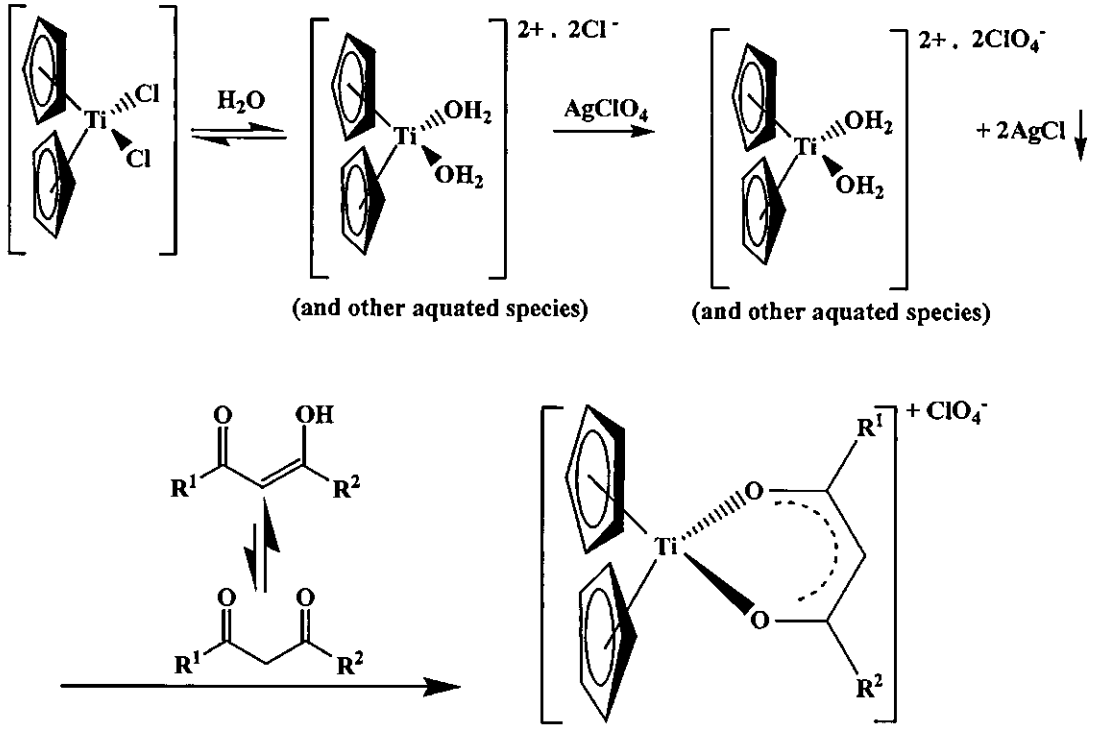

Scheme 2. 8: Synthetic route to mono-β-diketonato titanocene(IV) complexes.

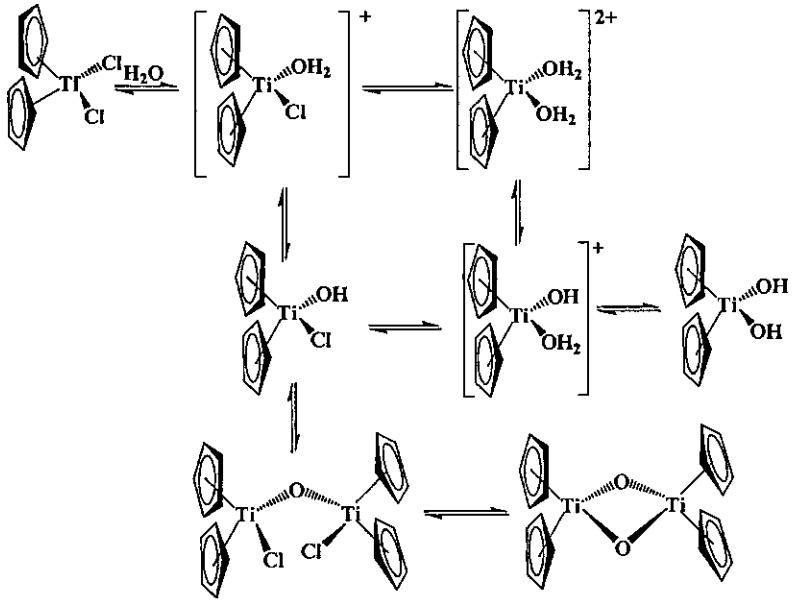

Scheme 2. 9: The hydrolysis of titanocene in aqueous media.

All mono chelates prepared by Doyle were very stable, with exception of the perchlorates which detonate easily. Mono chelates are slightly soluble in water and virtually insoluble in most organic solvents. In an effort to obtain a chelate which would be more soluble in

organic solvents, the dipivaloylmethane complex was synthesized, however, solubility was not significantly better.

2.2.2 *Bis*-β-diketonato Titanium(IV) Complexes

The reaction of titanocene dichloride with an excess of ethanol in the presence of a base in acetonitrile, causes the splitting off of one of the cyclopentadienyl rings to yield $[CpTiCl(OEt)_2]$.[60] The replacement of one chlorine and one cyclopentadienyl group was also observed in the reactions of titanocene dichloride with the fluoro-beta-diketones, trifluorobenzoylacetone (Htfba) and thenoyltrifluoroacetone (Htta), to yield [CpTiCl(β-diketonato)$_2$] complexes.[60] Fraser and Newton synthesized neutral cyclopentadienyl chelates of the type *cis*-$M(C_5H_5)Cl(\beta\text{-diketonato})_2$ from the β-diketones, 2,4-pentanedione (Hacac), 1-phenyl-1,3-butanedione (Hba), 1,3-diphenyl-1,3-propanedione (Hdbm) and the metallocene dichloride Cp_2MCl_2 (M = Ti, Zr), in the presence of the hydrogen halide acceptor triethylamine, NEt_3.[44] Separation of the amine and titanium complex can be done by extraction with benzene or toluene (Scheme 2. 10). These chlorocyclopentadienyl *bis*(β-diketonato) metal(IV) complexes (M = Zr, Hf, Ti) are moisture sensitive and hydrolyzes easily.[44]

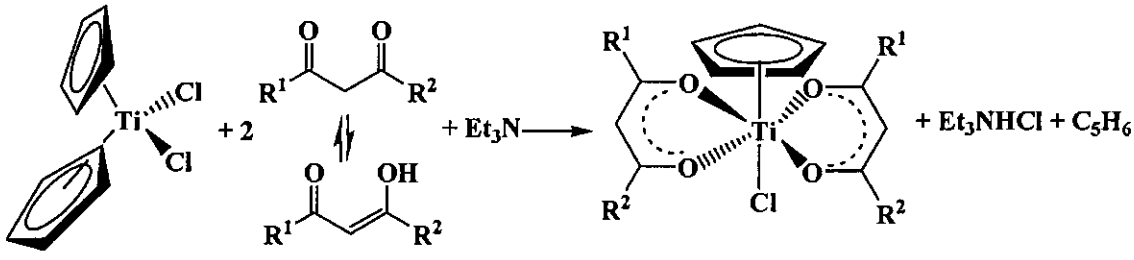

Scheme 2. 10: Reaction and formation of chlorocyclopentadienyl *bis*(β-diketonato)metal(IV) complexes.[44]

Another series of *bis*-β-diketonato metal complexes (M = Sn, Ge, Zr, Hf and Ti) can be synthesized from the β-diketonato and corresponding metal tetrahalides in an anhydrous organic solvent according to Scheme 2. 11.[45]

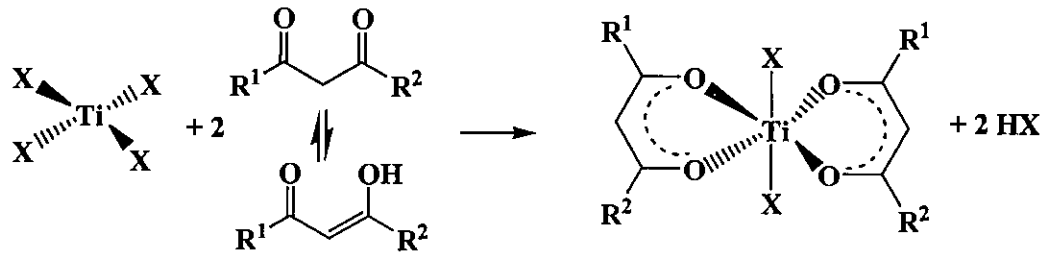

Scheme 2. 11: General synthesis of [Ti(β-diketonato)$_2$X$_2$] complexes, X = halogen or alkoxide.

The reactions of *bis*-β-diketonato metal complexes are highly susceptible to hydrolysis but relatively difficult to dissolve in water.[46] If the complex is dissolved in a water-soluble solvent such as acetonitrile, and water is added, the complex reacts under hydrolysis according to Scheme 2. 12.[47] Water rapidly replaces the relative labile group, X, which may be a halogen or an alcohol. The order of stability against hydrolysis, which depends on the hydrolyzed group X, is:

(more readily hydrolyzed) I < Br < Cl < F < OEt (more stable against hydrolysis)

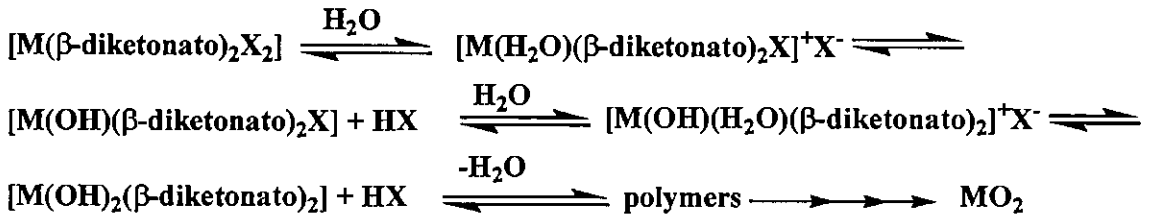

Scheme 2. 12: Hydrolysis of *bis*-β-diketonato metal complexes.[47]

2.2.3 Titanium(IV) Alkoxide Complexes

The titanium(IV) alkoxide complexes generally receive a great deal of attention because of their ease of hydrolysis and reactivity with hydroxylic molecules. The original method of preparation involved the reaction of sodium alkoxide and titanium tetrachloride in the appropriate alcohol.[37]

$$TiCl_4 + 4NaOR \rightarrow Ti(OR)_4 + 4NaCl$$

The addition of a base, typically ammonia, to mixtures of transition metal halides and alcohols allow the synthesis of homoleptic alkoxides and phenoxides for a wide range of metals. Anhydrous ammonia was used in the preparation of titanium alkoxides where the reaction is forced to completion by precipitation of ammonium chloride.[48] The $Ti(OR)_4$ compounds are usually insoluble polymers linked by oxygen bridges. [37]

$$TiCl_4 + 4ROH + 4NH_3 \rightarrow Ti(OR)_4 + 4NH_4Cl$$

When a proton-accepting reagent such as ammonia is not used, the reaction proceeds only as far as the $Ti(OR)_2Cl_2$ derivatives.

$$TiCl_4 + 2ROH \rightarrow Ti(OR)_2Cl_2 + 2HCl$$

Another synthetic route for complexes of the type $Ti(OR)_4$ involves phenolysis of metal sulfides, transesterification, and alcohol interchange. A mixture of phenol and aluminium sulfide is rapidly converted into the phenoxide upon heating, with evolution of H_2S.[49] Similarly, titanium and silicon phenoxides can be prepared directly from their sulfides.[50, 51]

$$TiS_2 + 4PhOH \rightarrow Ti(OPh)_4 + 2H_2S$$

The alkyls of the group IV metals, MR_4 (M = Ti, Zr, Hf), undergo rapid reactions with common alcohols and phenols yielding the corresponding tetra-alkoxides or tetra-phenoxides, and four equivalents of alkane.[52, 53] The use of alkoxides to synthesize new alkoxides by the process of alcohol interchange has been widely applied for a large number of elements.

$$M(OR)_n + nR'OH \rightarrow M(OR')_n + nROH$$

In general, the facility of interchange of alkoxy groups by alcoholysis follows the order: *tertiary* < *secondary* < *primary*.[54] Hence, the *tert*-butoxides of titanium and zirconium will undergo rapid exchange with methanol or ethanol. An extra driving force here is the large degree of oligomerization of methoxides or ethoxides in general over *tert*-butoxides.[55] However, it is possible in some cases, by fractionating out more volatile components, to partly reverse this order of reactivity.[56, 57]

New alkoxide compounds $M(OR')_4$ can also be obtained from another titanium alkoxide $M(OR)_4$ by alcohol exchange in the reaction of titanium alkoxide with an organic ester. The new alkoxide can be obtained if the ester produced is more volatile than the ester added and can be fractioned out of the mixture. This method proved useful for the preparation of tertiary alkoxides since it appears to be much less prone to steric factors than alcohol exchange by using the relevant alcohol HOR'.[58]

$$M(OR)_4 + 4R'OOCMe \rightarrow M(OR')_4 + 4ROOCMe$$

Treatment of titanocene dichloride in a solvent with an alcohol or phenol in the presence of a base replaces one or both chlorides. Moisture has to be excluded in the reaction. [59, 60]

$$Cp_2TiCl_2 + n\text{ROH} + n\text{base} \rightarrow Cp_2Ti(OR)_nCl_{2-n} + n\text{base.HCl}$$

The formation of five and seven membered metallocyclic compounds is achieved similarly by reaction of either 1,2-benzenediol (for the five membered metallocyclic compound) or 2,2-biphenyldiol (for the seven membered metallocyclic compound) with titanocene dichloride in the presence of sodium amide, $NaNH_2$.[59] Phthalocyaninatotitanium(IV)oxide can undergo axial substitution to form a seven membered metallocyclic-phthalocyaninato compound (see Figure 2. 1). This axial substitution is a very simple reaction involving only the stirring of the two reagents phthalocyaninatotitanium(IV) oxide and 1,2-biphenyldiol for a few hours in DCM.[61]

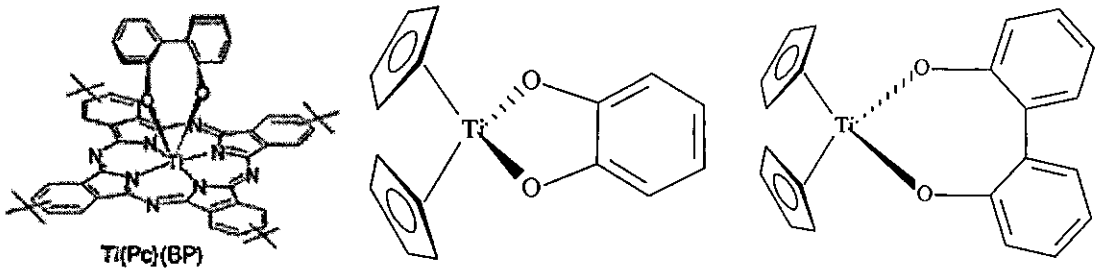

Figure 2. 1: Cyclic dialcohol compounds of titanium.[59, 61]

2.2.4 β-Diketonato Titanium(IV) Alkoxide Complexes

The general synthesis of M(β-diketonato)$_2$(OR)$_2$ complexes involves the reaction of β-diketones with metal alkoxides and is generally carried out in anhydrous organic/aromatic solvents, affording the "desired metal-diketone".[62, 63] The delivering alcohol can be removed from the reaction mixture by fractional distillation. By employing stoichiometric amounts of reactants, pure diketonatos and mixed alkoxide-diketonatos of titanium can be prepared in this way.[64]

$$M(OR)_n + m\ \beta\text{-diketone} \rightarrow M(\beta\text{-diketonato})_m(OR)_{n-m} + m\text{ROH}$$

A series of tetraalkoxytitaniums with acetylacetone or ethyl acetoacetate in a molar ratio of 1:1 or 1:2 respectively, formed Ti(β-diketonato)(OR)$_3$ and Ti(β-diketonato)$_2$(OR)$_2$ respectively.[65]

$$Ti(OR)_4 + 1(\beta\text{-diketone}) \rightarrow Ti(\beta\text{-diketonato})\ (OR)_3 + HOR$$

$$Ti(OR)_4 + 2(\beta\text{-diketone}) \rightarrow Ti(\beta\text{-diketonato})_2(OR)_2 + 2HOR$$

Diisobutoxybis(2,4-pentadionato)titanium(IV), $Ti(acac)_2(OCH_2CH(CH_3)_2)_2$, was obtained similarly by reacting acetylacetone and titanium(IV)isobutoxide in a ratio of 2:1 in acetonitrile under a stream of dry nitrogen.[66]

Mixed-ligand complexes of the type, Ti(β-diketonato)(β-diketonato′)$(OR)_2$, can be prepared in solution *via* ligand exchange, as observed by ^1H NMR studies.[67]

$$\mathbf{Ti(\beta\text{-}dik)_2(OR)_2 + Ti(\beta\text{-}dik')_2(OR)_2 \rightleftharpoons 2Ti(\beta\text{-}dik)(\beta\text{-}dik')(OR)_2}$$

Six hours of refluxing of stoichiometric amounts of $Ti(acac)_2Cl_2$ and 1,1'-methylenebis(2-naphtol) in CH_3CN under a nitrogen atmosphere at room temperature, yielded the cyclic bi-alcohol compound illustrated in Figure 2. 2.[68]

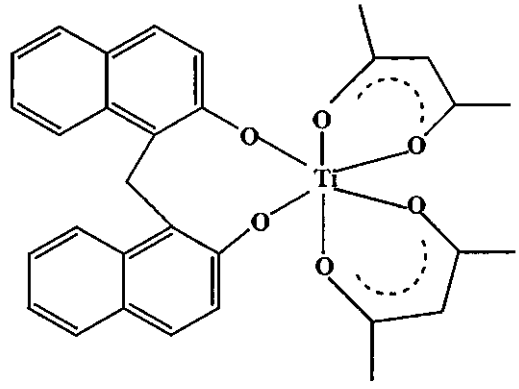

Figure 2. 2: A cyclic bi-alcohol β-diketonato titanium(IV) complex.

2.2.5 Stereochemistry of *bis*-β-diketonato Titanium(IV) Complexes

The six-coordinated octahedrally configured bis-β-diketonato complexes of the type, [Ti(β-diketonato)$_2X_2$] (X = halogen or alkoxide), can occur with the X groups in a *trans*- or *cis*-position (Figure 2. 3). The different *cis*- and *trans*-isomers of the octahedrally configured [Ti(β-diketonato)$_2X_2$] compounds are referred to by three *cis* and *trans* prefixes, as follows: the first specify the relative position of the halogens (Y), the second specifies the relative orientation of R^1 and the third the relative orientation of R^2. The number of possible isomers in the *cis* and *trans* forms depend on whether the bound β-diketone in the 1 and 5 positions have the same (symmetrically substituted, one *cis* and one *trans*) or different substituents (asymmetrically substituted, three *cis* and two *trans* isomers), see Figure 2. 3.

The *trans*-configuration is preferred due to steric reasons, but experimentally the *cis*-configuration is found to be the most stable isomer.[69, 70, 71, 72, 39] The higher stability of the *cis*-configuration was attributed to electronic effects. Since titanium(IV) is a d^0 system, only ligand → metal π electron donation is involved in the metal *d*-orbitals. In the *cis*-configuration, three of the empty *d*-orbitals (t_{2g} or d_{xy}, d_{yz} and d_{xz}) of titanium is involved in the pπ–dπ back donation by the β-diketonato ligands, while in the *trans*-configuration only two *d*-orbitals (d_{xy} and d_{xz}) can interact with the β-diketonato π electrons.[73]

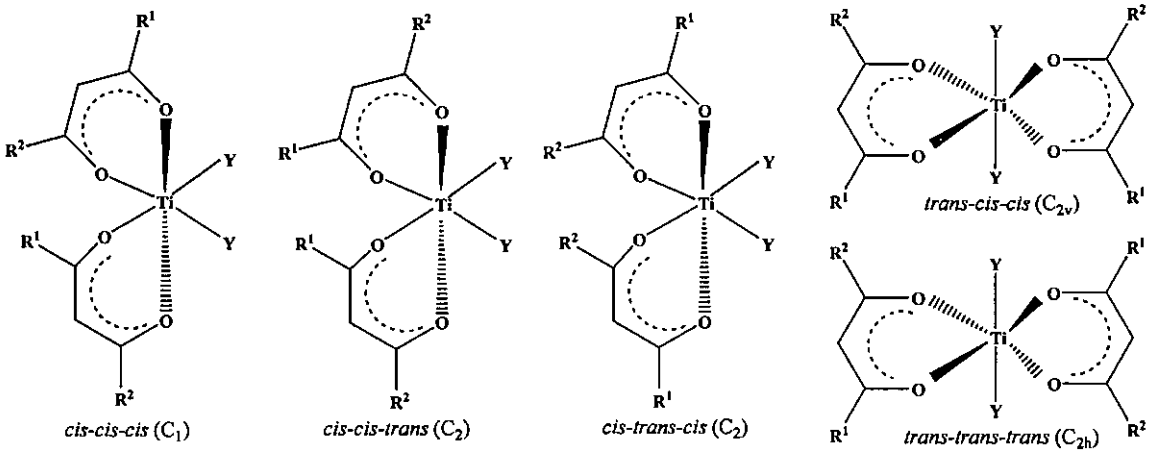

Figure 2. 3: The structures of possible isomers of *bis*-β-diketonato metal complexes, $[Ti(R^1COCHCOR^2)_2Y_2]$. Three *cis*-conformations (*cis-cis-cis*, *cis-cis-trans* and *cis-trans-cis*) and two *trans*-conformations (*trans-cis-cis* and *trans-trans-trans*) are possible for an unsymmetrical β-diketonato ligand. For a symmetrical β-diketonato ligand, *e.g.*. $CH_3COCHCOCH_3$ (acac) or PhCOCHCOPh (dbm) only one *cis*- and one *trans*-conformation is possible.

In the solid state, only one *cis* isomer was found to crystallize for a variety of [Ti(β-diketonato)$_2$Y$_2$] (Y = halogen or alkoxide) complexes (see Table 2. 2). In solution, however, all three *cis* isomers were detected by variable-temperature ^{1}H and ^{19}F NMR for a variety of [Ti(β-diketonato)$_2$X$_2$] (X = halogen or alkoxide) complexes.[74, 75] The stereochemistry of the complex, $[Ti(ba)_2Cl_2]$, for example, can be inferred from NMR spectra, as follows: the *cis-cis-cis* isomer (point group C_1) has no symmetry and therefore may give rise to two methyl, two phenyl, and two ring proton resonances. The other four isomers, *cis-cis-trans* (point group C_2) *cis-trans-cis* (C_2), *trans-cis-cis* (C_{2v}) and *trans-trans-trans* (C_{2h}), all possess at least one twofold axis. These isomers, as Figure 2. 3 indicates, should give a single resonance for each type of group.

Table 2. 2: Summary of crystallographic structural data of selected Ti(β-diketonato)$_2$X$_2$] with X = Cl, OEt, OMe, O^{t}Bu complexes.

Complex	Configuration	Bond lengths (Å) and angles (°)				
		Ti-O (alkoxy)/Ti-Cl		Ti–O(diketonato)		X–Ti–X (octahedral angles)
		Mean	Range	Mean	Range	Range
Ti(ba)$_2$(OEt)$_2$[39]	*cis-cis-trans*	1.808	1.803(7)–1.812(8)	2.025	1.977(5)-2.082(7)	81.6(2)–100.3(3)
	cis-cis-trans	1.797	1.782(7)–1.811(7)	2.015	1.977(5)–2.064(7)	80.9(2)–100.3(3)
Ti(ba)$_2$(O^{t}Bu)$_2$[71]	*cis-cis-cis*	1.785	1.773(7)–1.797(7)	2.044	1.986(6)–2.109(6)	79.4(2)–101.8(3)
Ti(ba)$_2$(OMe)$_2$[76]	*cis-trans-cis*	1.788	1.786(5)–1.789(4)	2.020	1.980(4)–2.094(5)	82.3(2)–99.7(2)
*Ti(tfba)$_2$(OEt)$_2$[72]	*cis-cis-trans*	1.760		2.050	2.009(1)–2.090(2)	79.0(1)–101.7(1)
**Ti(bzee)$_2$(OEt)$_2$[76]	*cis-trans-cis*	1.786	1.780(3)–1.792(3)	2.043	1.973(3)–2.115(3)	80.1(2)–100.5(2)
Ti(ba)$_2$Cl$_2$[39]	*cis-trans-cis*	2.293	2.285(1)–2.301(1)	1.953	1.910(2)–1.999(2)	83.9(1)–96.0(1)

*Htfba = trifluorobenzoylacetone

**Hbzee = Ethylbenzoylacetate.

2.3 Electrochemistry

2.3.1 Cyclic Voltammetry.

Cyclic voltammetry (CV) is one of the most versatile electroanalytical techniques for the study of electroactive species. For examining the electrochemical properties of a chemical substance or material, CV is one of the most often used techniques. For the study of biosynthetic reaction pathways and electrochemically-generated free radicals, organic chemists often apply this technique.[76, 77] An increasing number of inorganic chemists have been using cyclic voltammograms to evaluate the effects of ligands on the oxidation/reduction potential of the central metal ion in complexes and multinuclear clusters.[78] Stationary electrode polarography (linear sweep and cyclic voltammetry) has become the most powerful electroanalytical technique in providing information on the thermodynamics of redox processes, kinetics of heterogeneous electron transfer reactions, coupled chemical reactions, *etc.* Since the characteristic shape and position of the voltammetric waves fingerprint the individual electrochemical properties of redox systems, the technique has rightly been termed 'electrochemical spectroscopy'.[79] The theoretical development of this technique was initiated by Randles[80] and Sevcik[81], while the theory was extended to irreversible charge transfer processes by Delahay.[82]

The effectiveness of cyclic voltammetry results from its capability for rapid observation of the redox behaviour of compounds over a potential range. From a simple experiment, information of thermodynamics and reaction kinetics of the reactant may be observed. The rate and nature of a chemical reaction coupled to the electron transfer step can be studied, and both reduction potential and heterogeneous electron transfer rates can be measured. For the selection of the proper oxidizing agent, CV can be used for the conversion of the metal complex into an intermediate. Electrochemistry is the way to study the influence of ligand sets in redox properties.[83] Knowledge of the electrochemistry of a metal complex can be useful in the selection of the proper oxidizing agent to put the metal complex in an intermediate oxidation state. Electrochemical methodology has been exploited as a novel means of introducing functional groups and removing blocking agents.[84]

2.3.1.1 The Basic CV Experiment - Important Parameters

Cyclic voltammetry consists of cycling the potential of an electrode, which is immersed in an unstirred solution, and measuring the resultant current. The potential of the working electrode is controlled *versus* a reference electrode such as a saturated calomel electrode (SCE), a standard hydrogen electrode (SHE or NHE) or a silver/silver chloride electrode (Ag/AgCl). The voltammogram is a display of current (vertical axis) *versus* potential (horizontal axis). A cyclic voltammogram that was obtained with a glassy carbon working electrode immersed in a 3.0 mmol dm^{-3} ferrocene solution measured in 0.1 mol dm^{-3} tetrabutylammonium hexafluorophosphate/acetonitrile 25°C as supporting electrolyte and a scan rate of 100 mV s^{-1} is shown in Figure 2. 4. Important parameters of a cyclic voltammogram, *viz* cathodic peak potential (E_{pc}), anodic peak potential (E_{pa}), cathodic peak current (i_{pc}) and anodic peak current (i_{pa}), are shown in Figure 2. 4.

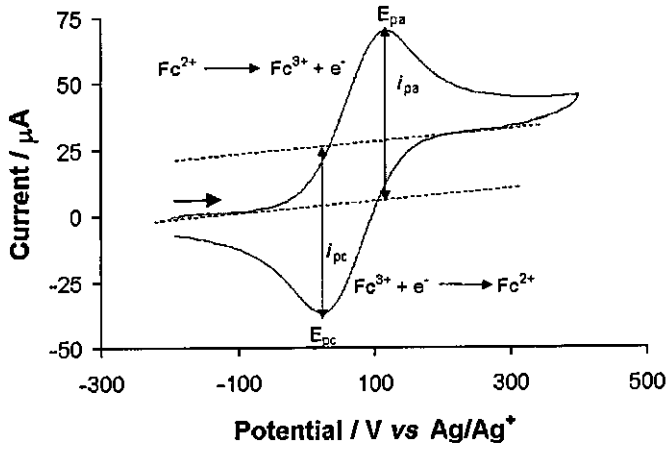

Figure 2. 4: Cyclic voltammogram of a 3.0 mmol dm^{-3} ferrocene measured in 0.1 mol dm^{-3} tetrabutylammonium hexafluorophosphate/acetonitrile on a glassy carbon electrode at 25°C, scan rate 100mV s^{-1}.[85] The arrow designates the direction of the scan.

Peak anodic and cathodic currents are obtained by extrapolating a baseline as illustrated in Figure 2. 4. From the separation between the peak potential, ΔE_p, the number of electrons transferred in the electrode reaction (n) for a reversible couple can be determined as follows:

$$\Delta E_p = E_{pa} - E_{pc} \approx \frac{0.059\ V}{n}$$

Peak separation increases due to slow electron transfer kinetics at the electrode surface. If at higher scan rates, the ΔE_p values increase, it can be deduced that the rate of electron transfer between the substrate and electrode is slow compared to the scan rate.[86] The theory predicts 59 mV for a one electron transfer process, but in practice a system with potential difference, ΔE_p, up to 90 mV, is still considered as an indication of a reversible couple. A redox couple may or may not be electrochemically reversible. From electrochemical reversibility, it is deduced that the rate of electron transfer between the electrode and substrate is fast enough to maintain the concentration of oxidized and reduced forms in equilibrium with each other at the electrode surface. The formal reduction potential, E°', is the average of the forward and return peak potential for the electrochemically reversible redox couple, and is given by the equation:

$$E^{0'} = \frac{E_{pa} + E_{pc}}{2}$$

This $E^{0'}$ is an estimate (but not exactly the same) of the polarographic $E_{1/2}$ value (the value that was given to the potential where the current is half the value of that on the current plateau):[87]

$$E_{1/2} = E^{0'} + (RT/nF)\ln(D_R/D_O)$$

D_R is the diffusion coefficient of the reduced species and D_O the diffusion coefficient of the oxidized species.

Another characteristic of reversible systems is the dependence of the peak height on the square root of the scan rate. The peak current as defined by the Randles-Sevcik equation at 298 K, is:

$$i_p = \left(2.69 \times 10^5\right) n^{\frac{3}{2}} A D^{\frac{1}{2}} \nu^{\frac{1}{2}} C$$

where C is the concentration of the substrate (mol cm^{-3}), D is the diffusion coefficient ($cm^2 s^{-1}$), i_p is the peak current (amperes, A), and A is the electrode surface area (cm^2). In the studies of electrode mechanism and analytical applications, the relationship between peak

current and concentration is shown to be important. For an electrochemical reversible couple that is not followed by any coupled chemical reactions the value of i_{pc} and i_{pa} should be identical. That is,

$$\frac{i_{pa}}{i_{pc}} = 1$$

Systems can be electrochemically reversible ($\Delta E_p \leq 90$ mV), quasi-reversible (90 mV $\leq \Delta E_p \leq$ 150 mV) or irreversible ($\Delta E_p > 150$ mV) [88] (See Figure 2. 5). A chemically reversible couple is where both the oxidation and reduction processes take place. In chemical irreversible systems, only oxidation (or reduction) is possible.

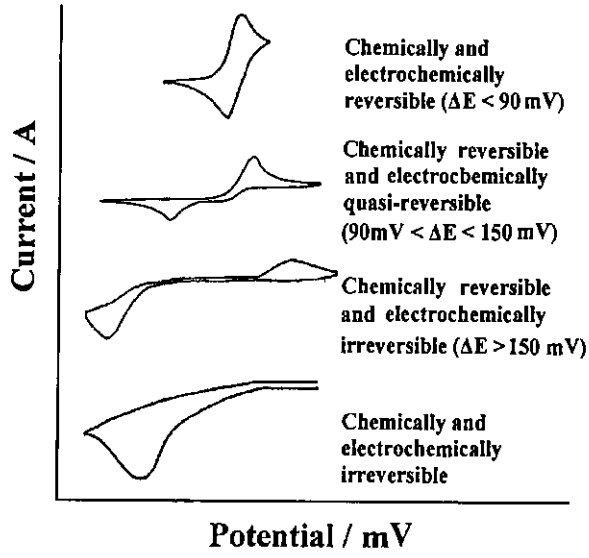

Figure 2. 5: A schematic representation of the cyclic voltammogram expected for an electrochemical reversible (top CV), quasi-irreversible (middle two CV's) or irreversible (bottom CV) system. Reference to chemical reversibility or irreversibility is included.

2.3.1.2 Solvents and Supporting Electrolytes in Electrochemistry

All electrochemical phenomena occur in suitable media, which consist of solvents containing a supporting electrolyte. Attention has to be given to how electrochemical and chemical properties of the electrode reaction may be affected by the solvent system. Important requirements are that the species under investigation must be stable and soluble in the solvent, and that the solvent has to allow electrical conductivity. It should be a good solvent for both electrolyte and analyte. An ideal electrochemical solvent should possess electrochemical and

chemical inertness over a suitable potential range for the species under investigation. Dipolar aprotic solvents are often used since they have large dielectric constants (≥ 10) and low proton availability. Acetonitrile, commonly used in anodic studies, is moderately nucleophilic, an excellent solvent for polar organic compounds, inorganic salts, and is stable after purification (with a dielectric constant of 37). Dichloromethane is a good choice if a strictly non-coordinating solvent is required.

In most electro-synthetic and electro-analytical experiments supporting electrolytes are used to increase conductivity in non-aqueous solution, which influences mass transfer. Ions of the supporting electrolyte carries the current. The concentration of material under investigation must therefore be at most 10% that of the electrolyte, to prevent the analyte acting as an electrolyte. Tetrabutylammonium hexafluorophosphate, $[NBu_4]^+[PF_6]^-$ or $TBAPF_6$, is widely used as a supporting electrolyte and soluble in CH_3CN. A solution of $TBAPF_6$ in acetonitrile exhibits a very wide accessible potential range, with positive and negative decomposition potentials of 3.4 V and -2.9 V (*vs.* SCE) respectively.[89] Diffusion of an electro-active species will be affected by the viscosity of the medium and the size of the solvating species.

LeSeur and Geiger[90] showed that the use of the non-coordinating supporting electrolyte, tetrabutylammonium tetrakis(pentafluorophenyl)borate, $[NBu_4]^+[B(C_6F_5)_4]^-$, improves the electrochemistry compared to the weakly coordinating supporting electrolyte, tetrabutylammonium hexafluorophosphate, $[NBu_4]^+[PF_6]^-$, in solvents of low dielectric strength, as illustrated in Figure 2. 6.

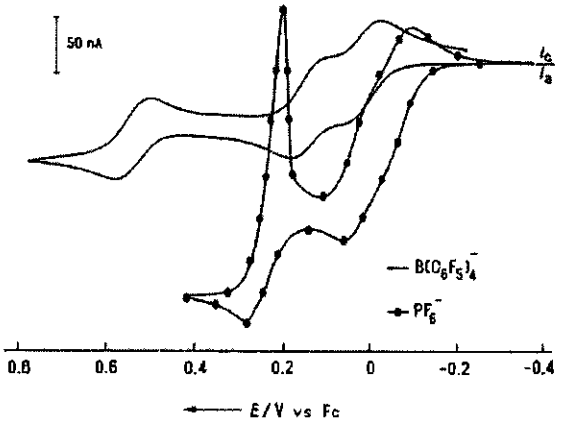

Figure 2. 6: Comparison of cyclic voltammograms of $[Fe(\eta\text{-}C_5H_4)_2]_3(SiMe_2)_2$ (1.0 mM) in dichloromethane (Pt electrode, 0.5 mm diameter) at ambient temperature with different electrolytes, i.e., $[NBu_4]^+[PF_6]^-$ (bottom) and $[NBu_4]^+[B(C_6F_5)_4]^-$ (top). Scan rate = 200 mV s^{-1}.

Ohrenberg *et al*[91] demonstrated that when using the non-coordinating solvent α-α-α-trifluorotoluene or (trifluoromethyl)benzene and the electrolyte tetrabutylammonium tetrakis(pentafluorophenyl)borate $[NBu_4]^+[B(C_6F_5)_4]^-$, reversible behaviour can be obtained for nickelocene and cobaltocene. They found that the Ni(II)/Ni(III) and Ni(III)/Ni(IV) couples yield a ΔE_p value of 75 mV, i_{pa}/i_{pc} ratios of 1 and $E^{0'}$ values of – 0.42 V and 1.10 V *vs.* Fc/Fc^+ respectively. The Co(III)/Co(II) couple showed reversible behaviour with an $E^{0'}$ value of – 1.35 V, while the Co(II)/Co(I) couple with an $E^{0'}$ value of – 2.48 V did not exhibit an i_{pa}/i_{pc} ratio of exactly 1, due to solvent destruction. The cyclic voltammograms illustrating reversible behaviour of cobaltocene and nickelocene are shown in Figure 2. 7.

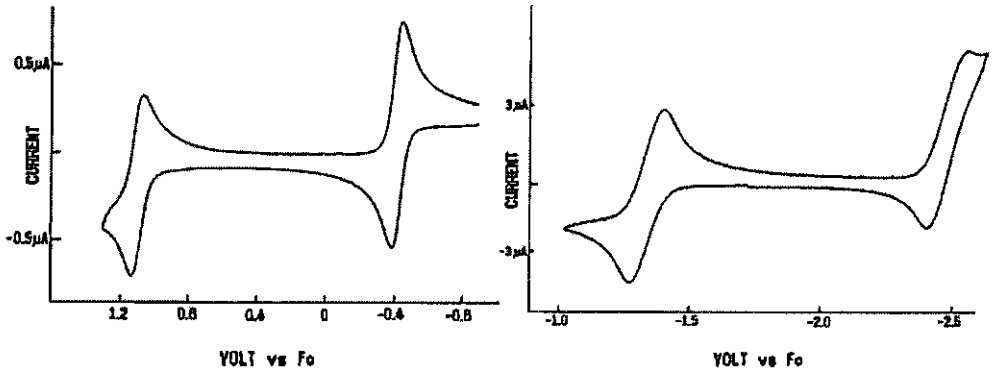

Figure 2. 7: The cyclic voltammogram of 0.5 mM nickelocene (supporting electrolyte 0.05 M each of $[NBu_4]^+[B(C_6F_5)_4]^-$ and $[NBu_4]^+[BF_4]^-$, left) and 1 mM cobaltocene (supporting electrolyte $[NBu_4]^+[B(C_6F_5)_4]^-$ (0.1 M), right) in α-α-α-trifluorotoluene, showing reversible electrochemistry utilizing a glassy carbon electrode. Scan rate of 100 mV s^{-1}.[91]

2.3.1.3 Reference Systems

In non-aqueous solvents, the NHE (standard hydrogen electrode) and SCE (saturated calomel electrode) are often impractical to use as reference electrodes. The recommendation by IUPAC is that all electrochemical data are to be reported *vs.* an internal standard. The Fc/Fc^+ couple is a convenient internal standard in organic media[92, 93, 94] (Fc^+/Fc couple: 400 mV *vs.* NHE).[92] In systems where the Fc^+/Fc couple overlaps with peaks of the analyte, cobaltocene ($E^{o'}$ = -918 mV *vs.* NHE),[92] or any of a variety of aromatic compounds, comprising a virtual continuum of reduction potentials, can be substituted. Potentials should then be related to the formal reduction potential, $E^{o'}$ (Fc^+/Fc), through a second experiment.

The Fc/Fc^+ couple has a ΔE_p value of 59 mV and is reversible under ideal conditions. The use of the formal reduction potential of ferrocene as an internal standard is illustrated in Figure 2. 8.

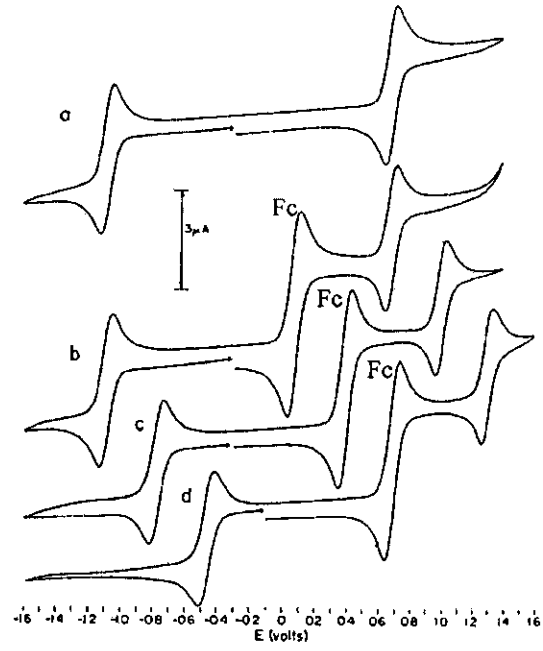

Figure 2. 8: Platinum button cyclic voltammetry at 50 mV/s of 0.005 M $[Ru(acac)_3]$ in CH_3CN with tetrabutylammonium perchlorate (TBAP = 0.1M), (b), (c) and (d) ferrocene added. (a) and (b) *vs.* $Ag/AgNO_3$ (0.01M), (c) *vs.* SCE and (d) *vs.* Cu wire.

Figure 2. 8(a) shows the cyclic voltammogram of *tris*(acetylacetonato)ruthenium(III) in acetonitrile. Figure 2. 8(b) shows the cyclic voltammogram of *tris*(acetylacetonato)-ruthenium(III) after the addition of a small amount of ferrocene to give $E^{0'}$ values of 0.602 and -1.157 V *vs.* Fc^+/Fc. For Figure 2. 8(c) and (d), a SCE and copper wire were used as reference electrodes respectively and the conditions used were similar to those found in Figure 2. 8(b). The values on the potential axis appear to be shifted, but formal potentials relative to Fc^+/Fc remain unchanged.[93]

2.3.2 Electrochemistry of some Titanium Complexes

2.3.2.1 Titanocene containing Compounds

Table 2. 3 gives the redox potentials of titanocene dichloride in solutions of THF, DCM and CH_3CN, with the supporting electrolyte being 0.2 M n-Bu_4NPF_6.[96] The redox properties of titanocene dichloride show a strong solvent dependence. In THF and DCM quasi-reversible redox character was observed with ΔE_p being 90 – 100 mV and i_{pa}/i_{pc} being 0.65 – 0.95. In CH_3CN irreversible redox character with only a small reoxidation peak, strongly shifted to the positive direction, and ΔE_p being 400 mV, was observed. By using the supporting electrolyte, tetrabutylammonium hexafluorophosphate, in DCM solution, however, the redox behaviour of titanocene dichloride improved to electrochemically quasi-reversible with ΔE_p = 117 mV and chemically reversible, with i_{pa}/i_{pc} = 0.92.[85] Refer to Figure 2. 9.

From the framework of a 'square scheme', Scheme 2. 13.[96], the above observations can be interpreted in terms of an electrochemical reduction step accompanied by the solvent molecule rapidly substituting one chloride ligand. The process of back electron transfer in strong coordinating solvents (CH_3CN) $E_{1/2}$ shifts to a more positive potential, than in weakly coordinating solvents (THF, DCM).

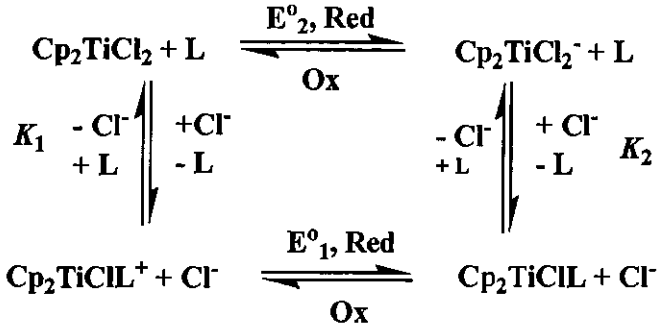

Scheme 2. 13: The 'square scheme' illustrating the reduction and oxidation of titanocene dichloride.[95]

The electrochemical characterization of a titanocene dichloride derivative, $[Cl_2TiCpC_5H_4(CH_2)_3NC_4H_4]$, (one of the cyclopentadienyl rings is functionalized with a

pyrrolyl ring (Py)), shows that the oxidation and reduction resemble the behaviour of the unsubstituted titanocene dichloride, Table 2. 3. The reduction of this titanocene dichloride derivative gives rise to irreversibility in CH_3CN, while in THF and DCM quasi-reversible behaviour reveals dependence on the solvent complexation ability.

Table 2. 3: Redox potentials in solutions *versus* Ag/Ag^+ and SCE (Pt electrode and supporting electrolyte 0.2 M *n*-Bu_4NPF_6) of Tc, $[Cl_2TiCpC_5H_4(CH_2)_3NC_4H_4]$ (Tc3Py) and Fc.[96] The last three rows give the data of Tc, with the supporting electrolyte, 0.2 mol dm^{-3} tetrabutylammonium hexafluorophosphate.[85]

Compound	Solvent	$E_{1/2}$ *vs.* Ag/Ag^+ / mV	$E_{1/2}$ *vs.* SCE / mV	ΔE_p / mV	i_{pc}/i_{pa}
Tc	THF	-1080	-760	90	0.90 – 0.95
	DCM	-950	-730	100	0.65 – 0.75
	CH_3CN	-800	-470	400	-
Fc	THF	200	530	100	1.0
	DCM	210	430	100	1.0
	CH_3CN	100	430	80	1.0
Tc3Py	THF	-1120	-790	95	0.7 – 0.9
	DCM	-980	-760	115	0.65 – 0.80
	CH_3CN	-845	-525	425	-
Tc	THF	-1077*	-	106	0.62
	DCM	-922*	-	117	0.83
	CH_3CN	-990*	-	304	0.92

*$E^{0'}$ value

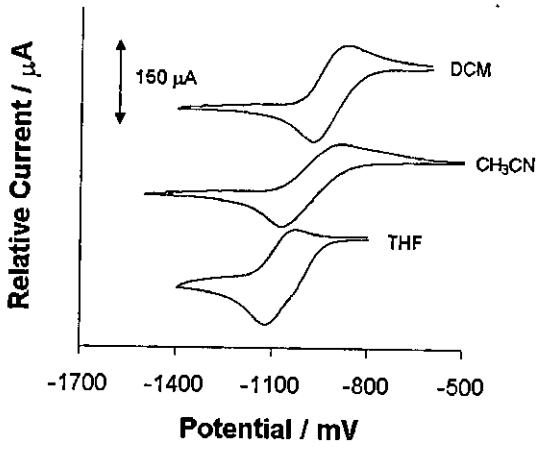

Figure 2. 9: The cyclic voltammograms of 3.0 mmol dm^{-3} titanocene dichloride *vs.* Ag/Ag^+ (0.2 mol dm^{-3} tetrabutylammonium hexafluorophosphate supporting electrolyte) in DCM (ΔE_p = 117 mV, E^{01} = -1160 mV *vs.* Fc/Fc^+), THF (ΔE_p = 106 mV, E^{01} = -1280 mV *vs.* Fc/Fc^+) and CH_3CN (ΔE_p = 304 mV, E^{01} = -900 mV *vs.* Fc/Fc^+) on a glassy carbon working electrode at 25°C, and a scan rate of 200 mV s^{-1}.

2.3.2.2 Titanium-β-diketonato and Related Compounds

Electrochemical data obtained from the titanium(III)-β-diketonato complex [Cp_2Ti(β-diketonato)], where β-diketonato = $acac^-$ or ba^-, shows that both the metal (peak at -0.85 or -0.86 V) as well as the β-diketonato ligand (peak at *ca* -2.5 V) are electrochemically active (Figure 2. 10).[97] Ti(III) can be reversibly oxidized in a one electron process at a potential, which is apparently independent of the β-diketonato ligand, when R = CH_3 or C_6H_5. For [$TiCp_2$(acac)] $E^{0'}$ = -0.86 V and for [$TiCp_2$(ba)] $E^{0'}$ = -0.85 V *vs.* Fc/Fc^+ in 0.2 M NBu_4PF_6/butyronitrile. The negligible influence of the β-diketonato ligand on the formal reduction potential was attributed to the presence of a highly localized centred frontier orbital, which dominates the redox chemistry.

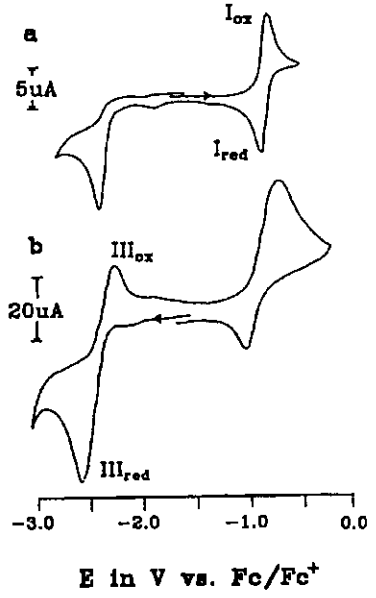

Figure 2. 10: CV of [Cp_2Ti (ba)] (2 mM) obtained in butyronitrile (0.2 M NBu_4PF_6) at a scan rate of 200 mV/s with a) 1 mm Pt disk electrode at 22°C, and b) a 5 mm glassy carbon disk electrode at -50°C.[97] The peak at -0.85 V represents the Ti^{3+}/Ti^{4+} couple while the peak at ± -2.5 V represents the reduction of the β-diketonato ligand.

The cyclic voltammogram of $[VCp_2(acac)](CF_3SO_3)$ in acetonitrile using a Pt working electrode (Figure 2. 11)[98] displayed a characteristic one electron quasi-reversible reductive couple for the V^{3+}/V^{4+} process with $E_{1/2}$ = -1.06 V (*vs.* Fc/Fc^+). An oxidative quasi-reversible redox couple, attributable to the V^{4+}/V^{5+} heterogeneous electron transfer process, was observed at 0.987 V (*vs.* Fc/Fc^+). The peak current ratio i_{pa}/i_{pc}, for oxidative, and i_{pc}/i_{pa}, for reductive couple for both the redox processes are nearly one, and the plots of i_p (peak current) *vs.* $v^{1/2}$ (v = scan rate) for each redox process are linear, implying a limited mass transfer of the one electron stoichiometric reaction:

$$[V^{V}Cp_2(acac)]^{2+} \leftrightarrow [V^{IV}Cp_2(acac)]^{+} \leftrightarrow [V^{III}Cp_2(acac)]^{0}$$

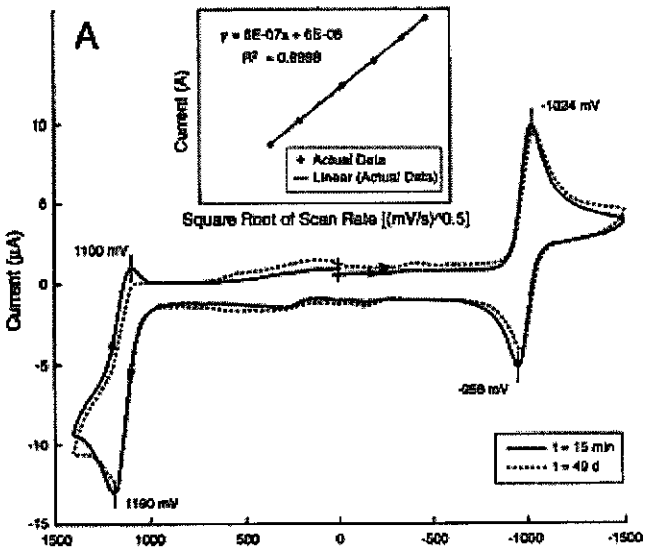

Figure 2. 11: Cyclic voltammograms of $[VCp_2(acac)](CF_3SO_3)$ in acetonitrile containing 0.1 M tetrabutyl ammonium trifluoromethane sulfonate, at a platinum working electrode, and scan rate = 200 mV/ s (—). CV taken after 49 days of storage (---). Inset: plot of *I* vs. *v*.[98]

The redox behaviour of Ti in the tetranuclear antitumor (4-acyl-5-pyrazolonato)-titanium species, *cyclo*-tetrakis[bis(4-benzoyl-3-methyl-1-phenylpyrazolon-5-ato)(μ-oxo)titanium(IV)] (Scheme 2. 14, left), and the mononuclear species (3-methyl-4-(neopentylcarbonyl)-1-phenylpyrazol-5-onato)$_2$Ti($OCH_2CH_2CH_3$)$_2$ (Scheme 2. 14, right) show a reversible redox couple in the cathodic region assigned to Ti^{III}/Ti^{IV}, with E_{pc} = -1.46 V (Figure 2. 12) and -1.71 V (voltammogram not shown) *vs.* Fc/Fc^+ respectively. Therefore, in the tetranuclear species all four Ti atoms undergo the same process and are indistinguishable. The Ti^{IV} atom has a greater tendency to be reduced to Ti^{III} in the mononuclear than in the tetranuclear species. [63]

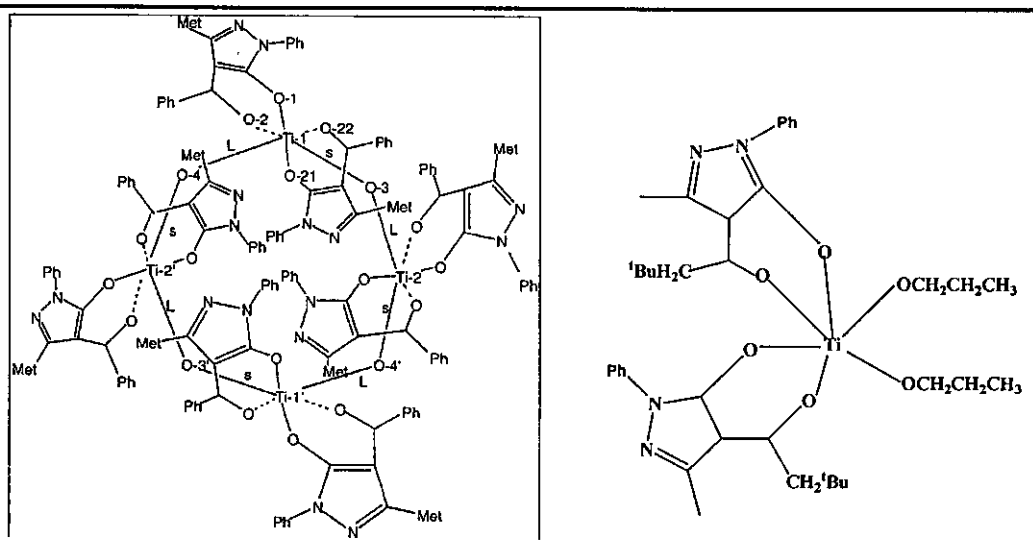

Scheme 2. 14: Structure of *cyclo*-tetrakis[bis(4-benzoyl-3-methyl-1-phenylpyrazolon-5-ato)(μ-oxo)titanium(IV)] (left) and (3-methyl-4-(neopentylcarbonyl)-1-phenylpyrazol-5-onato)$_2$Ti-(OCH$_2$CH$_2$CH$_3$)$_2$ (right)

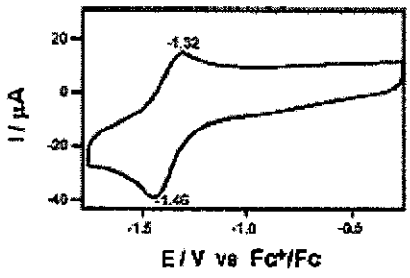

Figure 2. 12: Voltammogram of the antitumor compound *cyclo*-tetrakis[bis(4-benzoyl-3-methyl-1-phenylpyrazolon-5-ato)(μ-oxo)titanium(IV)] (structure shown in Scheme 2. 14 left).

2.4 Substitution Kinetics

2.4.1 Introduction

Chemical reactions are often grouped for convenience into the following types, i.e.: substitution, addition or elimination (perhaps involving free radical species), exchange (both intermolecular and intramolecular), solvolysis and redox reactions.[99] The different reaction types are represented below:

$$KX + LY \rightleftharpoons KLXY \quad \textbf{(addition/elimination)}$$

$$KX + LY \rightleftharpoons KY + LX \quad \textbf{(exchange)}$$

$$KX + HA \rightleftharpoons KA + HX \quad \textbf{(solvolysis)}$$

$$K_{ox} + L_{red} \rightleftharpoons K_{red} + L_{ox} \quad \textbf{(redox)}$$

$$KX + Y \rightleftharpoons KY + X \quad \textbf{(substitution)}$$

An addition reaction involves the addition of an incoming ligand (LY) to the complex (KX) in a solution. An elimination reaction is the opposite of an addition reaction. Oxidative addition and reductive elimination are two important classes of reactions in organometallic chemistry. Their relationship is shown below where n represents the number of ligands L on the metal M and m is the oxidation state of the metal.

$$L_nM^{(m)} + XY \rightleftharpoons L_nM^{(m+2)}\begin{matrix} X & Y \\ \diagdown & \diagup \end{matrix}$$

In oxidative addition reactions, the metal in the complex L_nM is oxidized to an oxidation state of two units higher, and the coordination number of the metal complex increases by two units. Oxidative addition is a combination of addition and change of oxidation state. The metal ion can act as the transmitter of electrons and facilitates electron transfer between coordinated ligands. The change of a pair of electrons in the central atom from a non-bonding to a bonding role can formally reduce a single molecule into two donor fragments upon which further chemistry might be carried out.[100] Latent or real coordination sites on the metal are

necessary for the oxidative addition of XY to certain d^8 systems, converting them into octahedral d^6 complexes.[101] Addition and elimination reactions can be used as catalysts in these reactions, for example, in the synthesis of acetic acid.

Exchange reactions involve the ligand exchange between complexes. This type of reaction also includes the substitution of the ligand of a complex with another ligand of the same type in the solution, for example in water exchange reactions. The reactions are important for medical applications, whereby isotopic complexes can be synthesized *via* exchange reactions to be used for cancer therapy.

Solvolysis is the chemical reaction in which the solute (KX) and solvent (HA) react to form a new compound (e.g. KA or KXKA). If the solvent is water, hydrolysis is a more appropriate term.

Oxidation-reduction or redox reactions involve all chemical processes in which atoms have their oxidation numbers (oxidation states) changed. It involves two species, the oxidant (K_{ox}), which receives electron(s), and the reductant (L_{red}), which looses electron(s). However, this kinetic simplicity cloaks a range of mechanisms, involving electron transfer, atom or group transfer, ligand substitution, addition or dissociation. An important application of redox reactions is the electroplating of the cathodes and anodes of batteries.

Substitution reactions involve the replacement of one ligand or group (the leaving group, X) by another (the entering group, Y) at a central element (K), with no change in oxidation state or coordination number of the central atom.[100] It is fairly obvious that the act of substitution requires a temporary change in the coordination number of the reaction centre. A special case of substitution is the exchange of a ligand with a solvent molecule. Metal ions or complexes that generally react rapidly (within a few seconds) are said to be labile. Whereas, if substitution is slow (taking minutes or longer), the reaction is considered inert.[101] There are various factors that determine whether a complex is labile or inert. The ligand interchange in metal complexes can occur in two ways,[101] either by (a) a combination of solvolysis and ligation, *e.g.*

$$Co(CN)_5Cl^{3-} + H_2O \rightarrow Co(CN)_5H_2O^{2-} + Cl^-$$

$$Co(CN)_5H_2O^{2-} + N_3^- \rightarrow Co(CN)_5N_3^{3-} + H_2O$$

or (b) by simple interchange with replacement of one ligand by another without direct intervention of the solvent, *e.g.*

$Pt(dien)Br^+ + Cl^- \rightarrow Pt(dien)Cl^+ + Br^-$

Indirect substitution of the type indicated by (a) above, appears to be mostly involved in octahedral complexes, while direct substitution is favoured by square planar complexes. This situation could perhaps be predicted in view of the more crowded conditions with octahedral as compared to square planar complexes.

The different reaction types shortly discussed above are an overview of reactions, but do not explain which mechanism the reactions follow. The accurate mode of mechanism of a specific reaction is important for the conditions of reactions to be optimized to minimise costs. The formation of undesirable products should be restricted and this can only be done if the reaction mechanism is familiar. In this study, substitution of six-coordinate octahedral titanium complexes is studied; therefore, a discussion of the mechanism, stereochemistry and factors influencing octahedral substitution is appropriate.

2.4.2 Mechanisms of Substitution Reactions at Octahedral Complexes

Octahedral substitution reactions proceed *via* two basic mechanisms or pathways, *i.e.,* an associative and dissociative mechanism. The reaction that proceeds *via* an associative path is illustrated in Equation 2. 1:

Equation 2. 1 $$M\text{-}X + Y \longrightarrow [X\text{-}M\text{-}Y]^{\#} \longrightarrow M\text{-}Y + X$$

In the first step the reaction proceeds *via* an associative mechanism, A. The complex binds with the incoming ligand, producing an intermediate of increased coordination number. A seven-coordinate intermediate is formed, the bond between the leaving ligand and metal ion weakens and a new complex is formed. The reaction that proceeds *via* dissociative mechanism, D, is illustrated in Equation 2. 2:

Equation 2. 2 $$M\text{-}X \rightleftharpoons [M + X]^{\#} \overset{Y}{\rightleftharpoons} M\text{-}Y + X$$

The ligand is lost in the first step and an intermediate of reduced coordination number is formed. The five-coordinate intermediate reacts with an incoming ligand to form the final product. Few reactions proceed, however, strictly *via* one of the above-mentioned two mechanisms. In practice bond formation and bond breaking happen simultaneously during the formation of activated complexes. This reaction pathway is called, interchange, I. The I mechanism may be dominated by bond breaking (I_d) or bond formation (I_a) during the transition state. The substitution reaction that proceeds *via* an interchange mechanism is illustrated in Equation 2. 3:

Equation 2. 3 $$M\text{-}X + Y \rightleftharpoons [X\text{-}M\text{---}Y \longleftrightarrow Y\text{-}M\text{---}X]^{\#} \rightleftharpoons M\text{-}Y + X$$

The possible mechanisms for octahedral substitution reactions are illustrated below:

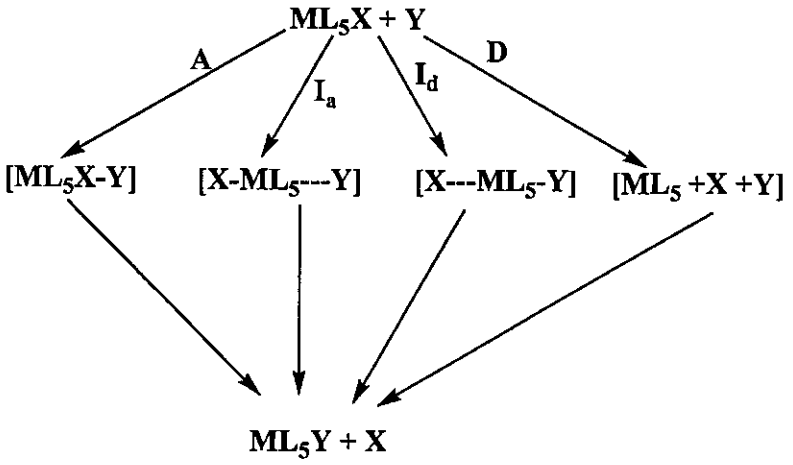

2.4.2.1 Dissociative Mechanism (*D*)

Bond breaking is the rate-determining step for the reaction proceeding *via* a dissociative mechanism. The total reaction is described in Equation 2. 4:

$$ML_5X \underset{k_{-1}}{\overset{k_1}{\rightleftharpoons}} ML_5 + X \quad \textbf{(rate determining step)}$$

$$ML_5 + Y \xrightarrow{k_2} ML_5Y \quad \textbf{(fast)}$$

Equation 2. 4

The second step is fast due to the fact that the metal in the five-coordinate intermediate, ML_5 is unsaturated and therefore very reactive. The steady-state (or stationary-state) hypothesis assumes a very small concentration of the intermediate, ML_5, and requires that the rates of formation and reaction of the intermediate should be equal. This in turn requires that the rate of change of $[ML_5]$ be zero during much of the reaction. The rate law will be written as in Equation 2. 5.

Equation 2. 5 $$\text{Rate} = \frac{k_1 k_2 [ML_5X][Y]}{k_{-1}[X] + k_2[Y]}$$

Following Equation 2. 5, the reaction rate is dependent on the concentration of incoming ligand, Y, and complex, ML_5X. One criterion for this mechanism is that the intermediate, ML_5, be detectable during the reaction.

If in Equation 2. 5 $k_2[Y] >> k_{-1}[X]$, which is usually true at high concentration of the incoming ligand, the reaction rate become independent of the concentration of the incoming ligand, with Equation 2. 5 then becoming Equation 2. 6, a first-order process.

Equation 2. 6 $$\text{Rate} = k_1 [ML_5X]$$

The following reaction is an example of a dissociative mechanism reaction:

Equation 2. 7 $$\mathbf{[Co(TPPS)(H_2O)_2]^{3-} + NCS^- \rightleftharpoons [Co(TPPS)(H_2O)(NCS)]^{4-} + H_2O}$$

The first-order reaction rate in Equation 2. 6 was obtained for the substitution reactions of Co(III)-complexes with various monodentate ligands. The positive activation volume of +15.4(6) $cm^3\ mol^{-1}$ for the reaction in Equation 2. 7 is indicative of a dissociative mechanism.

2.4.2.2 Associative Mechanism (*A*)

In an associative mechanism, the first step, namely the formation of an intermediate with an increased coordination number, is the rate-determining step. It is followed by a faster reaction in which the leaving ligand is lost:

$$ML_5X + Y \underset{k_{-1}}{\overset{k_1}{\rightleftharpoons}} ML_5XY \qquad \textbf{(rate determining step)}$$

$$ML_5XY \xrightarrow{k_2} ML_5Y + X \qquad \textbf{(fast)}$$

By applying the stationary-state approach the rate law becomes,

$$\text{Rate} = \frac{k_1 k_2 [ML_5X][Y]}{k_{-1} + k_2} = k[ML_5X][Y] \qquad \text{where } k = \frac{k_1 k_2}{k_{-1} + k_2}$$

This is a second-order equation regardless of the concentration of Y. If the reaction is performed under pseudo first order conditions, the rate equation becomes,

$$\text{Rate} = k_{obs}[ML_5X] \text{ with } k_{obs} = k[Y]$$

Once it was thought that the I_d mechanism dominated octahedral substitutions, but more recently it emerged that the associative mode of activation is perhaps just as common - with a range of geometries possible for such transition states.[100]

2.4.2.3 Interchange Mechanism (*I*)

In an interchange (*I*) reaction, a rapid equilibrium between the incoming ligand and the six-coordinate reactant forms an ion pair or loosely bonded molecular combination. The

intermediate species does not change in coordination number and is not directly detectable. This intermediate species reacts to form the product and releases the initial ligand.

$$ML_5X + Y \underset{k_{-1}}{\overset{k_1}{\rightleftharpoons}} ML_5XY$$

$$ML_5XY \xrightarrow{k_2} ML_5Y + X$$

When the second step is slow, with $k_2 << k_{-1}$, the reverse reaction of the first step is fast enough for this step to be independent of the second step, and the first step is an equilibrium with $K_1 = k_1/k_{-1}$. Applying the stationary-state hypothesis:

$$\text{Rate} = k_1[ML_5X][Y] - [ML_5XY](k_{-1} + k_2)$$

If $[Y] >> [ML_5X]$, the concentration of the unstable transition species may be large enough to significantly change the concentration of ML_5Y, but not that of Y. Under this condition in terms of the total initial reactant concentration of ML_5X and Y, which will be called $[M]_0$ and $[Y]_0$ it follows that:

$$[M]_0 = k_1[ML_5X] + [ML_5XY]$$

Assuming the concentration of the final product, $[ML_5Y]$, is too small to change the concentration of the incoming ligand Y significantly, then

$$[Y]_0 \cong [Y]$$

From the stationary-state equation:

$$k_1([M]_0 - [ML_5XY])[Y]_0 - k_{-1}[ML_5XY] - k_2[ML_5XY] = 0$$

The reaction rate becomes:

$$\text{Rate} = k_2[ML_5XY] = \frac{k_2K_1[M]_0[Y]_0}{1 + K_1[Y]_0 + \left(k_2/k_{-1}\right)} \cong \frac{k_2K_1[M]_0[Y]_0}{1 + K_1[Y]_0}$$

where k_2/k_{-1} is very small and can be omitted, because $k_2 << k_{-1}$ is required for the first step to be in equilibrium.

If $K_1[Y]_0 << 1$, the reaction rate depends on the concentration of incoming ligand [Y]:

Rate = $k_1K[M]_0[Y]_0$

If $K_1[Y]_o >> 1$, reaction rate is independent of incoming ligand's concentration [Y]:

Rate = $k_2[M]_0$

The difference between the two variations on the interchange mechanism I_d (dissociative interchange) and I_a (associative interchange) lies in the degree of bond formation in the first step of the mechanism. If bonding between the incoming ligand and the metal is more important, it is an I_a mechanism. If bond breaking between the leaving ligand and the metal is more important, it is an I_d mechanism. The distinction between the two possibilities is subtle, and careful experimental design is required to determine which description fits a given reaction.

2.4.3 Factors Influencing the Mechanism of Octahedral Substitution Reactions.

2.4.3.1 Introduction

There are various factors that influence the rate of octahedral substitution reactions. These factors give important information concerning reaction mechanism. The rate of substitution in an octahedral reaction is influenced by the central metal ion, the incoming ligand, leaving and non-labile ligands, the nature of the solvent as well as activation parameters. The type of mechanism that the reaction follows can be determined by the influence the above-mentioned factors have on the rate of reaction.

2.4.3.2 Influence of the Central Metal Ion

The size, charge and electron configuration of the metal ion are factors that can influence the rate of substitution of a complex. It can also be used to develop more insight into the type of mechanism a reaction follows. An increase in the positive charge of a metal ion will result in a stronger metal-ligand bond. The stronger metal-ligand bond will oppose dissociation, which will result in a decrease in the rate of reaction that follows a dissociative mechanism. Therefore, the higher positive charge of the metal ion will generally encourage an associative mechanism, since with bond formation the incoming ligand will be favoured. A large central metal ion accommodates the incoming ligand more easily, favouring an associative mechanism.

An example of illustrating the influence of the charge (oxidation state) of the central metal ion on the reaction rate, is the substitution reaction of the $[MO(H_2O)(CN)_4]^{(n-2)-}$ complexes of W(IV)[102] and $[M(H_2O)(CN)_4]^{(n-1)-}$ complexes of Re(V)[103] with thiocyanate ions. The reaction of $[W^{IV}O(H_2O)(CN)_4]^{2-}$ with thiocyanate ions is approximately 800 times faster than the corresponding reaction of $[Re^{V}(H_2O)(CN)_4]^{-}$. Another example of how the increase of the metal ion's positive charge resulted in slower reaction rates, is the water exchange reaction of $[Cr^{II}(H_2O)_6]^{2+}$ and $[Cr^{III}(H_2O)_6]^{3+}$, which were found to be in order of 10^8 dm^3 mol^{-1} s^{-1},[104] and 10^{-6} dm^3 mol^{-1} s^{-1},[105] respectively.

2.4.3.3 The Effect of the Leaving Group[106]

An increase in the electronegativity of the leaving group should result in a decrease in the reaction rate for both dissociative and associative substitution reactions. An increase in the electronegativity of the leaving group gives rise to a stronger metal-ligand bond. The stronger metal-ligand bond will oppose dissociation, which will result in a decrease in the rate of the reactions that follow a dissociative mechanism. In an associative mechanism, the higher electronegativity of the leaving group leads to a decrease in the positive charge of the metal

ion (bond formation the negatively charged incoming ligand will be less favoured), resulting in a decrease in the reaction rate. The rate of the aquation of the pentaammine complexes $[Cr^{III}(NH_3)_5X]^{2+}$ and $[Co^{III}(NH_3)_5X]^{2+}$ decreased by a factor 4000 and 100 respectively as the electronegativity of the leaving group X = F^-, Cl^-, Br^- and I^- decreased (see Table 2. 4).[107, 100] The mechanisms of these substitution reactions were interpreted as I_a and I_d for the chromium(III) and cobalt(III) systems respectively.[100]

Table 2. 4: Comparison of the rate constants of the substitution reaction $[M^{III}(NH_3)_5X]^{2+} + H_2O \rightleftharpoons [M^{III}(NH_3)_5(H_2O)]^{3+} + X^-$ for X = F^-, Cl^-, Br^- and I^-, M = Cr and Co, T = 298 K, illustrating the influence of the electronegativity, κ_x, of the leaving group X on the reaction rate.

Compound	10^7 k (s^{-1})		κ_x
	Cr	Co	
$[M^{III}(NH_3)_5F]^{2+}$	2.5	0.86	4.1
$[M^{III}(NH_3)_5Cl]^{2+}$	95	18	2.8
$[M^{III}(NH_3)_5Br]^{2+}$	950	39	2.7
$[M^{III}(NH_3)_5I]^{2+}$	10340	83	2.2

An increase in the bulkiness of the leaving ligand favours a dissociative reaction because the five-coordinate activated complex can relieve strain. The increase in the reaction rate of the substitution of a PR_3-ligand from *cis*-$[Mo(CO)_4(PR_3)_2]$ with CO following a dissociative mechanism, is assigned to the increase in bulkiness of PR_3 as determined by the Tolman angle (see Table 2. 5).[108]

Table 2. 5: Rate constants of the substitution reaction *cis*-$[Mo(CO)_4(PR_3)_2]$ + CO $\rightleftharpoons$ $[Mo(CO)_5(PR_3)] + PR_3$ following a dissociative mechanism, illustrating the influence of steric repulsion on the reaction rate. [108]

PR_3	Tolman Cone Angle	k (s^{-1})
$PPhMe_2$	122°	$<10^{-6}$
PPh_2Me	136°	1.3×10^{-5}
PPh_3	145°	3.2×10^{-3}

The influence of the leaving ligand in octahedral substitution reactions can be studied by varying the leaving group (X) in a specific octahedral complex. The aquation of $[Co(NH_3)_5X]^{n+}$ was used to set up a series describing the lability of the leaving group (X) (see Table 2. 6).[109] The most labile species in the list are ClO_4^- and $CF_3SO_3^-$. The ease and rapid loss of trifluorosulphonate ligands is of great value in preparative coordination chemistry, especially when dealing with very inert centres like osmium(II).

Table 2. 6: The dependence of the rate constants for the aquation of $[Co(NH_3)_5X]^{n+}$ upon the nature of the leaving group, X.

X	$10^7 k_{aq}$ (s^{-1})	X	$10^7 k_{aq}$ (s^{-1})	X	$10^7 k_{aq}$ (s^{-1})
ClO_4^-	810 000	Me_2SO	180	$CF_3CO_2^-$	1.7
$CF_3SO_3^-$	270 000	I^-	83	$CH_3CO_2^-$	0.27
$4\text{-}NO_2C_6H_4SO_3^-$	6 300	H_2O	59	NO_2^-	0.12
ReO_4^-	3 120	Br^-	39	HCO_2^-	0.026
$(MeO)_3PO$	2 500	Cl^-	18	N_3^-	0.021
$MeSO_3^-$	2 000	$HCONMe_2$	15	NCS^-	0.0037
$(NH_2)_2CO$	510	SO_4^{2-}	8.9	PO_4^{3-}	0.0033
NO_3^-	240	$CCl_3CO_2^-$	5.8	NH_3	0.000 058

2.4.3.4 The Effect of the Incoming Ligand

The influence of the incoming ligand (Y) in octahedral substitution reactions

$$KX + Y \rightleftharpoons KY + X$$

can be studied by varying X during substitution in a specific octahedral complex. The rate of dissociative substitution reactions is independent of the incoming ligand, since the rate determining step in a dissociative reaction is bond breaking. The nucleophiles Br^-, SCN^-, CN^-, SO_3^{2-}, $S_2O_3^{2-}$, N_3^-, OH^-, NO_2^-, NH_3, thiourea, I^- and Cl^- all attack *trans*-$Rh(en)_2Cl_2^+$ (en = ethane-1,2-diamine) at the same rate, the results pointing towards an I_d or D mechanism.[110]

2.4.3.5 The Effect of the Solvent

The influence of the solvent lies in its ability to solvate the metal complex. The solvation influences the energetics of the activation process of the ground and activated states. It can also act as a nucleophile in the reaction to change the kinetic rate in an associative mechanism law to:

$$\text{rate} = (k_s + k_2[Y])[\text{complex}]$$

where k_s is the rate constant of the solvent pathway, k_2 the second order rate constant in the direct pathway in an associative substitution mechanism, and [Y] the concentration of the incoming ligand (see Scheme 2. 15). A large k_s is observed for solvents which have a good ability to donate electrons to the metal and coordinate strongly to the metal. The general order of solvation power by solvents is:[101]

$$\text{(strongly coordinating) } (CH_3)_2SO > CH_3NO_2,\ H_2O > ROH$$

Solvents like benzene and chloroform which coordinate very poorly to metals, have little or no influence on the reaction rate, since $0 \approx k_s << k_2$.

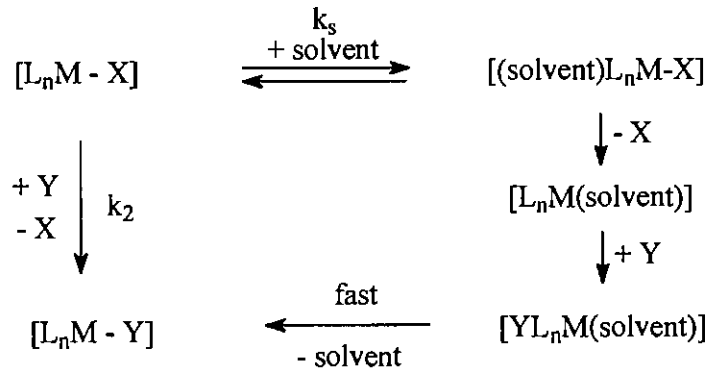

Scheme 2. 15: Schematic representation of the direct and solvent pathways for the associative mechanism of the substitution reaction $[L_nM - X] + Y \rightarrow [L_nM - Y] + X$.

2.4.3.6 The Influence of non-labile Ligands

The nature and position of ligands not participating in the reaction may have large influences on the reaction rate. The most important influence of these non-labile ligands is *cis* and *trans*-labilisation and steric effects.

The behaviour patterns of non-labile ligands can be identified from the study of a series of closely related complexes. An appropriate series of complexes is *cis*- and *trans*-$[Co(en)_2LX]^{n+}$ (en = ethane-1,2-diamine). This reaction is well characterized in terms of the rates of displacement of X (usually Cl^-, Br^- or NO_3^-) by H_2O and how the steric course of the process depend upon the nature and position of ligand L with respect to the leaving group X. Data of a whole range of species in which the two diaminoethanes are replaced by other nitrogen donors make extensive comparisons possible.[100] In the *bis*(1,2-diaminoethane) series, the labilization sequence is $OH^- > Cl^- \approx N_3^- > Br^- > NCS^-$ when it is *cis* to the leaving group, and $OH^- > N_3^- > CO_3^{2-} > Cl^- \approx Br^- > RCO_2^- > NCS^-$ when it is *trans*. In all cases, where both isomers are compared, the *cis* isomer is more labile than the *trans* isomer. This is especially marked in the case of the isothiocyanato complexes, where the factor difference is about 250. However, a satisfactory explanation for this observation has yet to be offered. [100]

2.4.3.6.1 Cis-labilisation of non-labile Ligands

An example of the effect of the *cis*-coordinated ligands on the reaction rate of the substitution of one H_2O ligand from different Cr(III)-complexes with NCS^- as an incoming ligand, is summarized in Table 2. 7. More electron-rich (better electron-rich donor) *cis* ligands increase the electron density on the metal (*i.e.* less positive) leading to faster substitution reactions.

Table 2. 7: Substitution reaction rate of the reactions of various Cr(III)-complexes with thiocyanate ion at 25°C.

Complexes	$k_1 \times 10^{-3}$ ($M^{-1} s^{-1}$)	Reference
$[Cr(H_2O)_6]^{3+}$	0.0018	111
$[Cr(NH_3)_5(H_2O)]^{3+}$	0.046	112
$[Cr(TMPP)(H_2O)_2]^{5+}$	0.74	113
$[Cr(TPPS)(H_2O)_2]^{3-}$	4.7	114

TMPP = *meso*-tetra(4-N-methylpyridyl)porphyrin
TPPS = *meso*-tetrakis(*p*-sulfonatophenyl)porphyrin

2.4.3.6.2 Trans-effect of non-labile Ligands

The nature of the ligand *trans* to the leaving group has a significant influence on substitution reaction rate. The *trans*-effect can be defined as the ability of the ligand *trans* with respect to the leaving group to decrease the activation energy of the reaction and the stabilization of transition state through the delocalization of the electron density. If a ligand has a large effect, it will weaken the metal-ligand bond *trans* to it, which will increase the substitution reaction rate that follows the dissociative mechanism. On the other hand, *trans*-ligands with strong electron withdrawing properties cause the incoming ligands with strong electron donating property to bind easily on the metal ions. This implies that the reactions that follow an associative mechanism will experience an increased reaction rate, which makes it difficult to differentiate between dissociative and associative mechanisms using this method of investigation.

A typical example of a reaction where a *trans* non-labile ligand has a large influence on the substitution reaction rate, is the reaction of $[Co(TPPS)(H_2O)X]^{n-}$ (TPPS = *meso*-tetrakis(*p*-sulfonatophenyl)porphyrin) with pyridine, where X = H_2O, pyridine and OH^- ion *trans* to the aqua ligand. The rate constants for the reaction determined as 9.6×10^2, 3.2×10^3 and 1.2×10^6 M^{-1} s^{-1} for X = H_2O, pyridine and OH^- ion, respectively indicating an increasing *trans* effect of X of H_2O < pyridine < OH^-.[115]

2.4.3.6.3 Steric effect of non-labile Ligands

Increased crowding of non-labile ligands at the reaction site decreases the rates of associative processes. Conversely, dissociative processes may be accelerated, as loose bonding in the transition state allows other groups room to move to relieve the strain.[116]

One of the well-known classic demonstrations of the steric effects in the operation of a dissociative mechanism is the aquation of cobalt(III) complexes involved in a series of substituted ethane-1,2-diamine complexes, *viz* *trans*-$[Co(R_nen)_2Cl_2]^+$.[117] Table 2. 8 contains

a summary of results for the replacement of chloride by water, and it shows that increasing the bulk of $R_n$en ligands leads to a marked increase in aquation rates. The simplest explanation is that of relief of steric strain on the formation of a dissociative transition state. The only defence left in favour of an associative process is to assign the rate variation to some electronic effect that dominates steric effects, since methyl substitution leads to an inductive increase in electron density at the cobalt center, as well as steric congestion.[118] It was shown that the electronic effects were much smaller than the steric effects by establishing very small substituents effects on rate constants for aquation of complexes $[Co(en)_2(X\text{-}py)Cl]^{2+}$ and *trans*-$[Co(X\text{-}py)_4Cl_2]^+$, where the substituents X-py = py, β-CH_3py, γ-CH_3py transmit their electronic effects to nitrogen and hence to the metal without causing major steric crowding.[119]

Table 2. 8: The rate constants for the acid hydrolysis reactions of $[Co(R_n en)_2Cl_2]^+$ with different diamine chains, at 25°C. ($R_n$en = amine complex)[119]

Amine Complexes	Structures	k x 10^{-3} (s^{-1})
Ethylenediamine	NH_2-CH_2-CH_2-NH_2	0.032
Propylenediamine	NH_2-CH_2-$CH(CH_3)$-NH_2	0.062
d,l-Butylenediamine	*d,l*-NH_2-$CH(CH_3)$-$CH(CH_3)$-NH_2	0.15
meso-Butylenediamine	*meso*-NH_2-$CH(CH_3)$-$CH(CH_3)$-NH_2	4.2
Tetramethylethylendiamine	NH_2-$C(CH_3)_2$-$C(CH_3)_2$-NH_2	33

2.4.3.7 Activation Parameters

The reaction rate generally increases with an increase in temperature. The rate constant's dependence on the temperature follows the Arrhenius equation:

$$k = A\, e^{\frac{-E_a}{RT}}$$

where E_a is the activation energy and provide useful information for the reaction mechanism. The magnitude and sign of the activation parameters, ΔH* (activation enthalpy), ΔS* (activation entropy), ΔG* (free energy of activation) and ΔV* (activation volume), obtained also gives information about the reaction mechanism. The theory of absolute reaction rates

postulates that an activated complex is in equilibrium with the reactants before the reaction takes place; and that the reaction rate is given by the rate of decomposition of the complex to form the reaction products (scheme 2.9).

$$A + B \overset{K_c^*}{\rightleftharpoons} [A{\cdot}B]^* \xrightarrow{k} \text{products}$$

Scheme 2.9: General scheme illustrating the transition state theory.

The rate constant, *k*, for a reaction is given by the expression:

$$k = \frac{RT}{Nh} K_c^*$$

where K_c^* is an equilibrium constant, R is the universal gas constant, h is Planck's constant, N is Avogradro's number and T is the absolute temperature. The free energy of activation, ΔG^*, is defined thermodynamically as

$$\Delta G^* = -RT \ln K_c^* = \Delta H^* - T\Delta S^*$$

where ΔH^* is the enthalpy of activation and ΔS^* is the activation entropy. The combination of the above equations results in

$$\ln\left(\frac{k}{T}\right) = \ln\left(\frac{RT}{Nh}\right) + \frac{\Delta S^*}{R} - \frac{\Delta H^*}{RT}$$

The rate constant k, and at different temperatures T can be used to determine ΔH^* and ΔS^*. The magnitude of ΔS^* gives information on the mechanism of substitution, i.e. associative or dissociative. A small negative or positive ΔS^* value generally indicates a dissociative mechanism, while a large negative ΔS^* value indicates an associative mechanism. Negative or near-zero ΔH^* values are rare and usually indicate a multistep process. If ΔS^* is not sensitive to the nature of the solvent for a specific reaction, it indicates solvation effects that do not play an important role in the reaction.[120]

The activation volume consists of two components; an intrinsic ΔV^{*}_{intr}, and a solvation ΔV^{*}_{solv} component. During the formation of a transition state, ΔV^{*}_{intr} reflects changes in volume due to variations in bond lengths and angles, while ΔV^{*}_{solv} reflects changes in solvation. For an associative mechanism, ΔV^{*} is large negative, due to the negative contribution from ΔV^{*}_{intr} (arises from the formation of the bond) and only minor contribution from ΔV^{*}_{solv}. For a dissociative mechanism ΔV^{*} is positive since ΔV^{*}_{intr} is positive due to bond cleavage, and ΔV^{*}_{solv} is negative due to an increase in electrostriction associated with the development of two ions in the transition state.[121] The activation volume is the most reliable activation parameter in determining the reaction mechanism.

An example of how ΔV^{*} gives information on the mechanism of a reaction follows from the aquation activation volumes for several pairs of pentaammine complexes. A clear distinction between negative values for chromium(III) and positive values for cobalt(III) was found (see Table 2. 9). These results were selected to involve only uncharged leaving groups and to minimize electrostriction complications. The results can be interpreted in terms of I_a and I_d mechanism for chromium(III) and cobalt(III) systems, respectively.[122]

Table 2. 9: Activation volumes for aquation reactions of chromium(III)- and cobalt(III)-pentaammine complexes: $[M(NH_3)_5L]^{3+} + H_2O \rightarrow [M(NH_3)_5(H_2O)]^{3+} + L$, involving uncharged leaving groups, L.

Leaving Group (L)	Activation Volumes, ΔV^{*} ($cm^3\ mol^{-1}$)	
	$M = Cr^{III}$	$M = Co^{III}$
OH_2	-5.8	+1.2
$OCHNH_2$	-4.8	+1.1
$OCHNMe_2$	-7.4	+2.6
$OC(NH_2)_2$	-8.2	+1.3
$OC(NMe_2)_2$	-3.8	+1.5
$OSMe_2$	-3.2	+2.0
$OP(OMe)_3$	-8.7	-

2.4.4 Examples of Substitution Reactions of Titanium Complexes.

Substitution reactions of titanium(IV)-halide and similar complexes were investigated by Burgess *et al.*[123] All the reactions investigated show two kinetically distinct steps:

$$Ti(LL)_2X_2 \xrightarrow[\text{fast}]{Y^-} Ti(LL)_2XY + X^- \xrightarrow[\text{slow}]{Y^-} Ti(LL)_2Y_2$$

LL = a variety of bidentate ligands such as HLL = 4-pyrone ethyl-maltol (Hetmalt), several 4-pyridinones, and related ligands; X = Cl^-, F^-, OMe^-, OEt^-, O^iPr^-, OPh^- and maltol; Y = Br^-, I^-, NCS^-, CN^-, water, 4,4'-bipyridyl, 2,2'-bipyridyl, pyrazine and ethyl-maltol.

By reducing the concentrations of the incoming group, it was possible to detect the relatively rapid first stage for some reactions. The rate constant for the first step of the reactions reported, is always at least 10 times faster than the second step. There is thus negligible coupling between two stages, and rate constants are determined independently. In all kinetic runs the nucleophile present was in large excess, so first-order kinetics was observed. The reactivities in terms of the incoming ligand, and the leaving and the non-leaving ligands were reported. In all cases the rate law for both the first and second stage of substitution is a two-term expression:

$$\frac{d[\text{complex}]}{dt} = \{k_1 + k_2[Y]\}[\text{complex}]$$

where k_1 is the rate constant of the solvent pathway, and k_2 the second order rate constant for the substitution reaction.

2.4.4.1 Results for different incoming Ligands

The effect of the incoming nucleophile on the two stages of the substitution reaction at $Ti(etmalt)_2Cl_2$ is illustrated in Figure 2. 13.

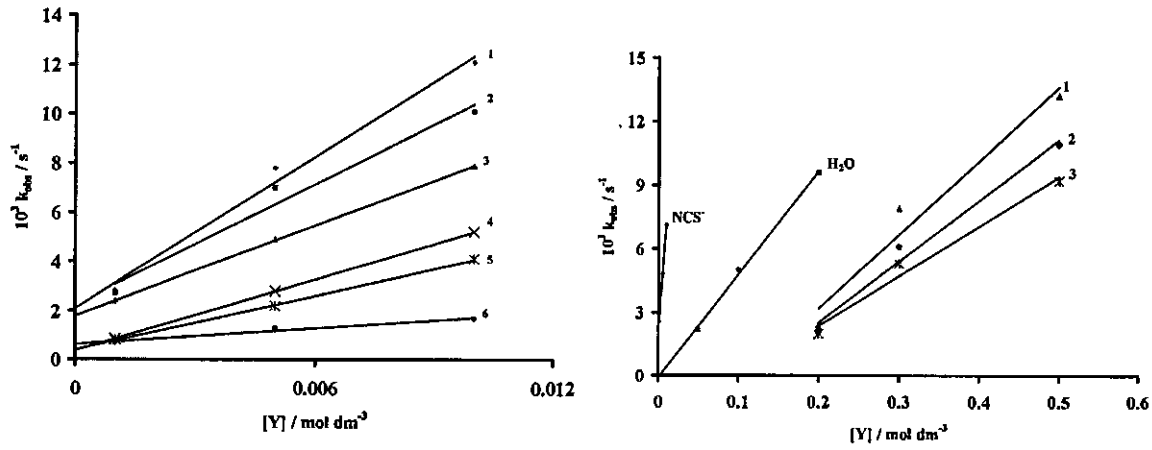

Figure 2. 13: Observed first-order rate constants for the first stage (left) and second stage (right) in nucleophilic attack at $Ti(etmalt)_2Cl_2$ in acetonitrile solution at 298.2 K, with 1 = MeOH, 2 = EtOH, 3 = ^{i}PrOH, 4 = Pyrazine, 5 = 2,2'-bipyridyl and 6 = malonic acid.

The intercepts (k_1) of the observed rate constant, k_{obs} ($k_{obs} = k_2[Y]$) *vs.* concentration of incoming nucleophile for the first stage (Figure 2. 13, left) is almost independant of the nature of the nucleophile, and is as expected for the common rate-limiting dissociation of the first chloride ligand. The intercepts for pyrazine, 2,2'-bipyridyl and malonic acid are in fact identical, while for isopropanol, ethanol and methanol they are successively slightly larger. There are small effects at low alcohol concentrations, but significant rate increases are attributed to favourable interaction with the leaving chloride ligand. It may be recalled that the rate constant for t-butyl chloride solvolysis in alcohol-water mixtures is very sensitive to solvation of the chloride, *e.g.* in ethanol containing 5% water, solvolysis is nearly six times faster than in pure ethanol.[124] The relative values obtained for k_2 for the first and second stages are as expected for the range of nucleophiles studied.

2.4.4.2 Results for different leaving Groups

The relative reactivities of different leaving ligands in nucleophilic attack at $Ti(etmalt)_2X_2$ are illustrated in Figure 2. 14. There is a small range of rate constants for the dissociative (k_1) pathway associated with the loss of the second halide or alkoxide (X^-) from $Ti(etmalt)_2(NCS)X$. Rate constants (k_2) for the dominant bimolecular pathway cover a range of over 20-fold for the complexes studied. The fluoride complex react more slowly (k_1 and k_2) than the chloride, consistent with stronger Ti-F bonding.

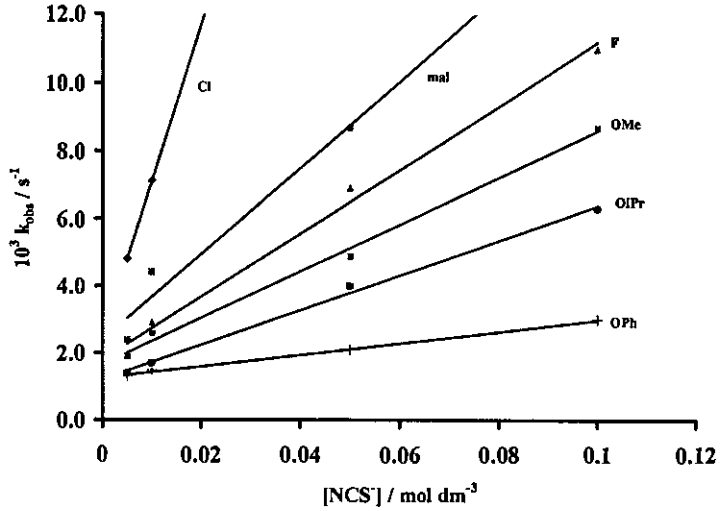

Figure 2. 14: Effect of leaving group variation. Observed first-order rate constants for the second stage in nucleophilic attack at $Ti(etmalt)_2X_2$ in acetonitrile at 298.2 K.

2.4.4.3 Results for different non-leaving Groups

The effect of changing non-leaving chelating ligands in $Ti(LL)_2Cl_2$ complexes on substitution reactivity is illustrated in Figure 2. 15. There is a relatively restricted range of rate constants, k_2, and a very restricted range of dissociation rate constants, k_1. For both dissociative and associative substitution, the pyrone complexes react fast, while the pyridinone complexes react slowly – with cyclopentadienyl, hydroxamate and tropolonate complexes reacting at intermediate rates. The very small effects on bimolecular thiocyanate attack are due to electron withdrawal or release by the chelating ligand assisting or discouraging entry of the incoming thiocyanate nucleophile. The most stable complexes are formed by ligands with the smallest k_2 values as shown in Figure 2. 15. The net electron density at titanium increases when a high degree of σ-electron donation is associated with strong ligand-metal bonding, *i.e.* effective positive charge increases on the central metal and discourages nucleophilic attack. The differences in k_2 values between the pyrone and pyridinone complexes correspond to about 75 and 90 kJ mol^{-1} in activation barrier differences of 15 kJ mol^{-1}.

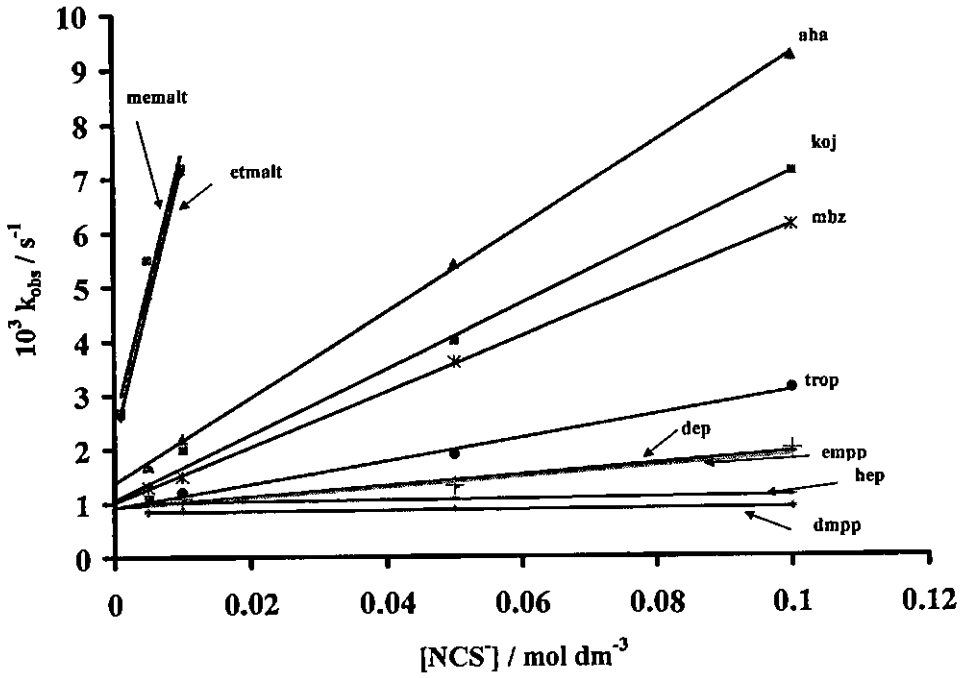

Figure 2. 15: Effect of non-leaving group variation. Observed first-order rate constants for the second stage in nucleophilic attack at $Ti(LL)_2Cl_2$ in acetonitrile at 298.2 K.

2.4.4.4 Bidentate Ligands as incoming Nucleophile.

The second step in the substitution reaction of $Ti(Cp)_2Cl_2$ with the bidentate ligand 4-pyrone ethyl-maltol (Hetmalt) or with 2,2'-bipyridyl, and of the substitution reaction of $Ti(etmalt)_2Cl_2$ with the bidentate ligand malonate (H_2mal) were proved to be ring closure of the bidentate ligand and not due to a second potentially bidentate ligand coordinated in a monodentate manner.[123] In Chapter 3 of this thesis, the substitution of the two Cl^- ligands from Ti(β-diketonato)$_2Cl_2$ with the bidentate ligand 2,2'-biphenyldiol will be reported.

2.5 References

[1] Mehrotra, R. C., Bohra, R. and Gaur, D. P., *Metal β-diketonates and Allied Derivatives*, Academic Press, New York, 1978.

[2] Pedersen, C. J., Salem, N. J. and Weinmayr, V., *US Pat.*, 2 875 223 (1959); Weinmayr, V., *Naturwissenschaften*, **45**, 311 (1958).

[3] Leipoldt, J. G., Basson, S. S., van Zyl, G. J, and Steyn, G. J. J., *J. Organomet. Chem.*, **418**, 241 (1991); Leipoldt, J. G. and Grobler, E. C., *Transition Met. Chem. (Weinheim, Ger.)*, **11**, 110 (1986); Leipoldt, J. G., Lamprecht, G. J and Steynberg, E. C, *J. Organomet. Chem.*, **402**, 259 (1991).

[4] Roodt, A., J. G. Leipoldt, J. G., Swarts, J. C. and Steyn, G. J. J., *Acta Cryst.*, **C48**, 547 (1992); Swarts, J. C., Vosloo, T. G., J. G. Leipoldt, J. G. and Lamprecht, G. J., *Acta Cryst.*, **C49**, 760 (1993); Lamprecht, G. J., Swarts, J. C., Conradie, J. and Leipoldt, J. G., *Acta Cryst.*, **C49**, 82 (1993); Haaland, A. and Nilsson, J., *Chem. Commun.*, 88 (1968); Yogev, A. and Mazur, Y., *J. Org. Chem.*, **32**, 2162 (1967).

[5] Cullen, W. R., Rettig, S. J. and Wickenheiser, E. B., *J. Mol. Catal.*, **66**, 251 (1991); Cullen, W. R. and Wickenheiser, E. B., *J. Organomet. Chem.*, 1989, **370**, 141

[6] du Plessis, W. C., Vosloo, T. G. and Swarts, J. C., *J. Chem. Soc., Dalton Trans.*, 2507 (1998).

[7] Kealy, T. J. and Pauson, P. L., *Nature*, **138**, 1039 (1951).

[8] Gero, A., *J. Org. Chem.*, 19, 469 (1954); Gero, A., *J. Org. Chem.*, **20**, 1960 (1955); Bell, R. P. and Davis, G. G., *J. Chem. Soc.*, 353 (1965).

[9] Campbell, R. D. and Gilow, H. M., *J. Am. Chem. Soc.*, **84**, 1440 (1962); Murthy, A. S. N., Balasubramanian, A., Rao, C. N. R. and Kasturi, T. R., *Can. J. Chem.*, **40**, 2267 (1962); Lowe, J. U. and Ferguson, L. N., *J. Org. Chem.*, **30**, 3000 (1965).

[10] Yogev, A. and Mazur, Y., *J. Org. Chem.*, **32**, 2162 (1967); Mills, S. G. and Beak, P., *J. Org. Chem.*, **50**, 1216 (1985).

[11] Moriyasu, M., Kato, A. and Hashimoto, Y., *J. Chem. Soc., Perkin Trans.* 2, 515 (1986).

[12] Burdett, J. L. and Rogers, M. T., *J. Am. Chem. Soc.*, **86**, 2105 (1964); Lowe, J. U. and Ferguson, L. N., *J. Org. Chem.*, **30**, 3000 (1965); Yogev, A. and Mazur, Y., *J. Org. Chem.*, **32**, 2162 (1967); Mills, S. G. and Beak, P., *J. Org. Chem.*, **50**, 1216 (1985); Sarella, D. J., Heinert, D. H. and Shapiro, B. L., *J. Org. Chem.*, **34**, 2817 (1969); Spencer, J. N., Holmboe, E. S., Kirshenbaum, M. R., Firth, D. W. and Pinto, P. B., *Can. J. Chem.*, **60**, 1178 (1982); Battesti, P., Battesti, O. and Selim, M., *Bull. Soc. Chim. Fr.*, 2214 (1974); Klose, G., Thomas, P., Uhlemann, E. and Marki, J., *Tetrahedron*, **22**, 2695 (1966).

[13] Geraldes, C. F. G. C., Barros, M. T., Maycock, C. D. and Silva, M. I., *J. Mol. Struct.*, **238**, 335 (1990).

[14] Moon, S. and Kwon, Y., *Magn. Reson. Chem.*, **39**, 89 (2001).

[15] Kawaguchi, S., *Coord. Chem. Rev.*, **70**, 51 (1986); Kawaguchi, S., in *Variety in Coordination of Ligands in Metal Complexes: Inorganic Concepts*, Kawaguchi, S., Eds., Springer Verlag, Berlin, **vol. 11**, pp. 79 – 119, 1988.

[16] Moriyasu, M., Kato, A. and Hashimoto, Y., *J. Chem. Soc., Perkin Trans.* 2, 515 (1986)

[17] du Plessis, W. C., Dawis, W. L., Cronje, S. J. and Swarts, J. C., *Inorg. Chim. Acta.*, **314**, 97 (2001).

[18] Yogev, A. and Mazur, Y., *J. Org. Chem.* **32**, 2162 (1967).

[19] Park, J. D., Brown, H. A. and Lachen, J. R., *J. Am. Chem. Soc.*, **75**, 4753 (1953).

[20] Ferguson, G., Glidewell, C. and Zakaria, C. M., *Acta Cryst.*, **C50**, 1673 (1994).

[21] Mullica, D.F., Karban, J.W. and Grossie, D.A., *Acta Cryst.*, **C43**, 601 (1987).

[22] Covey, W. D. and Leussing, D. L., *J. Am. Chem. Soc.*, **96**, 3860 (1974); Raghaven, N. V. and Leussing, D. L., *J. Am. Chem. Soc.*, **96**, 7147 (1974).

[23] Hauser, C. R., Swamer, F. W. and Adams, J. T., *Organic Reactions*, John Wiley & Sons, New York, **vol. 8**, pp. 59 – 196, 1958.

[24] Levine, R., Conroy, J. A., Adams, J. T. and House, C. R., *J. Am. Chem. Soc.*, **67**, 1510 (1945); Martin, D. F., Shamma, M. and Ferrielius, W. E., *J. Am. Chem. Soc.*, **80**, 4891 (1958); Martin, D. F., Shamma, M. and Ferrielius, W. E., *J. Am. Chem. Soc.*, **80**, 5851 (1958); Bloomfield, J. J., *J. Org. Chem.*, **27**, 2742 (1962); Vogel, A. I., *Practical Organic Chemistry*, 5th Ed., Longman Scientific & Technical, London, pp. 632, 1989.

[25] Hauser, C. R., Swamer, F. W. and Adams, J. T. in *Organic Reactions*, Adams, R., Blatt, A. H., Cope, A. C., Curtin, D. Y., McGrew, F. C. and Niemann, C., Eds., John Wiley & Sons, Inc., New York, **vol. 8**, pp. 62-63, 1954.

[26] du Plessis, W. C., *Synthesis, thermodynamics, electrochemical and kinetical aspects of ferrocene-containing β-diketones (M.Sc Thesis)*, University of the Orange Free State, 1996.

[27] Cravero, R. M., Gonzalez-Sierra, M. and Oliveri, A. C., *J. Chem. Soc., Perkin Trans*, 1067 (1993).

[28] Pettinari, C., Marchetti, F. and Drozdov, A., in *Comprehensive Coordination Chemistry II*, McCleverty, J. A. and Meyer, T. J., Eds., Elsevier Pergamon, United Kingdom, **vol. 1**, pp. 99, 2004.

[29] Pellicciari, R., Fringuelli, R. and Sisam, E., *J. Chem. Soc., Perkin I*, 2566 (1981).
[30] Pinnavalia, T. J. and Fay, R. C., *Inorg. Chem.*, 7, 502 (1968).
[31] Drew, M. G. B., Fowles, G. W. A. and Lewis, D. F., *Chem. Commun.*, 876 (1969); Guilard, R. and Lecomte, C., *Coord. Chem. Rev.*, **65**, 87 (1985); Bradley, D. C., Colapietro, M., Hursthouse, M. B., Rendall, I. F. and Vaciago, A., *Chem. Commun.*, 743 (1970); Schmidte, H. H. and Voets, U., *Inorg. Chem.*, **20**, 2766 (1981); Manek, E., Hinz, D. and Meyer, G., *Coord. Chem. Rev.*, **164**, 5 (1997); Vites, J. C. and Lynam, M. M., *Coord. Chem. Rev.*, **146**, 1 (1995); Vites, J. C. and Lynam, M. M., *ibid.*, **138**, 71 (1995).
[32] Bradley, D. C. and Copperthwaite, R. G., *Chem. Commun.*, 764 (1971); Crouch, P. C., Fowles, G. W. A. and Walton, R. A., *J. Chem. Soc. (A)*, 2172 (1968); Carr, S. G. and Smith, T. D., *J. Chem. Soc., Dalton Trans.*, 1887 (1972); Tornqvist, E. G. M. and Libby, W. F., *Inorg. Chem.*, **18**, 1792 (1970).
[33] Fowles, G. W. A. and Lester, T. E., *Chem. Commun.*, 47 (1967); Lappert, M. F. and Sanger, A. R., *J. Chem. Soc. (A)*, 874 (1971); Manek, E., Hinz, D. and Meyer, G., *Coord. Chem. Rev.*, **164**, 5 (1997); Vites, J. C. and Lynam, M. M., *Coord. Chem. Rev.*, **146**, 1 (1995); Vites, J. C. and Lynam, M. M., *ibid.*, **138**, 71 (1995); Quntar, A. A., Dembitsky, V. M. and Srebnik, M., *Org. Lett.*, **5**, 357 (2003).
[34] Vites, J. C. and Lynam, M. M., *Coord. Chem. Rev.*, **138**, 71 (1995); Haggerty, B. S., *J. Am. Chem. Soc.*, **114**, 10677 (1992); Flamini, A., and Giuliani, A. M., *Inorg. Chim. Acta.*, **112**, L7 (1986).
[35] König, E. and Herzog, S., *J. Inorg. Nucl. Chem.*, **32**, 613 (1970); Rosier, C., Niccolai, G. P. and Basset, J-M., *J. Am. Chem. Soc.*, **119**, 12408 (1997).
[36] Ellis, J. E. and Chi, K. M., *J. Am. Chem. Soc.*, **110**, 163 (1988).
[37] McAuliffe, C. A. and Barratt, D. S. in *Comprehensive Coordination Chemistry*, Wilkinson, G., Gillard, R. D. and McCleverty, J. A., Eds., Pergamon, Oxford, **vol.** 3, pp. 323-360, 1987.
[38] Wailes, P. C., Coutts, R. S. P. and Weigold, H., *Organometallic Chemistry of Ti, Zr and Hf*, Academic Press, New York, pp 62-75, 1974
[39] Dubler, E., Buschmann, R. and Schmalle, H. W., *J Inorg. Biochem.*, **95**, 97 (2003).
[40] Doyle, G. and Tobias, R. S., *Inorg. Chem.*, **6**, 1111 (1967).
[41] White, D. A., *J. Inorg. Nucl. Chem.*, **33**, 691 (1971).
[42] Moksdi, G. and Harding, M. M., *J. Organomet. Chem.*, **565**, 30 (1998).
[43] Burdett, J. L. and Rogers, M. T., *J. Am. Chem. Soc.*, **86**, 2105 (1964); Leipoldt, J. G. and Grobler, E. C., *Trans. Met. Chem.*., **11**, 110 (1986).
[44] Frazer, M. J. and Newton, W. E., *Inorg. Chem.*, **10**, 2142 (1971).
[45] Keller, H. J., Keppler, B. K. and Schähl, D., *A. Forsch.*, **32(8)**, 806 (1982).
[46] Blandamer, M. J. and Burgers, J., *Coord. Chem. Rev.*, **31**, 93 (1980).
[47] Keppler, B. K. and Heim, M. E., *Drugs of the Future*, **3**, 638 (1988).
[48] Nelles, J., *Chem. Abstr.*, **34**, 3764 (1940).
[49] Cunningham, G. L. and Robinson, R. S., *Chem. Abstr.*, **42**, 5045 (1948).
[50] Boyd, T., *Chem. Abstr.*, **46**, 6139 (1952).
[51] Malatesta, L., *Gazz. Chim. Ital.*, **78**, 753 (1948).
[52] Coates, G. E. and Ridley, D., *J. Chem. Soc.*, 1870 (1965).
[53] Latesky, S., McMullen, A. K., Rothwell, I. P. & Huffman, J. C., *Organometallics*, **4**, 902 (1985).
[54] Verma, I. D. and Mehrotra, R. C., *J. Chem. Soc.*, 2966 (1960).
[55] Mehrotra, R. C., *J. Indian Chem. Soc.*, **31**, 904 (1954).
[56] Bradley, D. C., Chakravarti, B. N., Chatterjee, A. K., Wardlaw, W. and Whitely, A., *J. Chem. Soc.*, 99 (1958).
[57] Mehrotra, R. C., *J. Indian Chem. Soc.*, **30**, 585 (1953).
[58] Mehrotra, R. C., *J. Am. Chem. Soc.*, **76**, 2266 (1954).
[59] Andrä, K., *J. Organomet. Chem.*, **11**, 567 (1968).
[60] Bharara, P. C., *J. Organomet. Chem.*, **121**, 199 (1976).
[61] Kobayashi, N., Muranaka, A. and Ishii, K., *Inorg. Chem.*, **39**, 2256 (2000).
[62] Keppler, B. K., Friesen, C., Moritz, H. G., Vongerichten, H. and Vogel, E., *Struct. Bonding.*, **78**, 97 (1991).
[63] Carusu, F., Massa, L., Gindulyte, A., Pettinari, C., Machetti, F., Pettinari, R., Ricciutelli, M., Costamagna, J., Canales, J. C., Tanski, J. and Rossi, M., *Eur. J. Inorg. Chem.*, 3221 (2003).
[64] Pettinari, C., Marchetti, F. and Drozdov, A., in *Comprehensive Coordination Chemistry*, McCleverty, J. A. and Meyer, T. J., Eds., Elsevier Pergamon, United Kingdom, **vol.** 1, pp. 105, 2004.
[65] Yamamoto, A. and Kambara, S., *J. Am. Chem. Soc.*, **79**, 4345 (1957).
[66] Fay, R. C. and Lindmark, A. F., *J. Am. Chem. Soc.*, **105**; 2118 (1983).
[67] Fay, R. C. and Lowry, R. N., *Inorg. Chem.*, **13**, 1310 (1974).
[68] Rao, P. V., Rao, C. P., Wegelius, E. K., Kolehmainen, E. and Rissanen, K., *J. Chem. Soc., Dalton Trans.*, 4469 (1999).
[69] Glidewell, C., Turner, G. M. and Ferguson, G., *Acta Cryst.* , **C52**, 11, (1996)
[70] Ferguson, G and Glidewell, C., *Acta Cryst.*, **C57**, 246 (2001).
[71] Schubert, U., Buhler, H. and Hirle, B., *Chem. Ber.*, **125**, 999 (1992).
[72] Wang, J. L., Miao, F. M., Fan, X. J., Feng, X. and Wang, J. T., *Acta Cryst.*, **C46**, 1633 (1990).
[73] Bradley, D. C. and Holloway, C. E., *Chem. Commun.*, 284 (1965).

[74] Serpone, N. and Fay, R. C., *Inorg. Chem.* **10**, 1835 (1967).
[75] Keppler, B. K., Friesen, C., Moritz, H. G., Vongerichten, H. and Vogel, E., *Struct. Bonding.*, **78**, 97 (1991).
[76] Bobbit, J. M. and Wills, J. P., *J. Org. Chem.*, **45**, 1978 (1980).
[77] Nelsen, S. F., Kessel, C. R., Brien, D. J. and Neinhold, F., *J. Org. Chem.*, **45**, 2116 (1980).
[78] Powers, M. J. and Meyer, T. J., *J. Am. Chem. Soc.*, **102**, 1289 (1980).
[79] Heinze, J., *Angew.Chem., Int. Ed. Engl.*, **23**, 831 (1984).
[80] Randles, J. E. B., *Trans. Faraday Soc.*, **44**, 327 1948).
[81] Sevcik, A., *Collection Czechoslov. Chem. Commun.*, **13**, 349 (1948).
[82] Delahay, P., *J. Am. Chem. Soc.*, **75**, 1190 (1953).
[83] Moock, K. H., Macgregor, S. A., Heath, G. A., Derrick, S. and Boere, R. T., *J. Chem. Soc., Dalton Trans.*, 2067 (1996).
[84] Mabbott, G. A., *J. Chem. Ed.*, **60**, 697 (1983).
[85] Erasmus, E., *Synthesis, substitution kinetics and electrochemistry of betadiketonato titanium and titanocene complexes with biomedical applications (M.Sc Thesis)*, University of the Free State, 2003.
[86] Bard, A. J. and Faulkner, L. R., *Fundamental Methods: Fundamentals and Applications*, John Wiley & Sons, New York, chapter 6, 1980.
[87] Nicholson, R. S. and Shain, I., *Anal. Chem.*, **36**, 706 (1964).
[88] van Benschoten, J. J., Lewis, J. Y., Heineman, W. R., Roston, D. A. and Kissinger, P. J., *J. Chem. Edu.*, **60**, 772 (1982).
[89] Kissinger, P. J. and Heineman, W. R., *Laboratory Techniques in Electroanalytical Chemistry*, Dekker, New York, chapter 13, 1984.
[90] Le Seur, R. J. and Geiger, W. E., *Angew. Chem., Int. Ed. Engl.*, **39**, 248 (2000).
[91] Ohrenberg, C. and Geiger, W. E., *Inorg. Chem.*, **29**, 2948 (2000).
[92] Koepp, H. M., Wendt, H. and Stehlow, H., *Electrochem.*, **64**, 483 (1960).
[93] Gagné, R. R., Koval, C. A. and Lisenky, G. C., *Inorg. Chem.*, **19**, 2855 (1980).
[94] Gritzner, G. and Kuta, J., *Pure and Appl. Chem.*, **56**, 461 (1984).
[95] Vallat, A., Roullier, L. and Bourdon, C., *J. Electroanal. Chem.*, **542**, 76 (2003).
[96] Vorotyntsev, M. A., Casalta, M., Pousson, E., Roullier, L., Boni, G. and Moise, C., *Electrochim. Acta*, **46**, 4020 (2001).
[97] Bond, A. M.,. Colton, R., Englert, U., Hűgel, H. and Merken, F., *Inorg. Chim. Acta*, **235**, 117 (1995).
[98] Ghosh, P., Ghosh, S., Navara,C., Narla, R. K., Benyumov, A. and Uckun, F. M., *J. Inorg. Biochem.*, **84**, 241 (2001).
[99] Purcell, K. F. and Kotz, J. C., *Inorganic Chemistry*, Holt-Saunders International Edition, Japan, pp. 359, 1977.
[100] Tobe, M. L. and Burgess, J., *Inorganic Reaction Mechanisms*, Addison Wesley Longman Inc., New York, pp. 18 – 20, 22, 128, 140-147, 163-165, 543, 1999.
[101] Wilkins, R. G., *The Study of Kinetics and Mechanism of Reaction of Transition Metal Complexes*, Allyn and Bacon, Inc., Boston, pp. 194, 200, 302, 1974.
[102] Roodt, A., Leipoldt, J. G., Basson, S. S. and Potgieter, I. M., *Transition Met. Chem.*, **13**, 336 (1988).
[103] Purcell, W., Roodt, A., Basson, S. S. and Leipoldt, J. G., *Transition Met. Chem.*, **14**, 224 (1989).
[104] Purcell, K. F. and Kotz, J. C., *Inorganic Chemistry*, Holt-Saunders International Edition, Japan, pp. 717, 1977.
[105] Wilkins, R. G., *The Study of Kinetics and Mechanisms of Transition Metal Complexes*, Allyn and Bacon, Inc., Boston, pp. 194, 200, 302, 1974.
[106] Lawrence, G. A., *Adv. Inorg. Chem.*, **34**, 145 (1989).
[107] O. Edwards, F. Monacellr and G. Ortaggi, *Inorg. Chimica Acta*, **11**, 47 (1974).
[108] D. J. Darensbourg and A. H. Graves; *Inorg. Chem.*, **18**, 1257 (1979).
[109] House, D. A., *Coord. Chem. Rev.*, **23**, 223 (1977); Edwards, J. O., Monacelli, F. and Ortaggi, G., *Inorg. Chim. Acta*, **11**, 47 (1974); Tobe, M. L., in *Comprehensive Coordination Chemistry*, Wilkinson, G., Gillard, R. D. and McCleverty, J. A., Pergamon Press, Oxford, **vol. 1**, pp. 281, 1987; Swaddle, T. W., *Adv. Bioinorg. Chem.*, **2**, 95 (1983); Swaddle, T. W., *Comments Inorg. Chem.*, **12**, 237 (1991); Lay, P. A., *Coord. Chem. Rev.*, **110**, 213 (1991); Uzice, J. L. and Lopez de la Vega, R., *Inorg. Chem.*, **29**, 382 (1990).
[110] S. A. Johnson, F. Basolo, R. G. Pearson; *J. Am. Chem. Soc.* **85**, 1741 (1963).
[111] Connick, R. E. and Switt, T. J., *J. Chem. Phys.*, **37**, 307 (1962).
[112] Ramasani, T. and Sykes, A. G., *J. Chem. Soc., Chem. Commun.*, 378 (1976).
[113] Leipoldt, J. G., Basson, S. S. and Rabie, D. R., *J. Inorg. Nucl. Chem.*, **43**, 3239 (1981).
[114] Ashley, K. R., Leipoldt, J. G. and Joshi, V. K., *Inorg. Chem.*, **19**, 1608 (1980).
[115] Ashley, K. R. and Leipoldt, J. G., *Inorg. Chem.*, **20**, 2326 (1981).
[116] Langford, C. H. and Gray, H. B., *Ligand Substitution Process*, W. A. Benjamin, Inc., New York, pp. 59, 1965.
[117] Pearson, R. G., Boston, C. R. and Basolo, F., *J. Am. Chem. Soc.*, **75**, 3089 (1953).
[118] Rodgers, G. E., *Introduction to Coordination, Solid state and Descriptive Inorganic Chemistry*, McGraw-Hill, New York, pp. 101 – 102, 1994.

[119] Basolo, F., Bergmann, J. G., Meeker, R. E. and Pearson, R. G., *J. Am. Chem. Soc.*, **78**, 2676 (1956).
[120] van Eldick, R., *Inorganic High Pressure Chemistry, Kinetics and Mechanism*, Elsevier Science Publishers B.V., Amsterdam, 1986.
[121] Whalley, E., *J. Chem. Phys.*, **38**, 1400 (1963).
[122] Tobe, M. L. and Burgess, J., *Inorganic Reaction Mechanisms*, Addison Wesley Longman Inc., New York, 1999, p. 165; van Eldick, R., in *High Pressure Chemistry and Biochemistry*, van Eldick, R. and Jonas, J., Eds., Reidel, Dordrecht, 1987, p. 344.
[123] Burgess, J. and Parsons, S. A., *Applied Organomet. Chem.*, **7**, 345 (1993).
[124] Wells, P. R., *Chem. Rev.*, **63**, 171 (1963).

3 Results and Discussion

3.1 Introduction

The synthesis and characterization of two phenyl containing β-diketones of the type $PhCOCH_2COR$, where R = C_4H_3S and $C_6H_4NO_2$, and Ph = C_6H_5, and a selection of new and known octahedral β-diketonato titanium(IV) complexes of the type Ti(β-diketonato)$_2Cl_2$ and Ti(β-diketonato)$_2$(biphen), where β-diketonato = acac (acetylacetonato, $CH_3COCHCOCH_3^-$), ba (benzoylacetonato, $C_6H_5COCHCOCH_3^-$), dbm (dibenzoylmethanato, $C_6H_5COCHCOC_6H_5^-$), tfba (trifluorobenozylacetonato, $C_6H_5COCHCOCF_3^-$), thba (theonylbenzoylacetonato, $C_6H_5COCHCOC_4H_3S^-$) and biphen = 2,2'-biphenyldiolato, are described in this chapter.

Spectroscopic characterization of the complexes includes techniques such as infra-red (IR) and ultra violet (UV/VIS) spectroscopy, elemental analysis (new complexes), proton nuclear magnetic resonance (^{1}H NMR) spectroscopy and the determination of the pK_a values for the β-diketones synthesized. The titanium complexes synthesized were electrochemically analysed by means of a cyclic voltammetry study.

Kinetic results include the conversion of β-diketone from the enol to the keto-isomer, hydrolysis of Ti(β-diketonato)$_2Cl_2$ complexes and substitution kinetics of chloride ligands from Ti(β-diketonato)$_2Cl_2$ with biphen.

The influences of group electronegativity (χ_R) of R groups on the β-diketonato ligand in titanium complexes are correlated to the results obtained.

3.2 Synthesis and Identification of Compounds.

Two phenyl-containing β-diketones, five octahedral bis-β-diketonato titanium(IV) complexes of the type Ti(β-diketonato)$_2$Cl$_2$, and five Ti(β-diketonato)$_2$(biphen) complexes were synthesized.

3.2.1 Synthesis of β-diketones

Two phenyl-containing β-diketones, PhCOCH$_2$COR, where R = C_4H_3S (**1**) and $C_6H_4NO_2$ (**2**), and Ph = C_6H_5, were prepared by Claisen condensation of acetophenone and the appropriate ester, under the influence of the hindered base, lithium diisopropylamide (LDA), according to Scheme 3. 1. Acetophenone and LDA were stirred under an inert atmosphere at 0°C for 30 minutes to abstract the methine proton of acetophenone. The ester (ethyl 2-thiophene carboxylate or methyl 4-nitro benzoate) was added and the reaction mixture was stirred at RT (room temperature) for 16 hours to yield the β-diketone, Hthba (1-phenyl-3-thenoyl-1,3-propanedione) in 13% yield and Hbnp (*para*-NO_2-dibenzoylmethane or 1-phenyl-4-nitrophenyl-1,3-propanedione) respectively. Hbnp was cleaned by partial recrystalization from acetone and water; the first fraction was impure while the second fraction yielded 15% pure Hbnp.

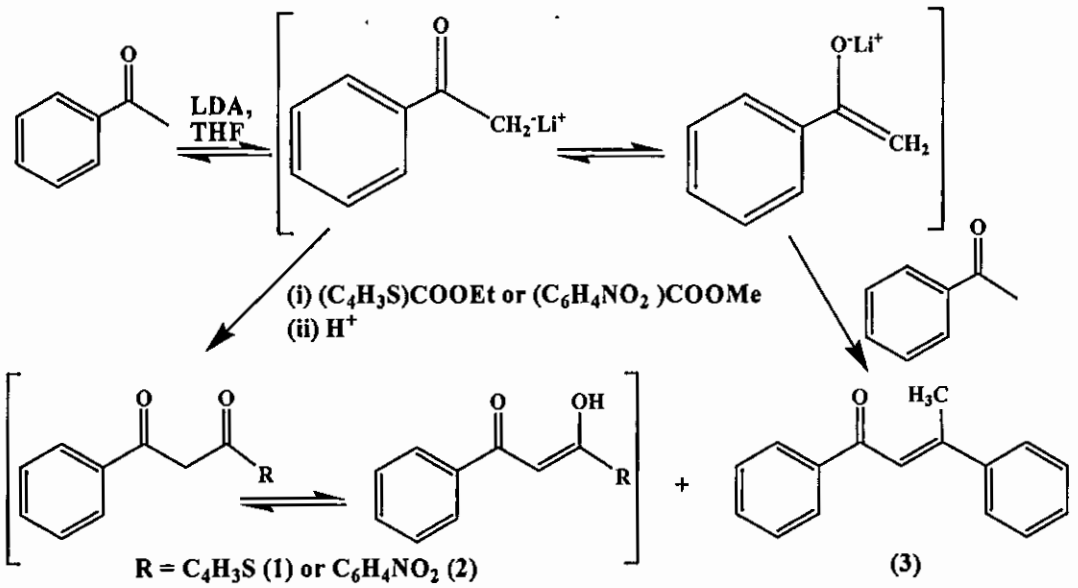

Scheme 3. 1: **Synthetic route utilized during the synthesis of phenyl-containing β-diketones Hthba (1) and Hbnp (2) with an appropriate ester by Claisen condensation in the presence of the base, lithium diisopropylamide, LDA. Self-condensation of acetophenone can also lead to an unwanted side product (3).**

Table 3. 1 gives the ^{1}H NMR shifts of the methine protons of a variety of β-diketones of the type, $PhCOCH_2COR$. Two factors contribute to the deshielding of the CH signal of the β-diketones. More conjugate systems and more electronegative R groups both result in a downfield shift. In comparing the methyl group and $PhNO_2$ for example, the aromatic $PhNO_2$ is more conjugated, with the nitro-group withdrawing electron density, resulting in a strong deshielded shift. The methyl group is electron donating, and less conjugate being a shielding group. The general trend in Table 3. 1 illustrates electron-withdrawing and aromatic groups shifting the CH resonances down-field.

Table 3. 1: **Comparison of ^{1}H NMR shifts of methine protons of β-diketones of the type $PhCOCH_2COR$.**

R group	χ_R [a]	NMR CH shifts
CH_3	2.34	6.19
Rc	1.99 [b]	6.28
Fc	1.87	6.48
CF_3	3.01	6.55
C_4H_3S	2.10 [c]	6.71
Ph	2.21	6.85
$PhNO_2$	2.11 [d]	6.91

[a] χ_R (Gordy scale) apparent group electronegativity values from reference [1] and [2]
[b] From reference [3]
[c] From reference [4]
[d] This study

β-Diketones exist in solution and in the vapour phase[5] as mixtures of enol and keto tautomers in equilibrium with each other. This equilibrium was studied by means of ^{1}H NMR for the β-diketones used in this study and will be discussed in section **3.3**.

3.2.2 Synthesis of Ti(β-diketonato)$_2$Cl$_2$ Complexes

The dichlorobis(β-diketonato)titanium(IV) $Ti(PhCOCHCOC_4H_3S)_2Cl_2$ (**4**), $Ti(PhCOCHCOPh)_2Cl_2$ (**5**), $Ti(PhCOCHCOCH_3)_2Cl_2$ (**6**), $Ti(CH_3COCHCOCH_3)_2Cl_2$ (**7**) and $Ti(PhCOCHCOCF_3)_2Cl_2$ (**8**) complexes were synthesized from the reaction of titanium(IV) chloride with the appropriate β-diketones in an organic solvent (dichloromethane, chloroform or toluene) as described by Fay *et al.*[6, 7] The synthesis involved mixing of $TiCl_4$ and the β-diketone, 120 minutes refluxing in an organic solvent, partial solvent removal and product precipitation by addition of hexane (see Scheme 3. 2).

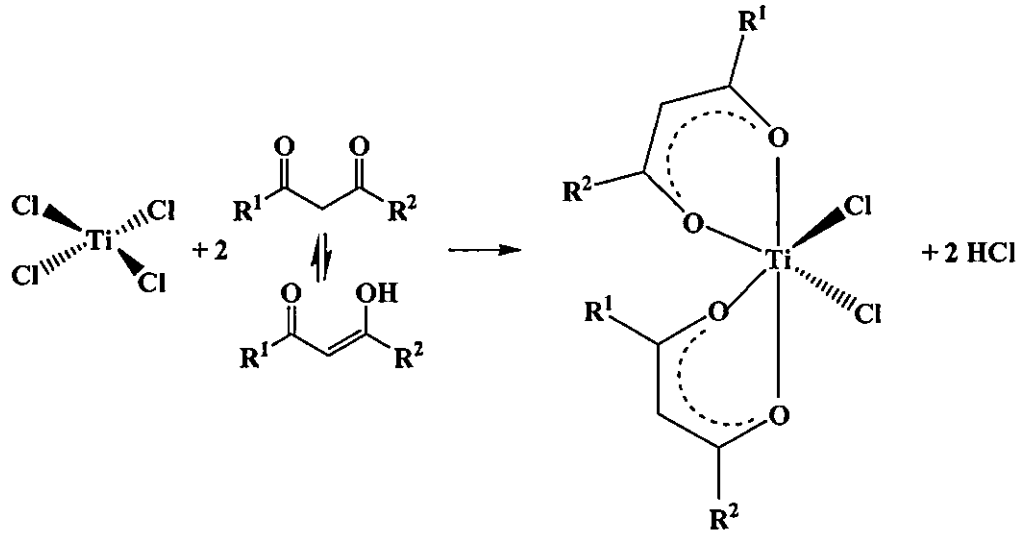

Scheme 3. 2: **Synthesis of dichlorobis(β-diketonato)titanium(IV) complexes, $Ti(PhCOCHCOC_4H_3S)_2Cl_2$ (4), $Ti(PhCOCHCOPh)_2Cl_2$ (5), $Ti(PhCOCHCOCH_3)_2Cl_2$ (6), $Ti(CH_3COCHCOCH_3)_2Cl_2$ (7) and $Ti(PhCOCHCOCF_3)_2Cl_2$ (8).**

The yields obtained in different solvents are given in Table 3.2. Yields of compounds (**4**) - (**7**) in toluene were similar. The much lower yield of the more acidic complex (**8**) may be ascribed to the fact that the electron withdrawing capability of the CF_3 groups makes the β-diketone a poorer electrophile, which in turn makes complex formation more difficult. Another contributing factor may be the titanium-fluorine single bond energy of 581 kJ mol^{-1} that is

higher than that of the titanium-oxygen single bond, (478 kJ mol^{-1}) [8], favoring Ti-F bond formation, leading to side products and a lower yield of (**8**). All products were stored under an argon atmosphere. The complexes of dichlorobis(β-diketonato)titanium(IV), **5-8**, are soluble in dichloromethane, chloroform, acetonitrile, acetone and benzene/toluene, but nearly insoluble in saturated hydrocarbons, ether and carbon tetrachloride. Complex 4 is insoluble in most organic solvents at room temperature, but soluble in hot acetonitrile and chloroform at 55°C. The complexes in solid state are attacked by moisture, and are hydrolyzed almost completely in solution, as they are extremely moisture sensitive. In the hydrolysis of $TiCl_2$(β-diketonato)$_2$, $Ti(OH)_2$(β-diketonato)$_2$ is formed, which is condensed by removal of water, to form [Ti(β-diketonato)$_2$O]$_2$, having Ti-O-Ti bridges (see Scheme 3. 3).[9] The structure of [$Ti(acac)_2O]_2$ was established by single crystal X-ray analysis.[10] Table 3. 3 shows the experimental time measured until precipitation started, when compounds **5-8** were dissolved in dry acetonitrile and treated with 6.25 % water. The yellow, white and orange precipitates were observed for benzoylmethanes, acetylacetonates and dibenzoylmethanes, respectively. The hydrolytic stability in acetonitrile increases in the order $Ti(tfba)_2Cl_2$ < $Ti(acac)_2Cl_2$ < $Ti(ba)_2Cl_2$ < $Ti(dbm)_2Cl_2$ (see Table 3. 3). The greater stability of $Ti(ba)_2Cl_2$ over $Ti(acac)_2Cl_2$ is in agreement with results obtained by Keppler and Heim in a 0.01% water in chloroform solution.[9] Serpone and Fay found $Ti(dbm)_2Cl_2$ more stable than $Ti(ba)_2Cl_2$ in a 0.2% water in CH_3CN solution.[7]

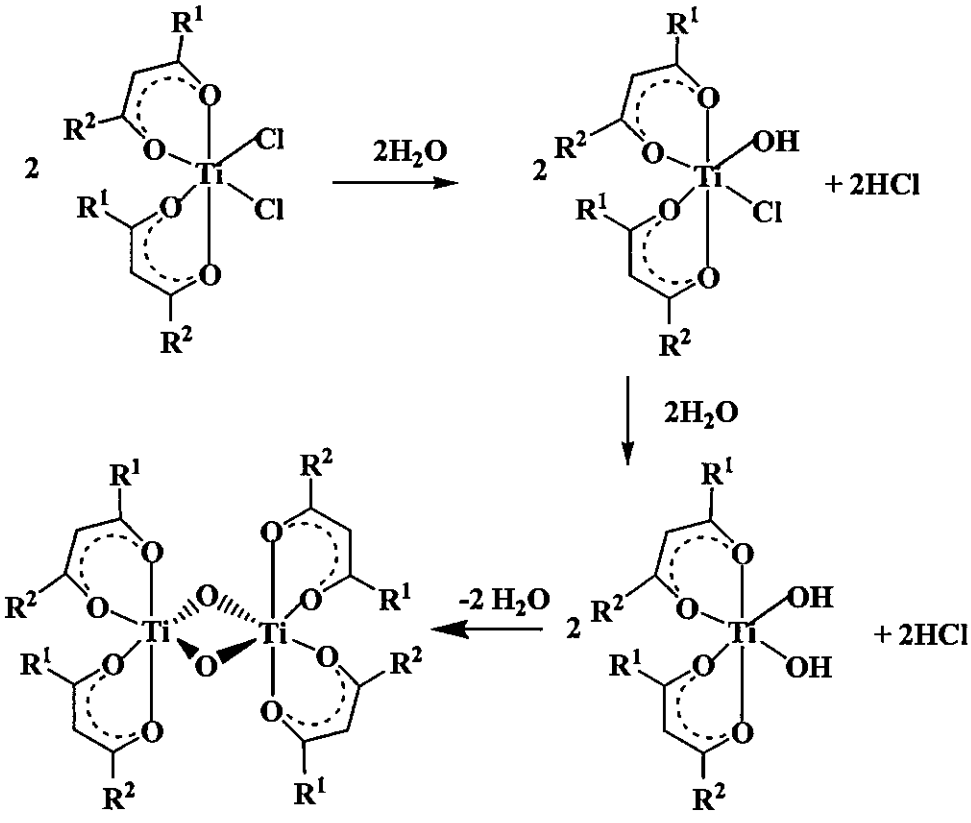

Scheme 3. 3: **Hydrolysis reaction of dichlorobis(β-diketonato)titanium(IV), $TiCl_2(R^1COCHCOR^2)_2$ complexes.**

Table 3.2: **Characterization data for the synthesis of dichlorobis(β-diketonato)titanium(IV), $TiCl_2(PhCOCHCOR)_2$.[a]**

R group	χ_R	% Yield in chloroform	% Yield in toluene	Methine ^1H NMR position / ppm
C_4H_3S	2.10	-	66	6.69
Ph	2.21	47	69	7.35
CH_3	2.34	77	70	6.69
CF_3	3.01	-	16	6.85

(a) $TiCl_2(CH_3COCHCOCH_3)_2$ was synthesized in DCM with a 78% yield.

Table 3. 3. **Results from hydrolysis experiments. The indicated amount of bis-β-diketonato titanium complex Ti(β-diketonato)$_2$Cl$_2$ was dissolved in 8 ml CH_3CN and treated with 0.5 ml H_2O. Time until precipitation sets in for different bis-β-diketonato titanium complexes was recorded.**

Complex	mass / mg	Time until precipitation sets in / min
4, Ti(thba)$_2$Cl$_2$ [(a)]	-	-
5, Ti(dbm)$_2$Cl$_2$	3.6	30
6, Ti(ba)$_2$Cl$_2$	3.2	3
7, Ti(acac)$_2$Cl$_2$	2.3	1
8, Ti(tfba)$_2$Cl$_2$	3.1	20 s

(a) Insoluble in CH_3CN

The $\nu_{C=O}$ bands of the free β-diketone ligands have been reported for Hacac at 1620 cm^{-1} and for Hba 1610 cm^{-1}. In the case of Hdbm the C-O band appears at 1605 cm^{-1}.[11] The ν_{CO} of Ti(acac)$_2$Cl$_2$ was found to be at 1520 cm^{-1} (lit.,[12] 1517 cm^{-1}), a shift of 100 cm^{-1} relative to the carbonyl stretching vibration in free acetylacetone (1620 cm^{-1}). No bands in the carbonyl region were found above 1600 cm^{-1} for **4-8.** The bands in the region 1500-1680 cm^{-1} may be assigned to coordinated C=O groups for **4-8.** Thus, on coordination the ν_{CO} frequency of the β-diketonato ligand is shifted to a lower value, as has been observed in several β-diketonato complexes of metals of the type M(β-diketonate)$_2$, for example in [(C$_5$H$_5$)$_2$Ti(β-diketonato)]$^+$ClO$_4^-$ where β-diketonato = acac, ba and dbm,[13] Cu(II) complexes of ba and dbm,[14] and Be(II) complexes of acac,[14] Mg(acac)$_2$, [15] Ca(hfac)$_2$(tmed),[16] Cu(bzac)$_2$[17] and Cu(acac)$_2$.[17]

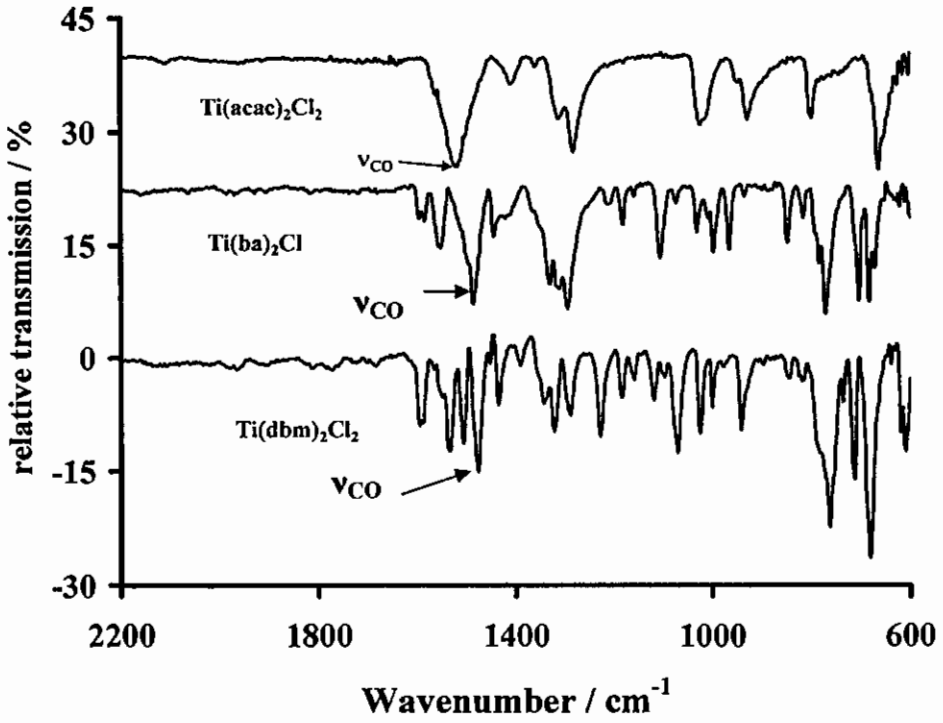

Figure 3. 1: **Infrared spectra for the complexes of dichlorobis(β-diketonato)titanium(IV) in KBr pellets.**

The method described by Serpone *et al.*[7] reported 94% yield for both $Ti(dbm)_2Cl_2$ and $Ti(ba)_2Cl_2$, while this study reports 77.1% and 60.65% yields for $Ti(ba)_2Cl_2$ and $Ti(dbm)_2Cl_2$ respectively. The melting point of $Ti(acac)_2Cl_2$ was found to be 192.66°C (lit.,[6] 191-192°C), $Ti(ba)_2Cl_2$ 238.12°C (lit.,[7] 209-210°C), and $Ti(dbm)_2Cl_2$ 144.69°C (lit.,[7] 262.5-263.5°C).

The ^1H NMR spectra of dichlorobis(β-diketonato)titanium(IV) complexes with β-diketonato = thba (**4**), dbm (**5**), ba (**6**), acac (**7**) and tfba (**8**) in $CDCl_3$ are easy to interpret (see Figure 3. 4). The methine protons' signal which resonates at a low field (6.0 - 7.35 ppm, integrates for 2 protons) for these complexes is a singlet. The methyl protons' signal (2.2 - 2.4 ppm, intergrating for 6 (**6**) and 12 (**7**) protons) in both ba and acac complexes are singlets. The aromatic protons' signals in the phenyl containing β-diketonato dichlorobis(β-diketonato)titanium(IV) complexes are broad multiplets. The six-coordinated, octahedrally configurated compounds can adopt both *cis*- and *trans*-configurations as illustrated in Figure 3. 2. The number of possible isomers in the *cis* and *trans*-forms depend on whether the bound β-diketone in the 1 and 5-positions have the same (symmetrically substituted) or different substituents (asymmetrically substituted). The proton NMR spectra of all dichlorobis(β-diketonato)titanium(IV) complexes are characteristic for the loss of protons from the β-

diketones, thereby suggesting binding of two oxygens to the titanium(IV) centre in the complexes.

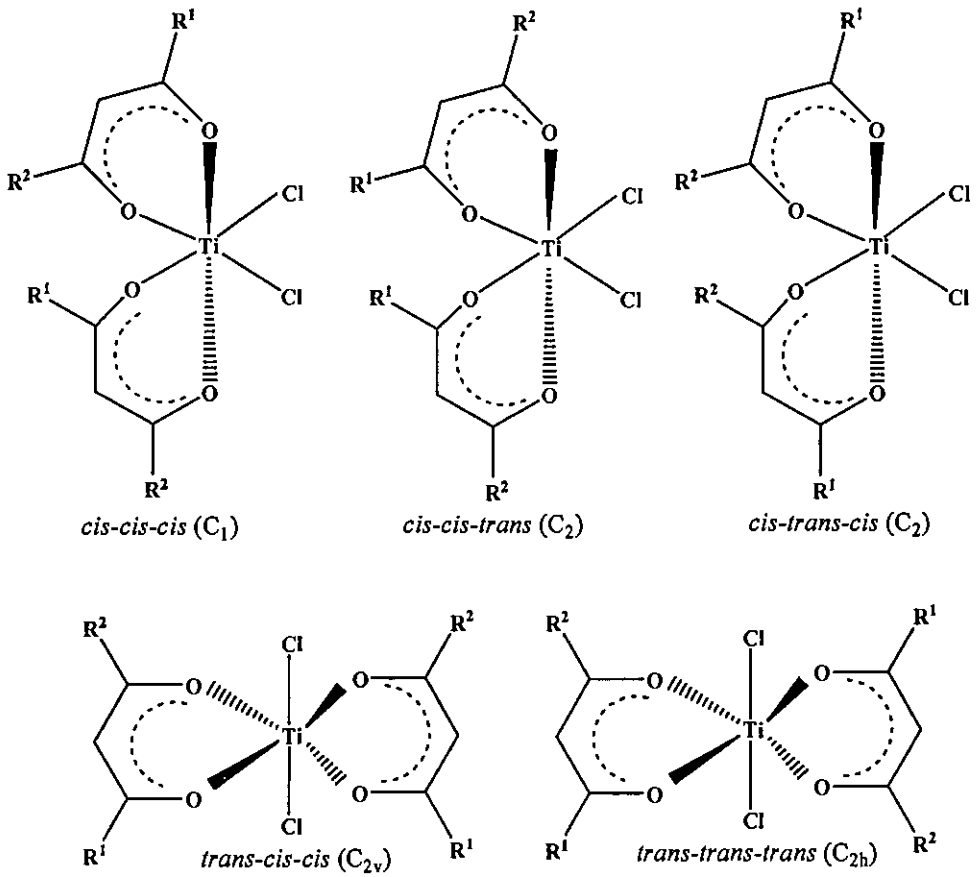

Figure 3. 2: **Isomers within the *cis*- and *trans*- forms of asymmetrically substituted bis(β-diketonato) complexes of the type, $Ti(R^1COCHCOR^2)_2Cl_2$, with $R^1 \neq R^2$.**

It is expected that the *cis* isomer of the symmetrically substituted $Ti(acac)_2Cl_2$ (7) complex shows one signal for the methine proton and two signals of the same intensity for the CH_3 group. For the *trans*-isomer, of (7), however, only one signal is expected for the methine proton and one signal for the CH_3 group. At room temperature (RT) the ^1H NMR shows only one signal for the methine proton and one signal for the CH_3 group. From a variable temperature ^1H NMR study it was concluded by Fay and Lowry[6] that (7) has a *cis* configuration in solution. The one methyl signal observed at RT in this study can be ascribed to the coalescence of the two methyl resonances due to a rapid exchange process which interchanges the methyl groups between the two non-equivalent sites of the *cis* isomer.

For the *cis* isomer of $Ti(dbm)_2Cl_2$ (5) shows one signal for the methine proton and two sets of signals of the same intensity for the Ph group is expected. Fay and Lowry[7] concluded from a

variable temperature ^{1}H NMR study on the methine proton signal that the *cis* configuration exists in solution. One methine signal and one set of broad signals at 7.40 – 7.71 (m, 12H, 4 x 3H, aromatic H) and 7.84 – 8.18 (m, 8H, 4 x 2H, aromatic H) were observed at RT in this study. The broad aromatic signals arise from interchanges of the phenyl groups between the two non-equivalent sites of the *cis* isomer.

The stereochemistry of the complex $Ti(ba)_2Cl_2$ (**6**) can be inferred from NMR spectra, as follows: the *cis-cis-cis* isomer (point group C_1) has no symmetry and, therefore, may give rise to two methyl, two phenyl, and two ring proton resonances. The other four isomers, *cis-cis-trans* (point group C_2), *cis-trans-cis* (C_2), *trans-cis-cis* (C_{2v}) and *trans-trans-trans* (C_{2h}), all possess at least a twofold axis. These isomers should give a single resonance for each type of group. In solution all three *cis* isomers were detected by variable-temperature ^{1}H and ^{19}F NMR for a variety of [Ti(β-diketonato)$_2$X$_2$] (X = halogen or alkoxide) complexes with unsymmetrical β-diketonato ligands.[5, 18]. In this study one methine protons' signal at 6.69 ppm and broad aromatic signals at 6.61 – 6.72 (s, 2H, 2 x CH), 7.39 – 7.66 (m, 6H, 2 x 3H, aromaticH) and 7.84 – 8.18 (m, 4H, 2 x 2H, aromaticH) were observed. These aromatic signals coalesce into three sharp signals at 60°C due to a fast equilibrium on the NMR timescale at 60°C between the three *cis* isomers (see Figure 3. 3).

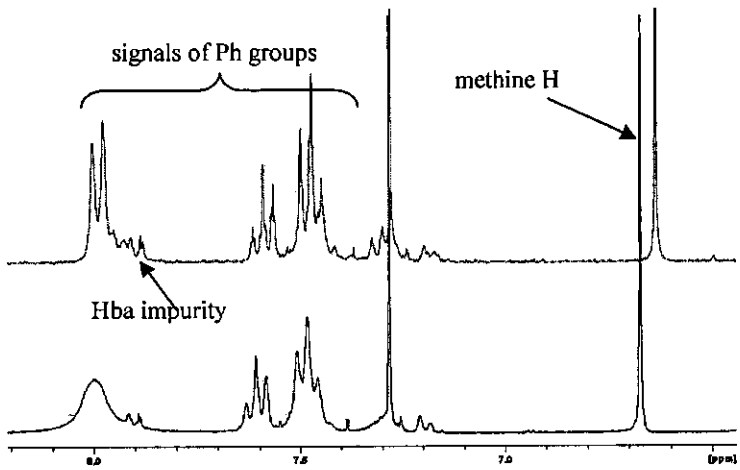

Figure 3. 3: **^{1}H NMR of $Ti(ba)_2Cl_2$ (6) in chloroform-*d* at 21°C (bottom) and at 60°C (top).**

The proton chemical shifts of the Ti(β-diketonato)$_2$Cl$_2$ complexes **4-8** are presented in Table 3. 4 and Figure 3. 4. The values for the enol form of the free β-diketones are included for the comparison.

Table 3. 4: **^{1}H NMR chemical shift data of dichlorobis(β-diketonato)titanium(IV) complexes and free β-diketones in $CDCl_3$.**

$Ti(R^1COCHCOR^2)_2Cl_2$				ν_{CO} of the titanium complex / cm^{-1}	pK_a of free β-diketone[c]	$Ti(\beta\text{-diketonato})_2Cl_2$		free β-diketone		δ[d] / ppm
abbreviation	R^1	R^2	$(\chi_{R1} + \chi_{R2})$ / (Gordy scale)			-CH / ppm	$-CH_3$ / ppm	-CH / ppm	$-CH_3$ / ppm	
4, thba[a]	Ph	C_4H_3S	4.31	-	9.21[b]	6.69	-	6.71	-	0.02
5, dbm	Ph	Ph	4.42	1593	9.35	7.35	-	6.85	-	0.50
6, ba	Ph	CH_3	4.55	1597	8.70	6.69	2.35	6.19	2.16	0.50
7, acac	CH_3	CH_3	4.68	1517	8.95	6.00	2.19	5.50	2.00	0.50
8, tfba	Ph	CF_3	5.22	-	6.30	6.85	-	6.55	-	0.30

[a] ^{1}H NMR values of $Ti(thba)_2Cl_2$ at 60°C in $CDCl_3$. It is insoluble in CD_3CN, $CDCl_3$, CD_3COCD_3 at RT.
[b] This study
[c] From reference[19]
[d] The difference in the resonances of the methine protons in $Ti(\beta\text{-diketonato})_2Cl_2$ and of the free β-diketone.

It can be seen from Table 3. 4 that the CH (methine) resonances of **5 - 7** are shifted to lower field by 0.50 ppm relative to the CH resonances of the enol form of the free β-diketone. The methyl resonance of **6** is shifted to lower field by 0.19 ppm. The CH resonances of $Ti(tfba)_2Cl_2$ also show a downfield shift of 0.3 ppm relative to the CH resonances of the enol form of trifluorobenzoylacetone. These downfield shifts are presumably a consequence of the intramolecular electric field of the highly dipolar *cis* isomers, providing additional confirmatory evidence for the *cis* configuration.[6] Low field shifts are not found and are not expected for *trans* isomers, since *trans* isomers have no molecular dipole moment along the C-H bond. The ^{1}H NMR spectra of all dichlorobis(β-diketonato)titanium(IV) complexes display single sharp resonances for the methine protons (-HC=C-) of the β-diketonato chelate ligands. The reason is that the two short *trans* Ti-O bonds of the *cis* isomer are propitious to reducing steric congestion of the ligands and optimising the opportunity for O to Ti π-bonding.

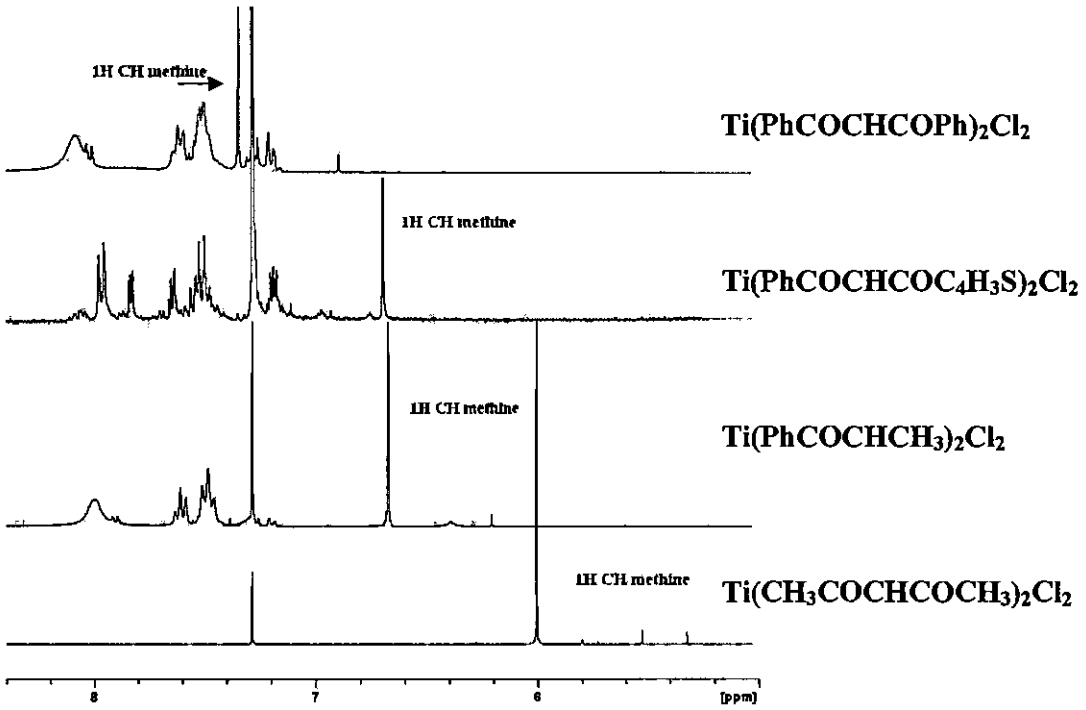

Figure 3. 4: ^{1}H NMR's of Ti(R^1COCHCOR^2)$_2$Cl$_2$ (from top to bottom): Ti(PhCOCHCOPh)$_2$Cl$_2$, Ti(PhCOCHCOC$_4$H$_3$S)$_2$Cl$_2$, Ti(PhCOCHCOCH$_3$)$_2$Cl$_2$ and Ti(CH$_3$COCHCOCH$_3$)$_2$Cl$_2$.

The substitution of methyl groups by phenyl groups in the β-diketone ligand of Ti(β-diketonato)$_2$Cl$_2$ results in down-field shifts because the aromatic ring protons are strongly deshielded by π-orbitals of the ring, resulting in ring-current effects. For example, when going from Ti(acac)$_2$Cl$_2$ to Ti(ba)$_2$Cl$_2$ to Ti(dbm)$_2$Cl$_2$, the CH signal shifts downfield by 0.66 and 0.69 ppm respectively, i.e. *ca* 0.68 ppm per phenyl ring. Similar results of downfield shifts for aluminium and boron compounds were noted by Smith *et al.*,[23] who reported a shift of 0.57 ppm per phenyl ring in the CH resonances for the series of compounds, B(acac)$_2$F$_2$, B(ba)$_2$F$_2$ and B(dbm)$_2$F$_2$.

3.2.3 Synthesis of Ti(β-diketonato)$_2$ bichelating Complexes

A variety of new titanium(IV) complexes, Ti(β-diketonato)$_2$(biphen) with β-diketonato = thba (**9**), dbm (**10**), ba (**11**), acac (**12**), tfba (**13**) and biphen = 2,2'-biphenyldiolato were synthesized.

The Ti(β-diketonato)$_2$(biphen) complexes **9-13** were obtained from the reaction of 2,2'-biphenyldiol with dichlorobis(β-diketonato)titanium(IV), according to Scheme 3. 4. The

synthetic route followed was similar to the one published by Rao *et al*[20] for the reaction between $Ti(acac)Cl_2$ and 1,1'-methylenedi-2-naphtol. The reaction proceeds in the absence or presence of sodium acetate.

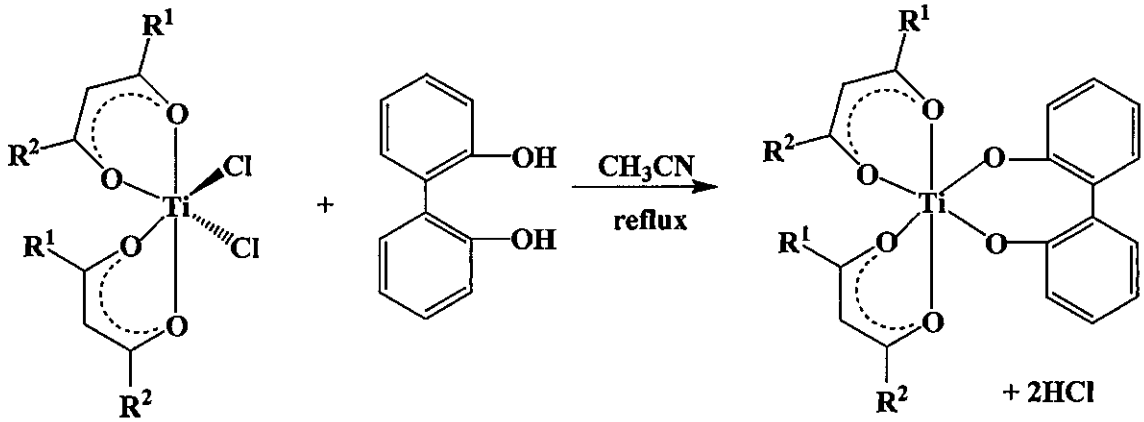

Scheme 3. 4: **The synthetic route utilized during the synthesis of biphenbis(β-diketonato)titanium(IV) complexes, $Ti(PhCOCHCOC_4H_3S)_2$(biphen) (9), $Ti(PhCOCHCOPh)_2$(biphen) (10), $Ti(PhCOCHCOCH_3)_2$(biphen) (11), $Ti(CH_3COCHCOCH_3)_2$(biphen) (12) and $Ti(PhCOCHCOCF_3)_2$(biphen) (13).**

To synthesize $Ti(acac)_2$biphen, **12**, stoichiometric amounts of $Ti(acac)_2Cl_2$, **7**, and 2,2'-biphenyldiol were dissolved in acetonitrile and refluxed under N_2 for 5 hours to yield the mixed ligand complex, Ti(acetylacetonato)$_2$(biphen), which started precipitating after 2 hours, in 77% yield. The reaction of $Ti(acac)_2Cl_2$ with 2,2'-biphenyldiol in ratio's of 1:2 or 1:3 yielded [Ti^{IV}(acetylacetonato)$_2$(biphen)] rather than the products possessing more than one 2,2'-biphenyldiol in the coordination sphere of titanium, for example the complexes, [Ti^{IV}(acetylacetonato)(biphen)$_2$]$^-$ or [Ti^{IV}(biphen)$_2$]. The excess of 2,2'-biphenyldiol ligand can be removed by washing the crude reaction mixture with methanol or ethanol.

Complexes **9**, **10**, **11** and **13** were prepared in a similar way to the reaction of $Ti(acac)_2Cl_2$ with 2,2'-biphenyldiol. These products were collected on removal of solvent from the reaction mixture under reduced pressure, and washed with methanol. Complex **13** contained some free 2,2'-biphenyldiol and could not be cleaned since both **13** and 2,2'-biphenyldiol dissolved in most organic solvents. The proton NMR spectra of all the complexes are characteristic of the loss of protons from the 2,2'-biphenyldiol (phenolic OH) ligand as can be seen from the resonances of the starting material and the ligand, thereby suggesting binding of two oxygens to the titanium(IV) centre in the complexes.

Ti(β-diketonato)$_2$(biphen) complexes can adopt only a *cis* orientation; one possible *cis* isomer if the bound β-diketone in the 1 and 5 position has the same (symmetrically substituted) substituents, or three possible *cis* isomers if the bound β-diketone in the 1 and 5 position has different substituents (asymmetrically substituted) (see Figure 3. 6). At 294K only one single set of sharp signals were observed for all the compounds, **9-13** (see Figure 3. 10). With decreasing temperature, the resonance signals broadened and split up into three to four signals. With further temperature lowering the split resonance signals sharpened again (see Figure 3. 7 for **11**, Figure 3. 8 for **9** and Figure 3. 5 for **13**).

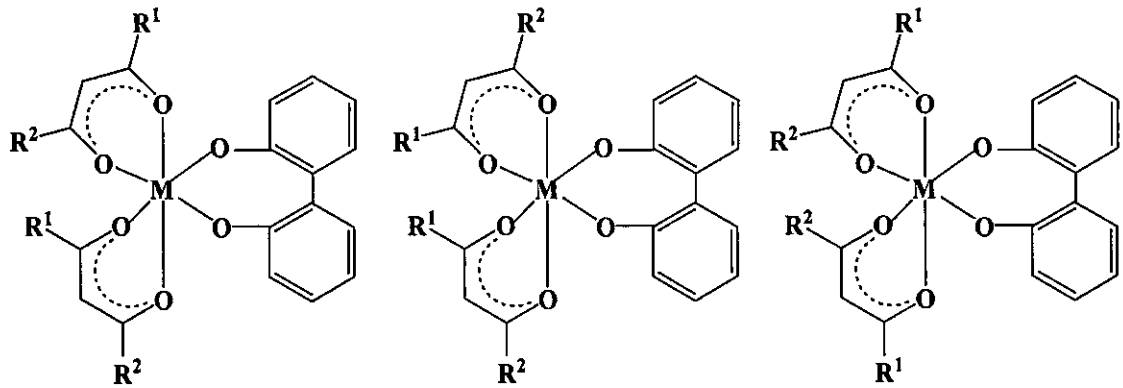

Figure 3. 6: **The three possible *cis*- isomers of asymmetrically substituted bis(β-diketonato) complexes of the type Ti(R^{1}COCHCOR^2)$_2$(biphen): *cis-cis* isomer (point group C$_1$, give rise to two proton resonances for each type of group), *cis-trans* (point group C$_2$, give a single resonance for each type of group), *trans-cis* (C$_2$, give a single resonance for each type of group)**

Figure 3. 7 illustrates the temperature dependence of the ^{1}H NMR resonances of the Ti(PhCOCHCOCH$_3$)$_2$(biphen) (11) complex in $CDCl_3$ solution. Below -40°C, four proton -CH_3 resonances are observed between 2.12 and 2.26 ppm, which, on raising the temperature, collapse into a singlet as a result of the rapid isomerization process which exchanges methyl groups between the four non-equivalent environments. On lowering the temperature the ring methine proton (-CH=) resonance at 6.47 ppm shows three resonance peaks in a 1:2:1 intensity. More than one -CH= resonance in this slow exchange region was not previously observed; Ti(PhCOCHCOCH$_3$)$_2$X$_2$ with X = F, Cl, Br, reveals a single, although considerably broadened resonance signal even at -65°C.[7] This may be due to poor NMR resolution or due to the fact that the exchange between the isomers was fast, even at low temperatures. Ti(PhCOCHCOCH$_3$)$_2$(O^{i}C$_3$H$_7$)$_2$ showed four resonances at -36.8°C for the resonance.[21] The benzoylacetonate phenyl region of the proton NMR spectrum of Ti(PhCOCHCOCH$_3$)$_2$(biphen) (11) is also temperature dependent. These phenyl groups

appear as sharp lines at ambient temperature, broadened below -20°C and sharpened again on cooling to -60°C. A fine structure caused by the overlapping of non-equivalent phenyl groups is observed. These observations are consistent with a rapidly interconverting mixture of the three *cis* diasterioisomers.

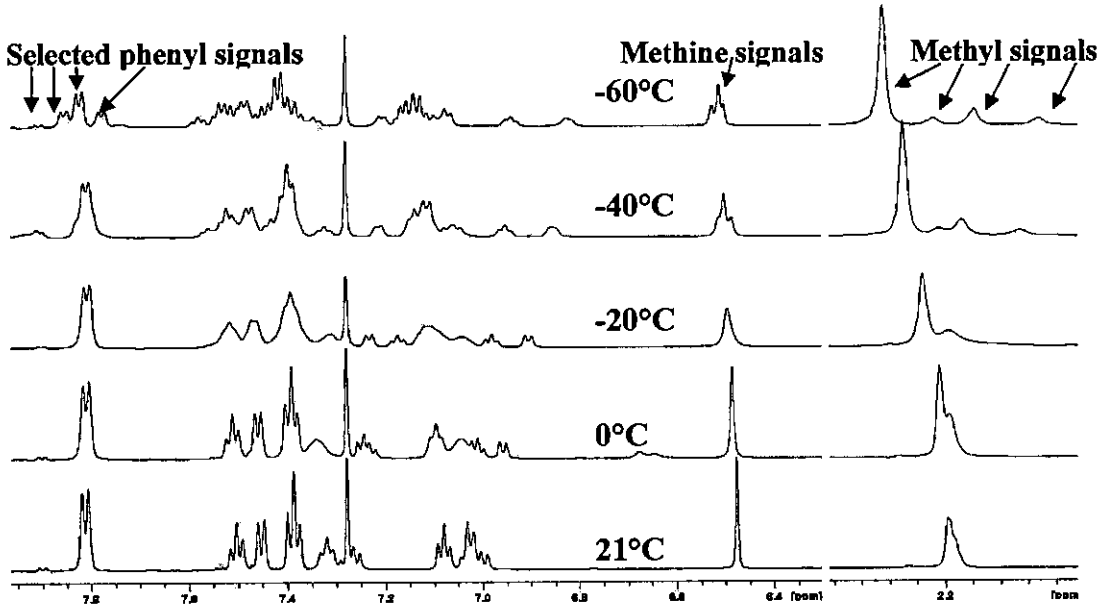

Figure 3. 7: **The temperature dependence of the proton resonances of $Ti(PhCOCHCOCH_3)_2$(biphen) (11) in $CDCl_3$ solution at the indicated temperatures. On the right is the methyl proton resonance at 2.19 ppm, enlarged.**

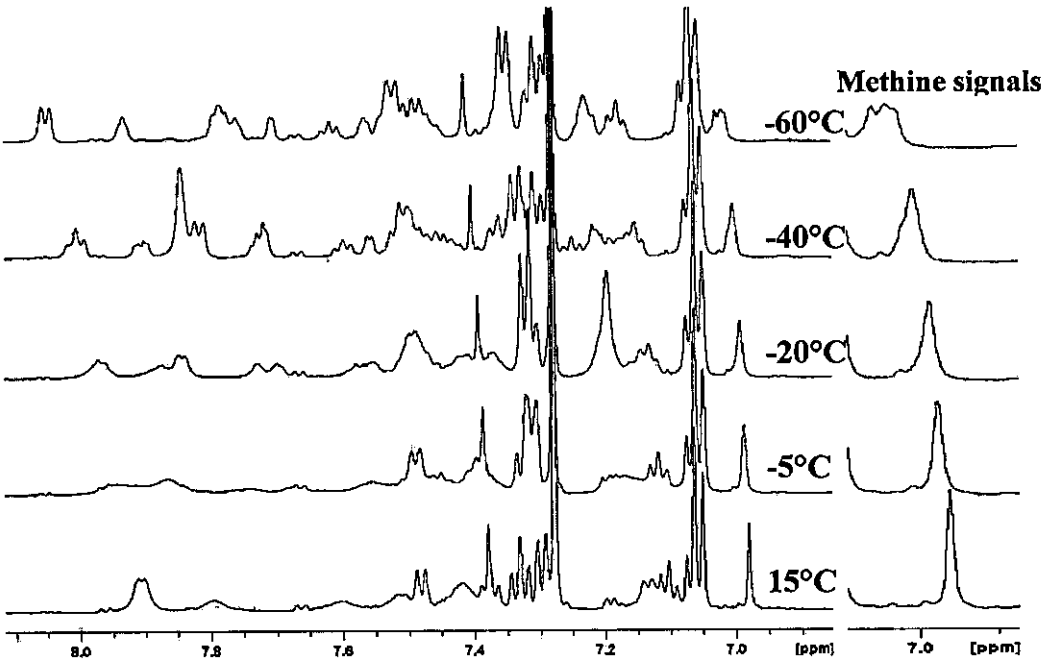

Figure 3. 8: **The temperature dependence of the proton resonances of Ti(PhCOCHCOC$_4$H$_3$S)$_2$(biphen) (9) in $CDCl_3$ solution at the indicated temperatures. On the right is the methine proton resonance at 6.98 ppm, enlarged.**

The ring methine proton (-CH=) resonance of Ti(PhCOCHCOC$_4$H$_3$S)$_2$(biphen) (**9**) at 6.98 ppm (Figure 3. 8) exhibits a single sharp peak at room temperature. On temperature lowering it broadens and split into three or four peaks at -60°C. The ring methine proton (-CH=) resonance of Ti(PhCOCHCOCF$_3$)$_2$(biphen) (**13**) at 6.9 ppm (Figure 3. 9) shows four distinguishable signals of three different intensities at -60°C, consistent with the existence of the three *cis* isomers of **13**, in $CDCl_3$ solution.

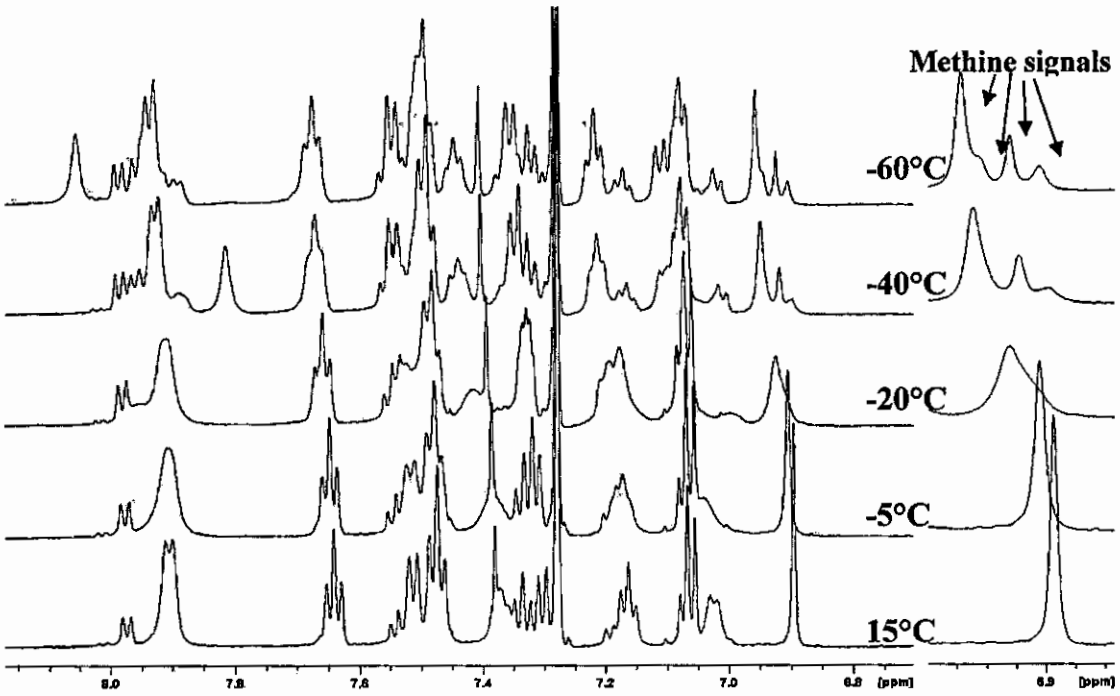

Figure 3. 9: **The temperature dependence of the proton resonances of Ti(PhCOCHCOCF$_3$)$_2$(biphen) (13) in $CDCl_3$ solution at the indicated temperatures. On the right is the methine proton resonance at 6.9 ppm, enlarged.**

^{1}H NMR shifts of Ti(β-diketonato)$_2$(biphen) complexes and the enol form of the free β-diketones are compared in Table 3. 5 and illustrated in Figure 3. 10. The CH and CH_3 resonances of [Ti(acac)$_2$(biphen)] (**12**) shifted to lower field. The methine resonances shifted 0.30 ppm lower to 5.80 ppm, relative to the corresponding resonance signals of the enol form of acetylacetone. NMR shifts of (**12**) are very similar to the methine and methyl resonance signals of Ti(acac)$_2$(CH_2($C_{10}H_6O$)$_2$), at 5.97 and 2.06 ppm respectively, as described by Rao *et al.*[20]

Table 3. 5: **^{1}H NMR shifts (in $CDCl_3$), carbonyl stretching frequencies, group electronegativities, melting points, UV/vis absorption maxima, and the yields of the biphenbis(β-diketonato)titanium(IV) complexes, Ti(β-diketonato)$_2$biphen. ^{1}H NMR shifts of the free β-diketone in $CDCl_3$ are included for comparison.**

Titanium complex		Ti(β-diketonato)$_2$biphen						Free β-diketone Ligand			δ [a] / ppm
	$\chi_{R1} + \chi_{R2}$	ν_{CO} / cm^{-1}	m.p (°C)	UV/ VIS max. (nm)	Yield (%)	-CH / ppm	-CH_3 / ppm	-CH / ppm	-CH_3 / ppm	pK_a	
9 Ti(thba)$_2$biphen	4.31	1658	>250	-	59	6.93	-	6.71	-	9.21	0.22
10 Ti(dbm)$_2$biphen	4.42	1589	244.9	342.0	12	7.18	-	6.85	-	9.35	0.33
11 Ti(ba)$_2$biphen	4.55	1584	>250	-	23	6.49	2.20	6.19	2.16	8.70	0.30
12 Ti(acac)$_2$biphen	4.68	1589	>250	335.9	77	5.80	2.05	5.50	2.00	8.95	0.30
13 Ti(tfba)$_2$biphen	5.22	1610	>250	-	51	6.90	-	6.55	-	6.30	0.35

[a] The difference in the resonance of the methine proton in Ti(β-diketonato)$_2$biphen and of the free β-diketone

The substitution of methyl for phenyl groups also results in downfield shifts. Thus, the methine CH resonances of $Ti(ba)_2$biphen and $Ti(dbm)_2$biphen are shifted to lower field by 0.69 and 1.38 ppm in relation to the CH resonance of the corresponding $Ti(acac)_2$biphen complex. In comparing the phenyl-containing biphenbis(β-diketonato)titanium(IV) complexes, it was found that there is an increase in NMR chemical shifts of 0.41, 0.44 and 0.69 ppm with regard to the CH resonances for $Ti(ba)_2$biphen of $Ti(tfba)_2$biphen, $Ti(thba)_2$biphen and $Ti(dbm)_2$biphen, respectively. These shifts may be due to inductive effects, suggested by the importance of the magnetic anisotropy of the phenyl group.

In the comparison of CH resonances of dichlorobis(β-diketonato)titanium(IV) complexes with biphenbis(β-diketonato)titanium(IV) complexes, it was found that there is an upfield shift of 0.20, 0.17 and 0.20 ppm for titanium(IV) complexes with β-diketonato = acac, dbm and ba respectively, and a downfield shift of 0.05 ppm for β-diketonato = tfba.

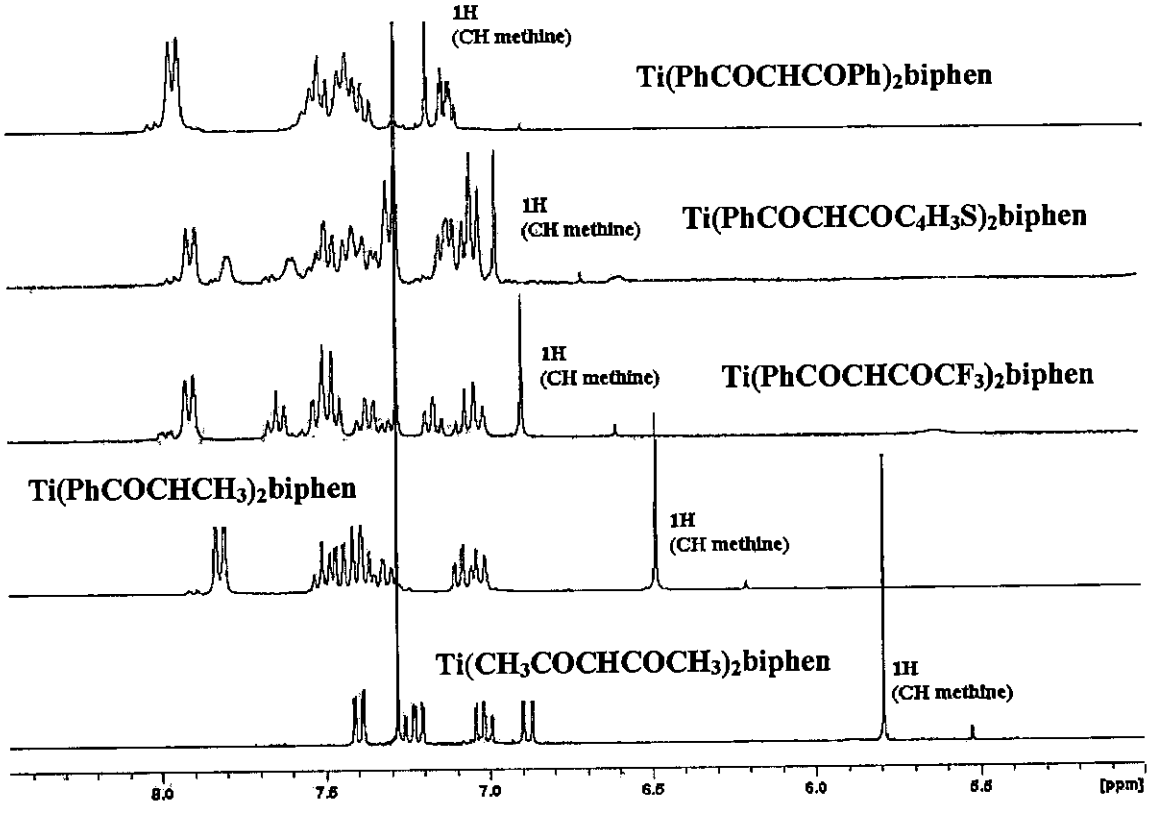

Figure 3. 10: **^{1}H NMR of (from top to bottom) $Ti(R^1COCHCOR^2)_2$(biphen) : $Ti(PhCOCHCOPh)_2$(biphen) (10), $Ti(PhCOCHCOC_4H_3S)_2$(biphen) (9), $Ti(PhCOCHCOCF_3)_2$(biphen) (13), $Ti(PhCOCHCOCH_3)_2$(biphen) (11) and $Ti(CH_3COCHCOCH_3)_2$(biphen) (12).**

There is an increase in the carbonyl stretching ν_{CO} (Table 3. 5), going from Ti(ba)$_2$biphen to Ti(thba)$_2$biphen *via* Ti(dbm)$_2$biphen and Ti(tfba)$_2$biphen complexes. The C-O (carbon-oxygen) bond order (bond strength) increases and the M-OC (metal-oxygen) bond order (bond strength) decreases. No deduction can be made from the sum of the group electronegativities of the R groups, and spectroscopic results.

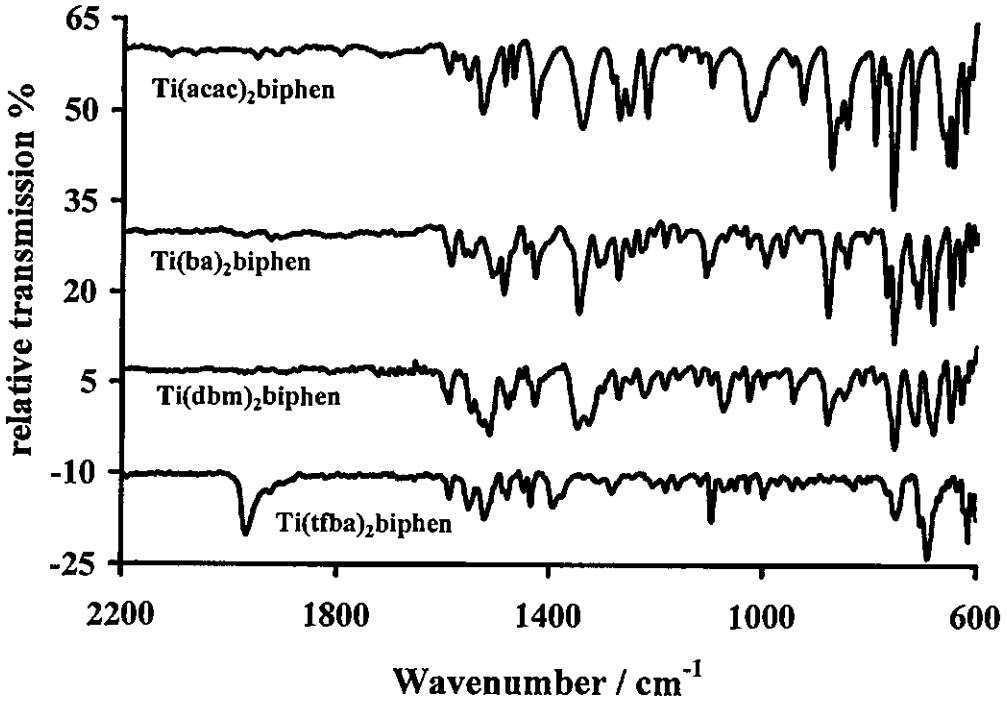

Figure 3. 11: **The infrared spectra for the complexes of biphenbis(β-diketonato)titanium(IV) in KBr-pellets.**

3.2.4 Properties of Ti(β-diketonato) and M(β-diketonato) complexes, M = metal

^{1}H chemical shifts of the methine proton of a variety of M(β-diketonato) complexes are summarized in Table 3. 6. The CH resonances of Ti(ba)$_2$X$_2$ (X = F or Cl) were very similar (6.6 - 6.7 ppm), but shifted to lower field by 0.4 – 0.5 ppm relative to the CH resonances of metal trisbenzoylacetonates M(ba)$_3$[22]. The methyl resonances are also shifted to lower field by 0.19 ppm. The CH resonances of Ti(dbm)$_2$Cl$_2$ exhibit analogous downfield shifts of 0.4 – 0.5 ppm relative to the CH resonances of Al(dbm)$_3$.[23] These shifts may in part be due to inductive effects. Comparing the chemical shifts of the β-diketonato -CH= proton of 5.89 -

6.05 ppm of metal benzoylacetonates[22], $M(ba)_3$ (M = Rh, Cr, Co, Al, Mn, Fe), with chemical shifts of 6.18-6.23 ppm of metal trifluoroacetylacetonates[24], $M(tfaa)_3$ (M = Cr, Co, Rh, Al, Ga, In, Mn, Fe), suggests the importance of magnetic anisotropy of the phenyl group.

The X-ray studies by Hon *et al.*,[25] of *cis*-$VO(ba)_2$ and *trans*-$Cu(ba)_2$ indicate that the phenyl and metal β-diketonate rings are nearly coplanar. By assuming exact coplanarity in solution, it was computed by McConnell[26] that in *trans*-$Cu(ba)_2$ the expected downfield shifts for the CH and methyl protons of the benzoylacetonate ligand, due to ring currents in the phenyl ring, are to be 0.53 and 0.10 ppm, respectively. By comparing the observed shifts of 0.69 and 0.16 ppm for $Ti(ba)_2Cl_2$ relative to $Ti(acac)_2Cl_2$, suggests that the observed downfield shifts are caused primarily by ring-current effects.

The -CH= proton resonance of the β-diketonato ligand in Ti(β-diketonato) complexes, is generally shifted to lower field with respect to the –CH= proton resonance of the free ligand, as is the case for other M(β-diketonato) complexes.

Table 3. 6: **^{1}H NMR chemical shifts (in ppm) of the methine proton of a variety of M(β-diketonato) complexes.**

tfaa-complexes		ba-complexes		acac-complexes		dbm-complexes	
$In(tfaa)_3$[c]	5.89	*cis*-$Rh(ba)_3$[a]	6.18	$Ti(acac)_2biphen$[d]	5.80	$Al(dbm)_3$[b]	6.91
trans-$Ga(tfaa)_3$[c]	5.92	*trans*-$Rh(ba)_3$[a]	6.18	$Ti(acac)_2F_2$[e]	5.87	$B(dbm)F_2$[b]	7.18
trans-$Al(tfaa)_3$[c]	5.98	*trans*-$Co(ba)_3$[a]	6.22	$Ti(acac)_2$	5.97	$Ti(dbm)_2biphen$[d]	7.18
cis-$Rh(tfaa)_3$[c]	5.99	*trans*-$Al(ba)_3$[a]	6.22	$(CH_2(C_{10}H_6O)_2)$		$Ti(dbm)_2F_2$[e]	7.25
trans-$Rh(tfaa)_3$[c]	6.01	*cis*-$Co(ba)_3$[a]	6.23	$Ti(acac)_2Cl_2$[d]+[f]	6.00	$Ti(dbm)_2Cl_2$[e]	7.35
cis-$Co(tfaa)_3$[c]	6.05	$Ti(ba)_2biphen$[d]	6.51	$B(acac)F_2$[b]	6.04		
trans-$Co(tfaa)_3$[c]	6.05	$Ti(ba)_2F_2$[e]	6.58				
		$B(ba)_2F_2$[e]	6.61				
$Ti(tfba)_2biphen$[d]	6.90	$Ti(ba)_2Cl_2$[d]+[e]	6.69				
$Ti(thba)_2biphen$[d]	6.93						

[a] From reference 21
[b] From reference 22
[c] From reference 23
[d] This study
[e] From reference 6
[f] From reference 5

3.3 Properties of β-diketones.

3.3.1 The observed Solution Phase Equilibrium Constant, K_c.

All β-diketones exist in principle as a mixture of enol and keto forms, as shown in Scheme 3. 5. Although two enol isomers, (Ph-C(OH)=CH-CO=R and Ph-CO-CH=C(OH)-R), exist in equilibrium, in practice, only one set of enol tautomer signals is observed on the NMR. It implies that either only one tautomer exists, or the conversion from one enol tautomer to another is fast on the NMR time scale.

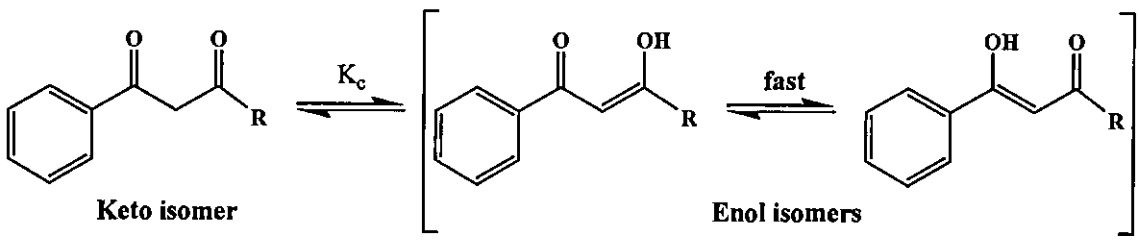

Scheme 3. 5: **Keto-enol equilibrium for phenyl-containing β-diketones.**

By interpreting NMR spectra of the enol tautomers, the measured integral values of the enol tautomers indicate the total enol tautomer content in solution. This implies that K_c can conveniently be determined by using the integral values for suitable ^{1}H NMR signals as in Equation 3.1.

Equation 3.1 $$K_c = \frac{[\text{enol isomers}]}{[\text{keto isomer}]} = \frac{\text{integral value of } ^1\text{H NMR signal of a suitable enol}}{\text{integral value of } ^1\text{H NMR signal of a suitable keto}}$$

For example, when using methine signal integrals of a 44.9 mM $CDCl_3$ solution of PhCOC**H**=C(OH)CH_3 at δ = 4.1 (1H, keto) and δ = 6.2 (2H, enol) ppm in Figure 3. 14 B, $K_c = \frac{1}{0.0835} = 12.0$.

In this study, K_c values for β-diketones, in $CDCl_3$ solutions, were obtained from ^{1}H NMR spectroscopy at 298 K. The percentage of keto isomer can be calculated using (Equation 3.2).

Equation 3.2 $$\% \text{ keto isomer} = \frac{\text{I of keto isomer}}{\text{I of keto isomer} + \text{I of enol isomer}} \times 100$$

I = integral value of the NMR. For example, using the methine proton signals of PhCOC**H**=C(OH)CH_3 of benzoylacetone, the equilibrium % keto isomer at 298 K can be calculated using Equation 3.2. It becomes

$$\% \text{ keto isomer} = \frac{0.0835}{0.0835 + 1.000} \times 100 = 7.707\%$$

Results of a temperature NMR study of the keto-enol equilibrium of the four β-diketones in $CDCl_3$ are summarized in Table 3. 7. The variation of K_c with temperature may mathematically be quantified by

$$\ln(K_{c2}) - \ln(K_{c1}) = \frac{-\Delta H}{R}\left(\frac{1}{T_2} - \frac{1}{T_1}\right)$$

with K_{c2} and K_{c1} the equilibrium constants at temperatures T_2 and T_1, R = 8.314 $JK^{-1}mol^{-1}$ and $\Delta_r H$ the reaction enthalpy as defined elsewhere.[27, 28] The above equation also implies that a graph of $\ln K_c$ *vs.* 1/T should be linear, with slope $-\Delta_r H/R$. Figure 3. 12 illustrates the linearity for Hthba and Hba. Hacac and Hdbm did not show any variation over the experimental temperature range for the indicated concentrations in $CDCl_3$. K_c and ΔH values from Figure 3. 12 are summarized in Table 3. 7. The thermodynamic quantity 'Gibbs free energy', ΔG, and 'entropy', ΔS, may be calculated from the equations

$\Delta G = -RT \ln K_c$ &

$\Delta G = \Delta H - T\Delta S$.

The results at 298 K are summarized in Table 3. 7.

Table 3. 7: **The average equilibrium constant K_c at 298K for the equilibrium shown in Scheme 3. 5, and the thermodynamic data at 298 K relevant to this equilibrium for the β-diketones Hthba, Hba, Hacac and Hdbm at the indicated concentrations iu $CDCl_3$.**

β-diketones	Conc. / mM	K_C (298K)	ΔH / kJ mol^{-1}	ΔG / kJ mol^{-1}	ΔS / J K^{-1} mol^{-1}
Hthba	42.8	16.1	-10.2	-6.9	-11
Hba *	53.7	46.8	-16.4	-9.5	-23
Hacac	106.0	2.08	-	-1.8	-
Hdbm	38.9	22.7	-	-7.7	-

*** K_C is concentration independent, *e.g.*, for [Hba] = 44.9 mM, K_C = 12.0 for a $CDCl_3$ solution at 21°C.**

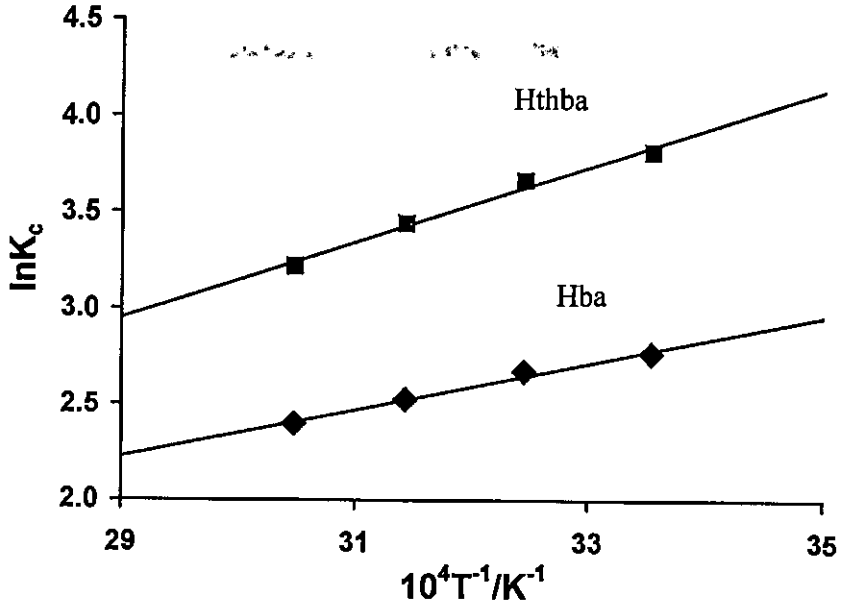

Figure 3. 12: **Temperature dependence of K_c for Hthba and Hba.**

There is a correlation between free energy and percentage enol for all the β-diketones, i.e., with decrease in % keto isomer, the free energy becomes more negative. As ΔG becomes more negative, i.e., thermodynamic driving force associated with keto-enol equilibrium becomes more favourable, the enol content of the β-diketones becomes larger. The values of ΔG in this study is in the same order that is found for a series of ferrocene-containing β-diketones, namely Hfctfa (K_C = 30, ΔG = -8.3 kJ mol^{-1}), Hfctca (K_C = 19.4, ΔG = -15 kJ mol^{-1}), Hfca (K_C = 43.4, ΔG = -6.2 kJ mol^{-1}), Hbfcm (K_C = 10.4, ΔG = -6.9 kJ mol^{-1}) and Hdfcm (K_C = 2.0, ΔG = -1.0 kJ mol^{-1}).[29] (Hfctfa = 1-ferrocenyl-4,4,4-trifluorobutane-1,3-dione, Hfctca = 1-ferrocenyl-4,4,4-trichlorobutane-1,3-dione, Hfca = 1-ferrocenylbutane-1,3-dione, Hbfcm = 1-ferrocenyl-3-phenylpropane-1,3-dione and Hdfcm = 1,3-diferrocenylpropane-1,3-dione)

3.3.2 Kinetics of Keto-Enol Conversion.

From the kinetic point of view, the equilibrium constant, K_c, can also be expressed in terms of the quotient of the rate of conversion of keto to enol isomers, and the rate of conversion of enol to keto isomers, as given by the reaction:

$$\text{Ph-CO-CH}_2\text{-CO-R} \underset{k_{-1}}{\overset{k_1}{\rightleftharpoons}} \text{Ph-CO-CH=C(OH)-R}$$

Keto isomer **Enol isomer**

In particular, $K_c = \frac{k_1}{k_{-1}}$, with k_1 and k_{-1} the rate constants for the conversion from keto to enol isomer, and conversion from enol to keto isomer, respectively.

It was found that aged samples of β-diketones become richer in enol content. On dissolving in $CDCl_3$, the formation of keto-isomer can be monitored until the solution's equilibrium position is reached.[29] For benzoylacetone in the solid state, it was found that after enough time has elapsed, the above equilibrium is essentially driven to the enol side. The keto content of a freshly prepared $CDCl_3$ β-diketone solution was for all practical purposes zero. When this solution is allowed to mature, the solution equilibrium position can again slowly be reached. In Figure 3. 14 A the ^{1}H NMR plot for an aged sample of the β-diketone, Hba, is shown directly after dissolution in $CDCl_3$, being mainly in the enol form. Figure 3. 14 B shows the same sample after being in solution for 100 minutes, i.e. at time infinity, at the keto-enol equilibrium position.

The formation of the keto isomer was monitored with time (See Figure 3. 13). The observed first order rate constant, k_{obs}, for the data in Figure 3. 13, was calculated from the following equation, utilizing the least squares fitting program MINSQ:[30]

$$\ln\left[\frac{C_0 - C_\infty}{C_t - C_\infty}\right] = k_{obs}t \text{ with } k_{obs} = k_1 + k_{-1}$$

C_0 = initial concentration expressed in % initial keto content, C_t = concentration at time (t) expressed as % keto content at time t.

A first-order treatment of the data obtained by NMR, describing the rate of conversion from enol to keto isomer at 20°C in $CDCl_3$, resulted in the observed first-order rate constant, k_{obs} = 0.0015 ± 0.0001 s^{-1} for a 44.9 mM $CDCl_3$ solution of Hba.

The observed rate constant, k_{obs}, is the sum of the forward and reverse rate constants, k_1 and k_{-1}. By solving $k_{obs} = k_1 + k_{-1}$ and $K_c = k_1/k_{-1}$ simultaneously, rate constants k_1 and k_{-1} are separated:

$k_{obs} = 0.0015(1)$ s^{-1}, $K_c = 12.0$, $k_{-1} = 1.5 \times 10^{-4}$ s^{-1}, $k_1 = 1.4 \times 10^{-3}$ s^{-1}.

The equilibrium constant, K_c, is concentration independent at high concentrations of the β-diketone. It decreases at low concentrations. For example, for Hba, K_c = 12.0 and 46.8 for a 44.9 and 53.7 mM $CDCl_3$ solution at 21°C respectively.

The rate of conversion of Hba from enol to keto (k_1 = 0.00015 s^{-1}, half-life of 1 hour) is faster than observed for ferrocene containing β-diketones Hfctfa (k_1 = 0.000002 s^{-1}, half-life of 96 hours), Hfca (k_1 = 0.000013 s^{-1}, half- life of 15 hours) and Hdfcm (k_1 = 0.000010 s^{-1}, half-life of 19 hours).[29] (Hfctfa = 1-ferrocenyl-4,4,4-trifluorobutane-1,3-dione, Hfca = 1-ferrocenylbutane-1,3-dione, Hdfcm = 1,3-diferrocenylpropane-1,3-dione).

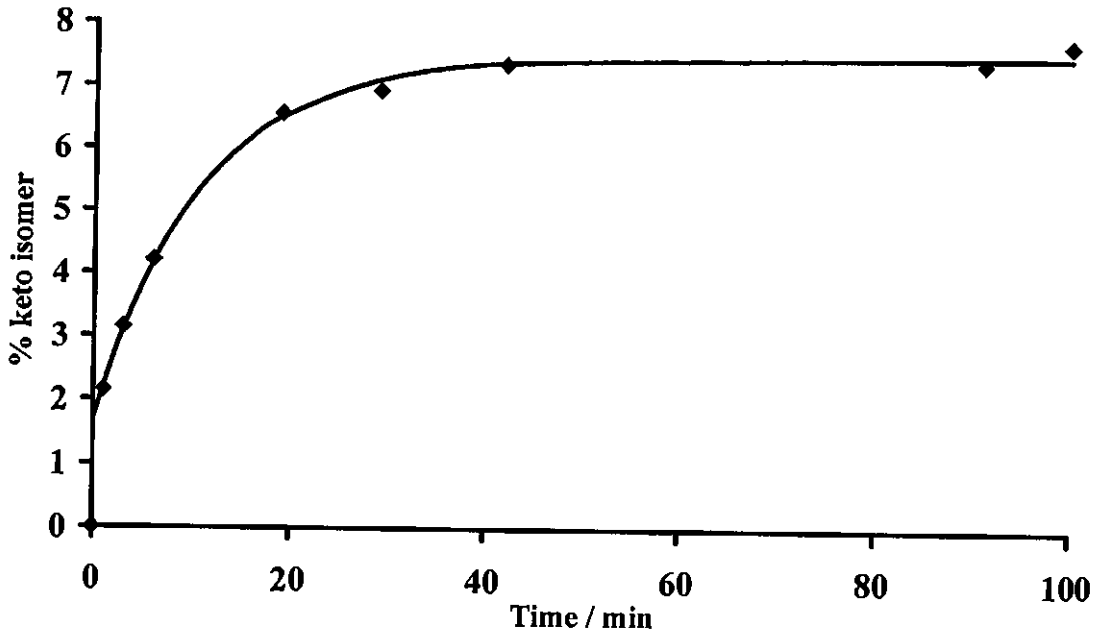

Figure 3. 13: **Time trace showing the conversion from enol to keto isomers for Hba at 20°C in $CDCl_3$. The observed first order rate constant is $k_{obs} = k_1 + k_{-1}$.**

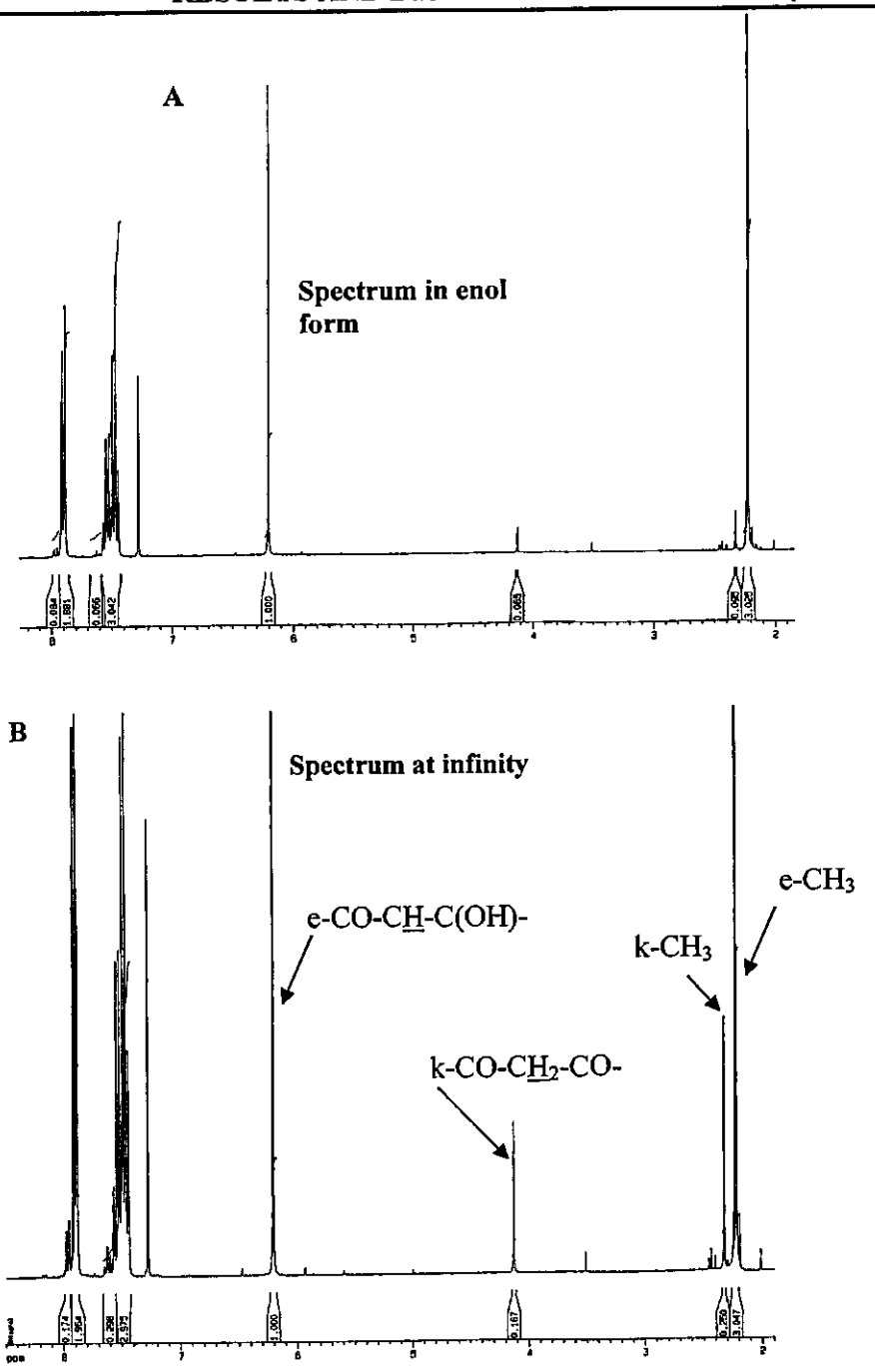

Figure 3. 14: **Spectrum A shows the ^{1}H NMR of a 44.9 mM $CDCl_3$ solution of Hba in enol form, at 294K, in $CDCl_3$. Spectrum B shows the ^{1}H NMR of Hba at equilibrium, at 294 K, in $CDCl_3$. The keto content is 7.707%. Assignments: δ_H (300 MHz; $CDCl_3$) enol-isomer, 2.12 (3H, s, CH_3), 6.20 (1H, s, $COC\underline{H}COH$), 7.50 (3H, m, C_6H_5), 7.90 (2H, d, C_6H_5); keto-isomer, 2.34 (3H, s, CH_3), 4.13 (2H, s, $COCH_2CO$), 7.59 (3H, m, C_6H_5), 7.98 (2H, d, C_6H_5). e = enol signal, k = keto signal.**

3.3.3 pK_a Determination.

The 'apparent' pK_a' values for the phenyl containing β-diketones, Hthba and Hbnp were determined in this study. The pK_a' values refer to the following process:

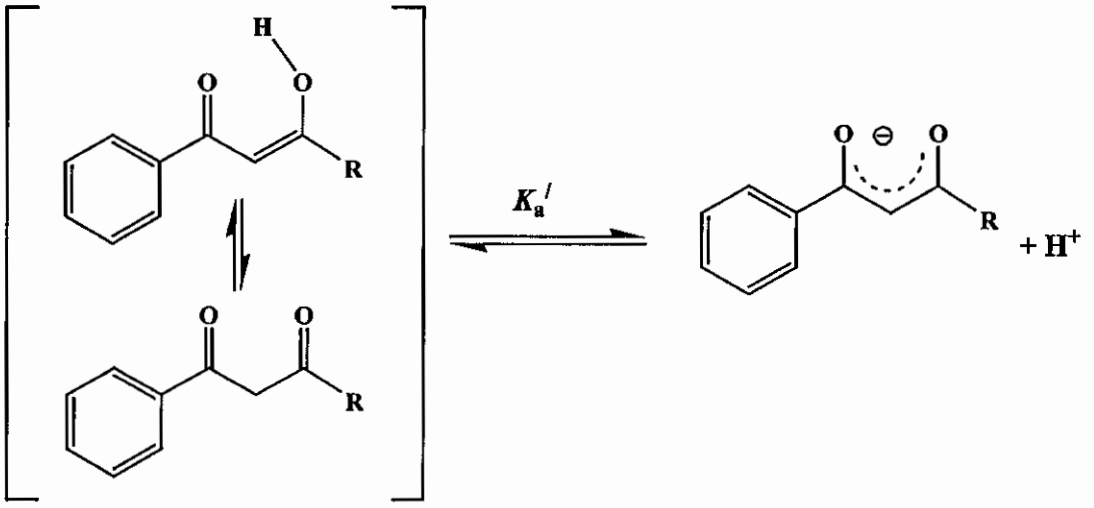

Scheme 3. 6: **Schematic representation of the acidic (enolic) and basic forms of the β-diketones, with R = $PhNO_2$, CH_3 and C_4H_3S.**

'Apparent' pK_a values were determined in this study, since no attempts were made to distinguish between the experimentally obtained 'apparent' pK_a value and the separate pK_a values for the enol and keto tautomers. The term, pK_a', will be used for the determined 'apparent' pK_a values. Since the β-diketones were not very soluble in pure or basic water, water-acetonitrile mixtures were used as solvent. It was found by du Plessis *et al.*[31] that such mixtures have much less influence on β-diketones' pK_a determination than do 1,4-dioxane, methanol, ethanol or propan-2-ol. The pK_a of Hacac measured under the same experimental conditions as used in this study, resulted in a pK_a of 9.07(1), which lies within experimental error, being the same as the best available published pK_a value for acetylacetone in water (8.878(5), where μ = 1 mol dm^{-3}, and 8.98, where μ = 0.0172 mol dm^{-3}).[32] The pK_a' of the β-diketones, Hthba and Hbnp, were determined in 10% acetonitrile/water mixture, with μ = 0.100 mol dm^{-3} ($NaClO_4$) at 20.0(1)°C. This was done by measuring the UV absorbance and pH data by titrating from high to low pH (or from low to high pH) and obtaining a least squares fit30 of the absorbance/pH data, using Equation 3. 3.

Equation 3. 3 $$A_T = \frac{A_{HA}\,10^{-pH} + A_A\,10^{-pK_a}}{10^{-pH} + 10^{-pK_a}}$$

A_T = total absorbance, A_{HA} the absorbance of the β-diketone in the protonated form, and A_A the absorbance of the β-diketone in deprotonated (basic) form. pK_a' values obtained from UV absorbance and pH data with titration from high to low pH, or from low to high pH, were within experimental error the same.

3.3.3.1 The pK_a of Hthba and Hbnp

The UV/Visible spectra of the protonated (acidic form) and deprotonated (basic form) of β-diketones, Hthba and Hbnp, are shown in **Figure 3.15**, with the peak absorption coefficients in Table 3.8. This table also gives the concentration of the β-diketones during the pK_a' determination, as well as pK_a' as determined from the data in **Figure 3.16**.

Table 3.8: pK_a values and molar extinction coefficients, ε, at corresponding wavelengths, λ_{max}, of the free β-diketones, Hthba and Hbnp, in 10% acetonitrile/water mixture.

β-diketone	pK_a'	λ_{max} (deprotonated) / nm [ε / $dm^3\ mol^{-1}\ cm^{-1}$]	λ_{exp} / nm	c / mol dm^{-3}
Hthba	9.21(5)	365 [9 354]	400	1.23×10^{-4}
Hbnp	8.02(7)	345 [22 868]	360	1.19×10^{-4}

The newly determined pK_a' values in this study fit in the series of increasing pK_a' values of β-diketones as follows (for each β-diketone, pK_a' is given in brackets):
(*strongest acid*) Hhfaa (4.71) < Htfba (6.30) < Hbnp (8.03) < Hba (8.70) < Hacac (8.95) < Hthba (9.21) < Hdbm (9.35) < Hbfcm (10.41) < Hdfcm (13.1) (*strongest base*).

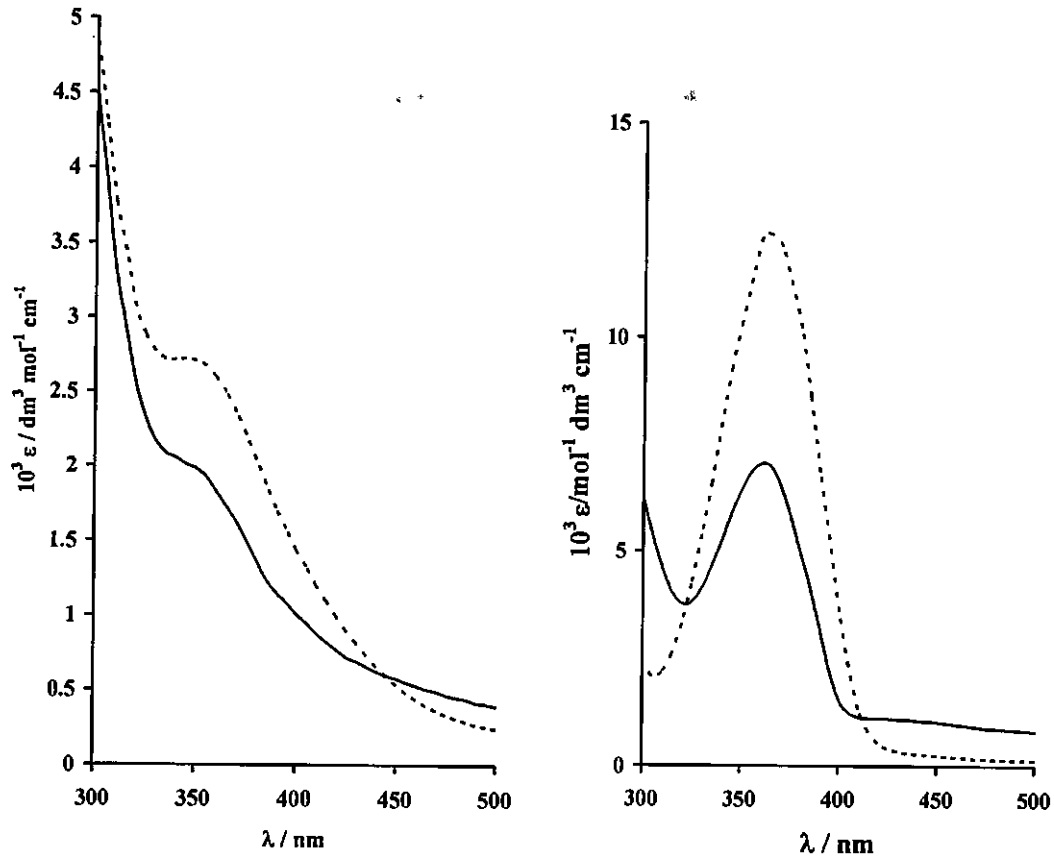

Figure 3.15: UV/visible spectra of the protonated (solid line) and deprotonated (dotted line) forms of the β-diketones, Hbnp (left) and Hthba (right), in 10% acetonitrile/water mixture. μ = 0.100 mol dm^{-3} ($NaClO_4$) at 20.0(1)°C.

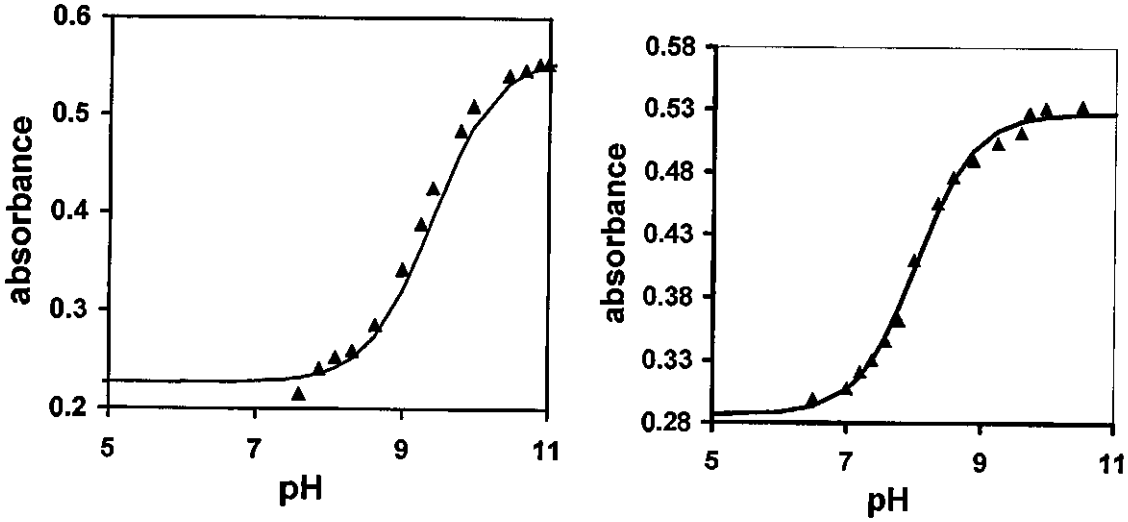

Figure 3.16: Effect of pH on absorbance, for Hthba at 400 nm (Left) and Hbnp at 360 nm (Right) in 10% acetonitrile/water mixture. μ = 0.100 mol dm^{-3} ($NaClO_4$) at 20.0(1)°C. The solid line represents the least square fit of Equation 3. 3.

3.4 Cyclic voltammetry

3.4.1 Introduction.

Cyclic voltammetry (CV) were conducted on representative examples of the synthesized titanium complexes. The formal reduction potentials of the redox active $Ti^{III/IV}$ centre in the synthesized complexes were determined. From the formal reduction potential an attempt was made to quantify the electronic influence (if any) of the different R substituents on the redox active metal centre of each of these compounds. The redox active couples vary from electrochemically reversible (defined as $\Delta E < 100$ mV since ferrocene showed electrochemically and chemically reversible behaviour with $\Delta E = 100$ mV in this study), quasi-reversible (defined for the purpose of this study as 100 mV $< \Delta E <$ 150 mV) to irreversible (defined as $\Delta E > 150$ mV). To minimize the liquid junction potentials and overpotentials, an in-house constructed Ag/AgCl-wire reference electrode was used. All formal reduction potentials ($E^{o\prime}$), peak anodic potentials (E_{pa}), and peak cathodic potentials (E_{pc}) are reported against an internal standard (Fc/Fc^+), and measured experimentally against Ag/AgCl. Ferrocene showed electrochemically and chemically reversible behaviour with ΔE = 100 mV and $i_{pa}/i_{pc} = 1.00$, at a scan rate of 50 mV s^{-1}. The cyclic voltammetric behaviour of the series of octahedral β-diketonato titanium(IV) complexes of the type, Ti(β-diketonato)$_2$Cl$_2$ and Ti(β-diketonato)$_2$(biphen), where β-diketonato = acac (acetylacetonato, $CH_3COCHCOCH_3^-$), ba (benzoylacetonato, $C_6H_5COCHCOCH_3^-$), dbm (dibenzoylmethanato, $C_6H_5COCHCOC_6H_5^-$) and tfba (trifluorobenozylacetonato, $C_6H_5COCHCOCF_3^-$), biphen = 2,2'-biphenyldiolato, were studied in CH_2Cl_2/0.1 mol dm^{-3} $[NBu_4][B(C_6F_5)_4]$.

3.4.2 Ti(β-diketonato)$_2$Cl$_2$ Complexes

Cyclic voltammetry results of the dichlorobis(β-diketonato) titanium(IV) complexes, [Ti(β-diketonato)$_2$Cl$_2$] with β-diketonato = acac$^-$, ba$^-$ and dbm$^-$, are shown in **Figure 3.17** and summarized in Table 3. 9. The $Ti^{III/IV}$ couple of these complexes is electrochemically quasi-reversible and chemically reversible, with ΔE = 114-134 mV and i_{pc}/i_{pa} = 0.6 - 1.0 at a scan rate of 50 mV s^{-1}. Ferrocene was added as an internal standard in order to compare the

electrochemical parameters of these complexes with each other. Generally an increase in scan rate result in an increase in ΔE_p of the $Ti^{III/IV}$ couple. This may be due to slow electron transfer. It is also clear that the ability of the β-diketone ligand to stabilise the oxidised metal centre improves in the order:

ba < acac ~ acac.

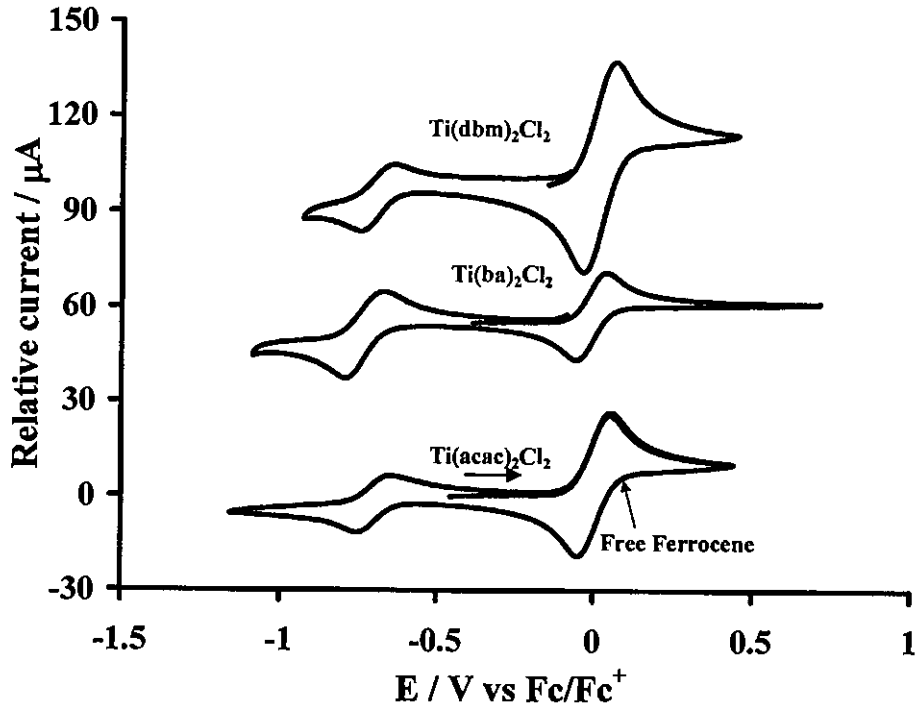

Figure 3.17: Cyclic voltammograms (CV) of the 2.0 mmol dm^{-3} solutions of bis-β-diketonato titanium complexes of the type $[TiCl_2(\beta\text{-diketonato})_2]$, with β-diketonato = acac$^-$, ba$^-$ and dbm$^-$, measured in CH_2Cl_2/0.1 mol dm^{-3} $[NBu_4][B(C_6F_5)_4]$ at a glassy carbon working electrode and a scan rate of 50 mV s^{-1}. T = 25°C. Scans initiated in the direction of the arrow.

Table 3. 9: **The cyclic voltammetry data obtained from voltammograms (*vs.* Fc/Fc^+) of various bis-β-diketonato titanium complexes of the type $[TiCl_2(\beta\text{-diketonato})_2]$ with β-diketonato = dbm^-, $acac^-$, ba^- measured in 0.1 mol dm^{-3} tetrabutylammonium tetrakis(pentafluorophenyl)borate/CH_2Cl_2 with a glassy carbon working electrode at 25°C, ferrocene added as an internal standard and a scan rate of 50, 100, 200 and 300 mV s^{-1}. Data tabulated is of the $Ti^{III/IV}$ couple. The concentration of the titanium complexes was 2.0 mmol dm^{-3}.**

Titanium complexes	scan rate	E_{pc} / mV	ΔE_p / mV	$E^{0\prime}$ / mV	i_{pc} / μA	i_{pc}/i_{pa} *
free Ferrocene***	50	-50	100	0	25.4	1.00
$[TiCl_2(dbm)_2]$	50	-766	114	-709	3.7	0.6
	100	-766	118	-707	4.8	0.7
	200	-772	130	-707	6.3	0.7
	300	-782	146	-709	7.5	0.6
$[TiCl_2(acac)_2]$	50	-763	116	-705	9.0	0.9
	100	-768	123	-707	10.7	0.8
	200	-785	144	-713	14.0	0.7
	300	-790	155	-713	17.1	0.8
$[TiCl_2(ba)_2]$	50	-794	134	-727	7.9	1.0
	100	-798	147	-725	11.0	0.8
	200	-807	165	-725	15.1	0.8
	300	-814	179	-725	18.2	0.7

* i_{pa}/i_{pc} **for ferrocene**

** **data for the** Fc/Fc^+ **couple and internal standard.**

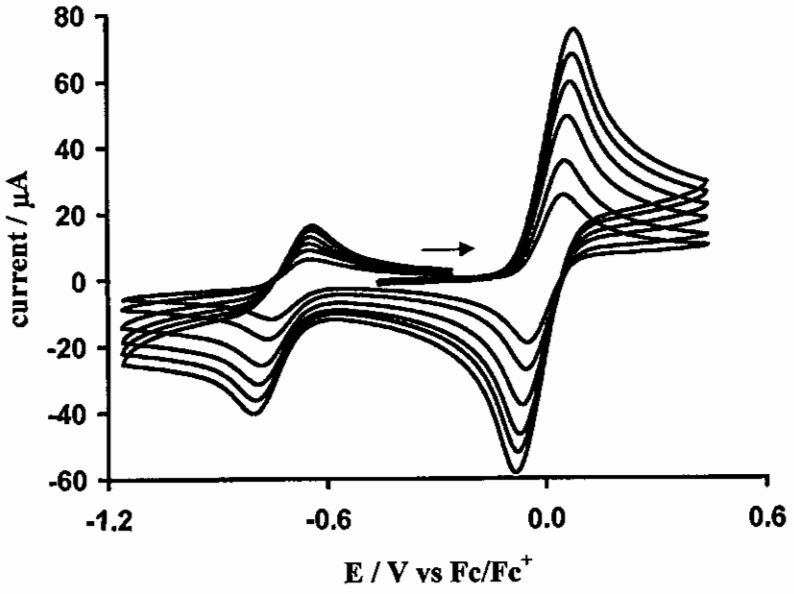

Figure 3. 18: **The cyclic voltammograms of a 2.0 mmol dm^{-3} $Ti(acac)_2Cl_2$ (supporting electrolyte is 0.1 mol dm^{-3} tetrabutylammonium tetrakis(pentafluorophenyl)borate) in dichloromethane witb a glassy carbon working electrode at 25°C and scan rates of 50, 100, 200, 300, 400 and 500 mV s^{-1}. Scans initiated in the direction of the arrow.**

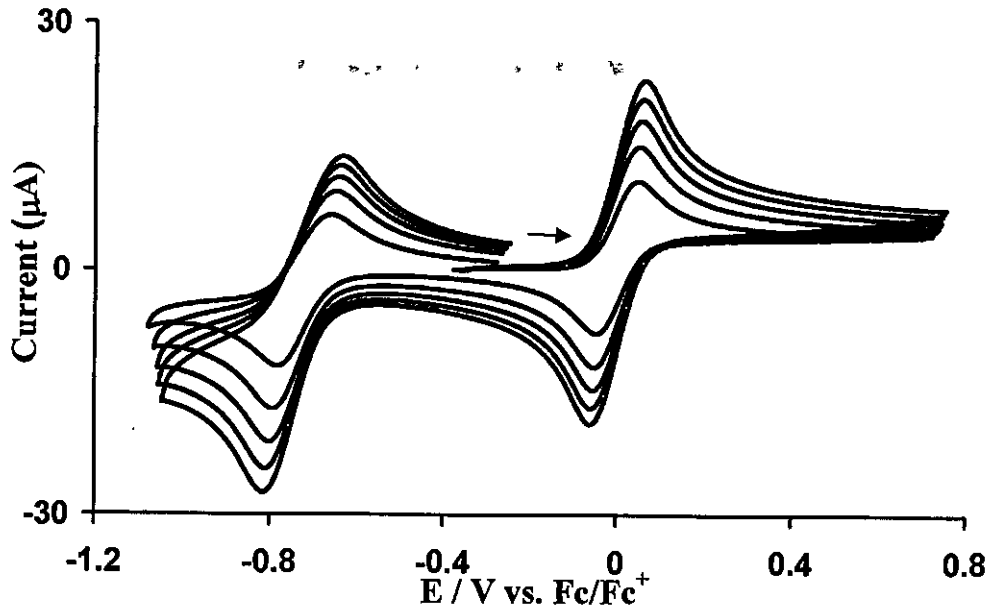

Figure 3. 19: **The cyclic voltammograms of 2.0 mmol dm^{-3} $Ti(ba)_2Cl_2$ (supporting electrolyte is 0.1 mol dm^{-3} tetrabutylammonium tetrakis(pentafluorophenyl)borate) in dichloromethane, with a glassy carbon working electrode at 25°C and scan rates of 100-500 mV s^{-1} (100 mV increments). Scans initiated in the direction of the arrow.**

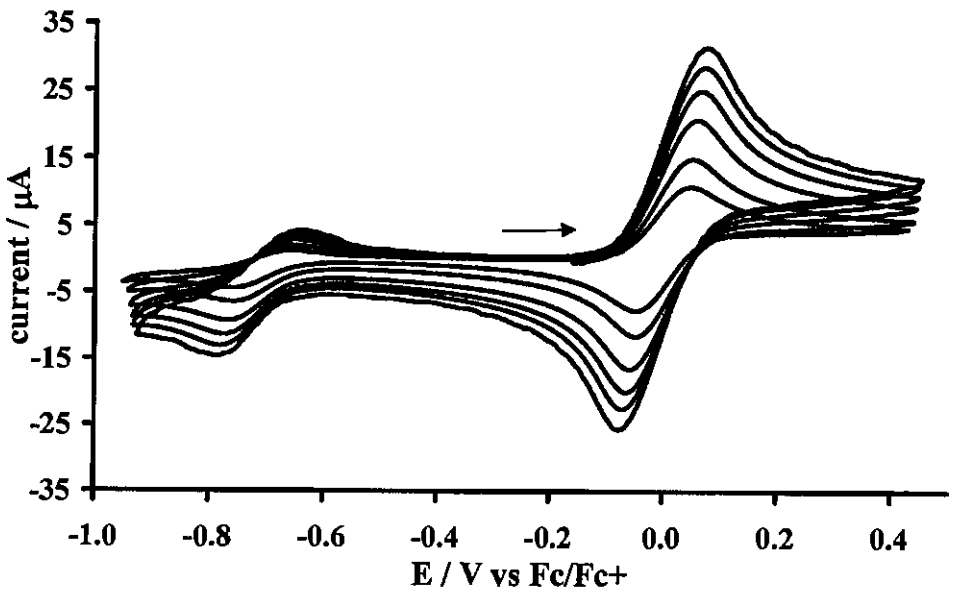

Figure 3. 20: **The cyclic voltammograms of 2.0 mmol dm^{-3} $Ti(dbm)_2Cl_2$ (supporting electrolyte is 0.1 mol dm^{-3} tetrabutylammonium tetrakis(pentafluorophenyl)borate) in dichloromethane with a glassy carbon working electrode at 25°C and scan rates of 100-500 mV s^{-1} (100 mV increments). Scans initiated in the direction of the arrow.**

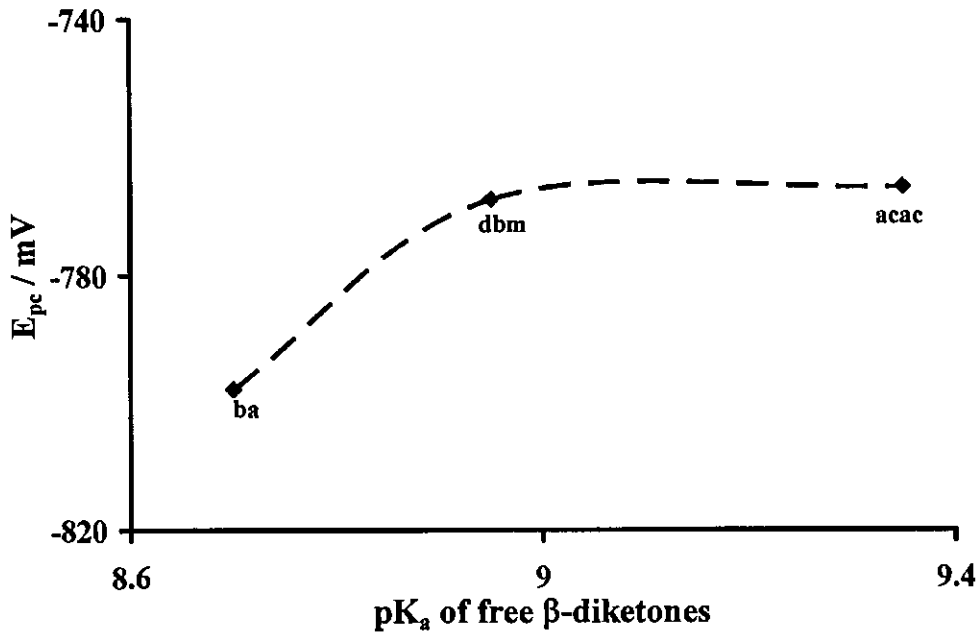

Figure 3. 21: **Graph of the relationship of peak cathodic potentials of the bis-β-diketonato titanium complexes, dichlorobis(β-diketonato)titanium(IV), of the type, $[TiCl_2(\beta\text{-diketonato})_2]$, with β-diketonato = acac$^-$, ba$^-$ and dbm$^-$, measured in 0.1 mol dm^{-3} tetrabutylammonium tetrakis(pentafluorophenyl)borate/CH_2Cl_2 with a glassy carbon working electrode, at 25°C, and a scan rate of 100 mV s^{-1}, *vs* pK_a for the free β-diketone. The β-diketonato ligands are as indicated.**

The general trend that is observed is that with increasing pK_a there is an increase in E_{pc} (Figure 3. 21). An increase in pK_a leads to the improved ability of the β-diketone to stabilise the Ti(IV) centre, thus an increase in E_{pc}, *i.e.,* Ti(IV) centre becomes a weaker oxidising agent.

3.4.3 Ti(β-diketonato)$_2$biphen Complexes

Cyclic voltammograms from dichlorobis(β-diketonato) titanium(IV) complexes, [Ti(β-diketonato)$_2$biphen], with β-diketonato = acac$^-$, ba$^-$, tfba$^-$ and dbm$^-$, at a scan rate of 100 mV s^{-1} and T = 25°C, are shown in Figure 3. 22 and summarized in Table 3.10. Free ferrocene is used as internal standard. The dichlorobis(β-diketonato) titanium(IV) complexes were found to exhibit an electrochemical quasi to irreversible Ti^{III}/Ti^{IV} couple according to:

$$Ti^{IV} + e^- \rightleftharpoons Ti^{III}$$

with 131 mV < ΔE_p < 215 mV for the one-electron transfer process involved. Electrochemical reversibility was observed with $i_{pa}/i_{pc} \sim 1$, except for the tfba complex where $i_{pa}/i_{pc} = 0.5$.

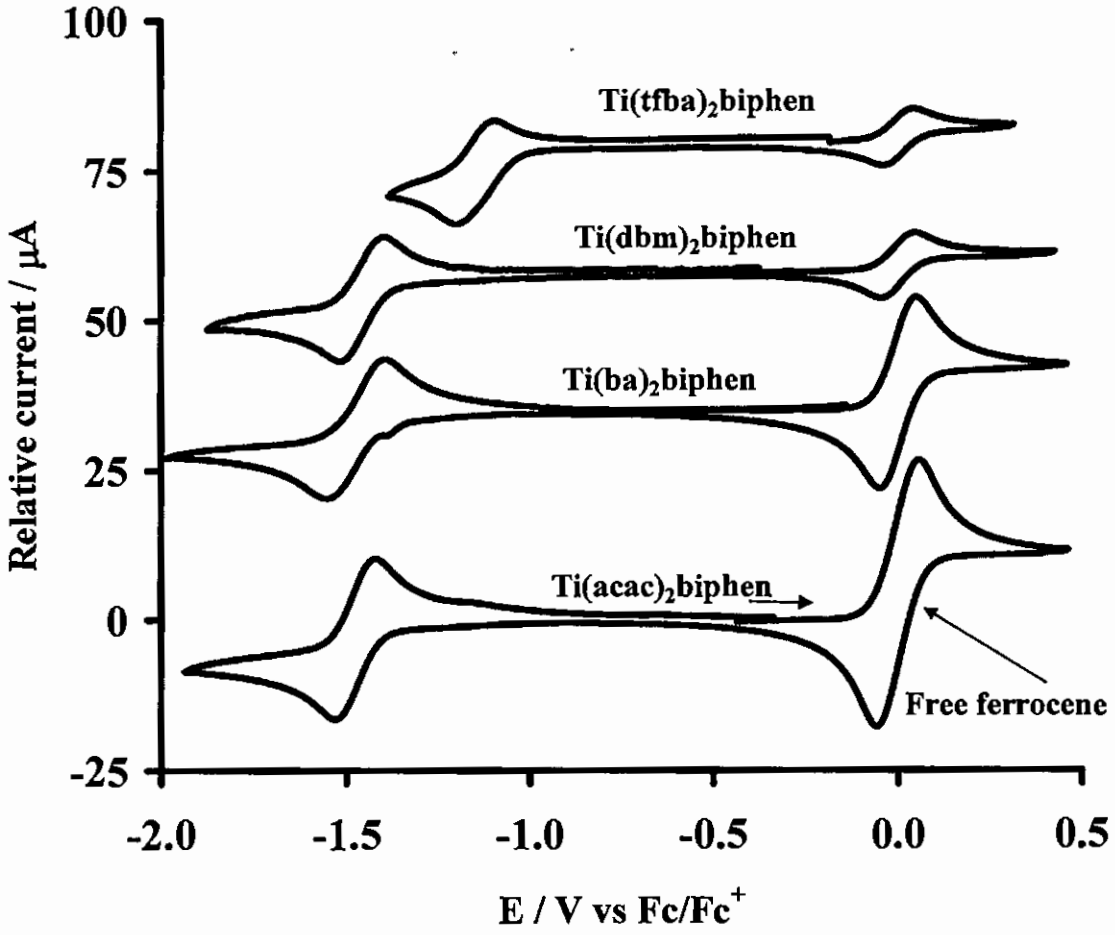

Figure 3. 22: **Cyclic voltammograms (CV) of the 2.0 mmol dm^{-3} solutions of bis-β-diketonato titanium complexes of the type [Ti(β-diketonato)$_2$biphen] with β-diketonato = acac$^-$, ba$^-$, dbm$^-$ and tfba$^-$ measured in CH_2Cl_2/0.1 mol dm^{-3} $[NBu_4][B(C_6F_5)_4]$ at a glassy carbon working electrode and a scan rate of 100 mV s^{-1}. T = 25°C. Scans initiated in the direction of the arrow.**

Table 3.10: The cyclic voltammetry data obtained from voltammograms (*vs.* Fc/Fc$^+$) of various bis-β-diketonato titanium complexes of the type, [Ti(β-diketonato)$_2$biphen], with β-diketonato = dbm$^-$, acac$^-$, ba$^-$ and tfba$^-$ measured in 0.1 mol dm^{-3} tetrabutylammonium tetrakis(pentafluorophenyl)borate/CH_2Cl_2, with a glassy carbon working electrode at 25°C, and a scan rate of 100 mV s^{-1}. Data tabulated is of the $Ti^{III/IV}$ couple. The concentration of the titanium complexes was 2.0 mmol dm^{-3}.

complexes	E_{pc} / mV	ΔE_p / mV	E^{01} / mV	$(\chi_{R1} + \chi_{R2})$ / (Gordy scale)	pK_a of β-diketonato	i_{pc} / μA	i_{pc}/i_{pa}
[Ti(dbm)$_2$biphen]	-1530	160	-1450	4.42	9.4	13.1	0.9
[Ti(acac)$_2$biphen]	-1551	170	-1478	4.68	8.95	22.9	0.9
[Ti(ba)$_2$biphen]	-1585	214	-1478	4.55	8.7	16.1	1.0
[Ti(tfba)$_2$biphen]	-1213	131	-1148	5.22	6.3	11.5	0.5

Cyclic voltammetry results at different scan rates of the [Ti(β-diketonato)$_2$biphen] complexes is given in Figure 3. 23 to Figure 3. 26 and Table 3.11 to Table 3. 14. It is once again clear from **Table 3.10** that the ability of the β-diketone to stabilise the Ti(IV) centre improves

moving from acac ~ ba towards dbm < tfba. This imply that the Ti(IV) centre becomes increasingly difficult to oxidise as more electron density is withdrawn from it by the substituents on the β-diketonato ligand. Furthermore, there is a significant difference in E_{pc} values between the biphen (± 1500 mV *vs.* Fc/Fc^+) the dichloro (± -800 mV *vs.* Fc/Fc^+) compounds, indicative of the shielding of the metal centre by the biphen ligand.

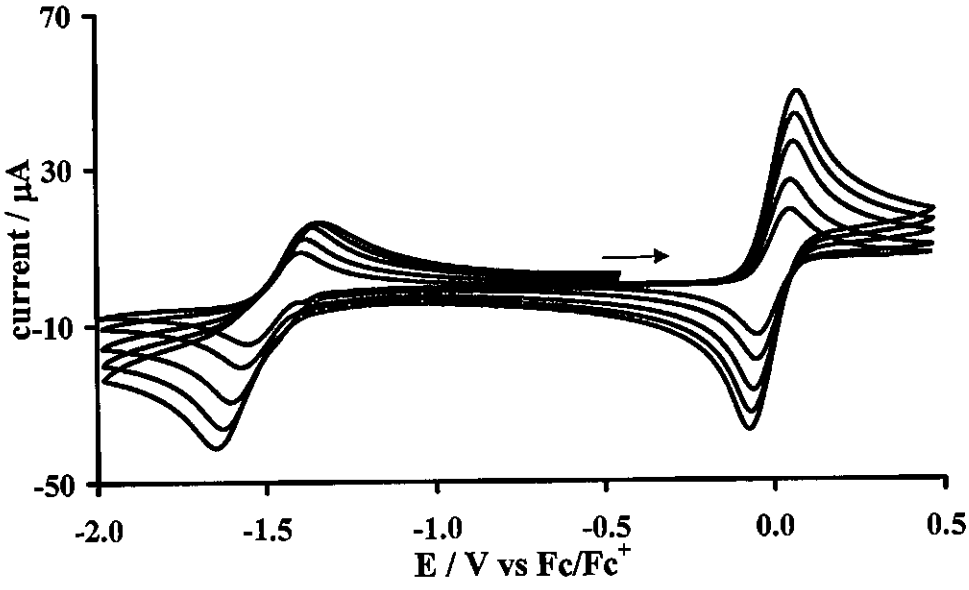

Figure 3. 23: **The cyclic voltammograms of a 2.0 mmol dm^{-3} $Ti(ba)_2$biphen (supporting electrolyte is 0.1 mol dm^{-3} tetrabutylammonium tetrakis(pentafluorophenyl)borate) in dichloromethane with a glassy carbon working electrode at 25°C and a scan rates of 50, 100, 200, 300 and 400 mV s^{-1} (100 mV increments). Scans initiated in the direction of the arrow.**

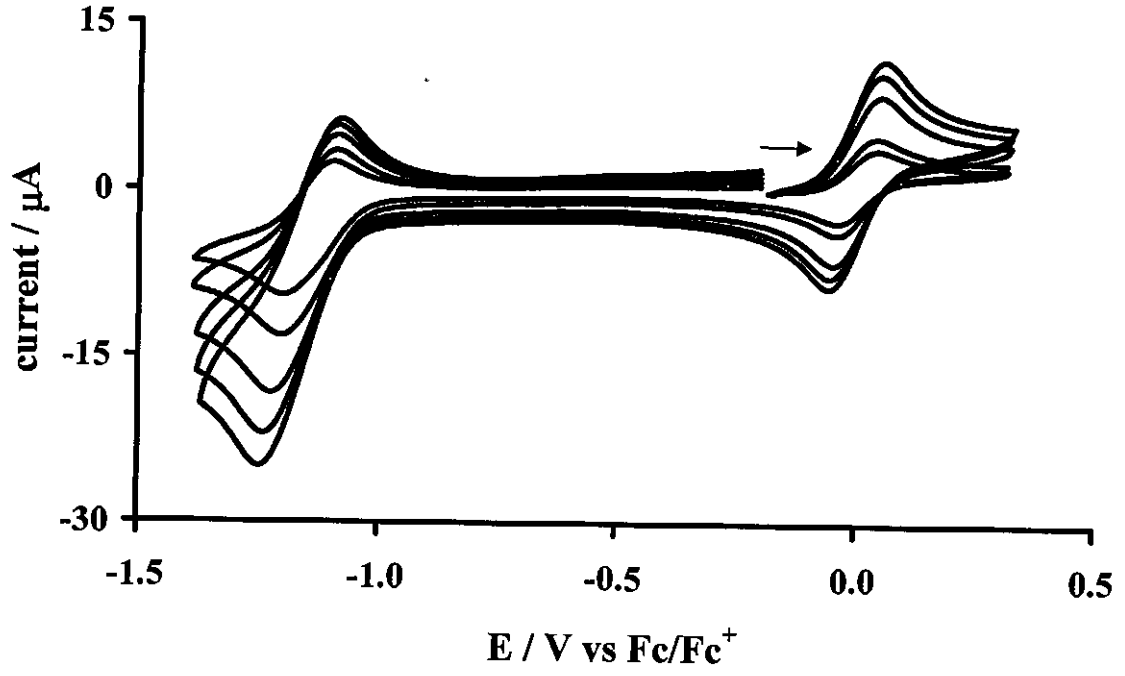

Figure 3. 24: **The cyclic voltammograms of 2.0 mmol dm^{-3} $Ti(tfba)_2biphen$ (supporting electrolyte is 0.1 mol dm^{-3} tetrabutylammonium tetrakis(pentafluorophenyl)borate) in dichloromethane with a glassy carbon working electrode at 25°C and scan rates of 50, 100, 200, 300 and 400 mV s^{-1}. Scans initiated in the direction of the arrow.**

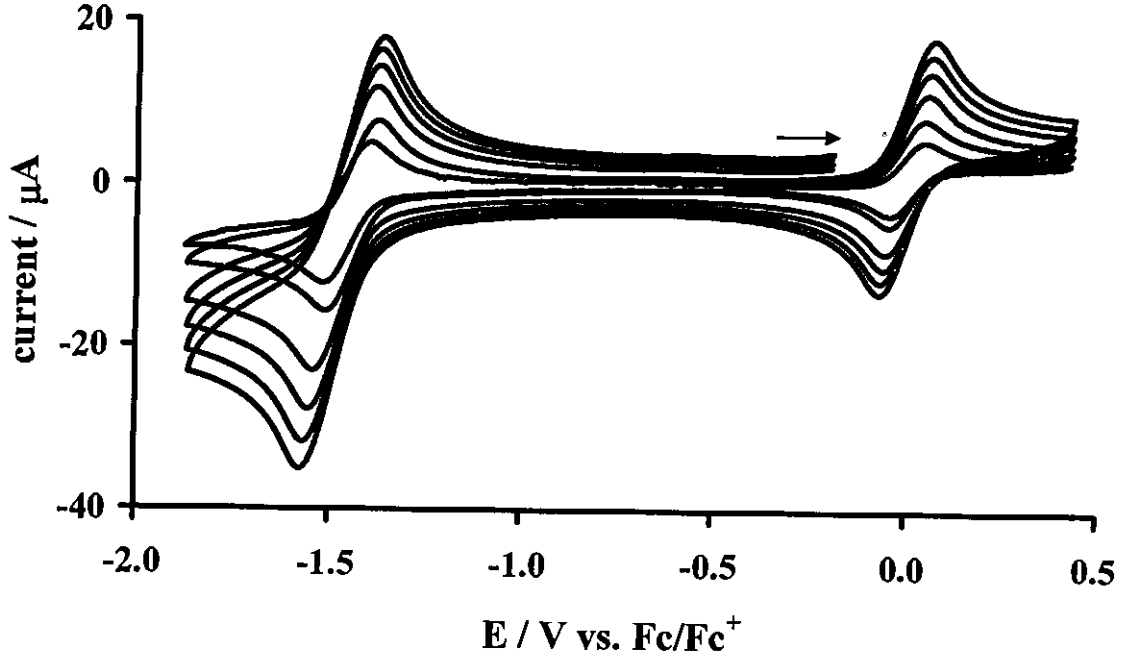

Figure 3. 25: **The cyclic voltammograms of 2.0 mmol dm^{-3} $Ti(dbm)_2biphen$ (supporting electrolyte is 0.1 mol dm^{-3} tetrabutylammonium tetrakis(pentafluorophenyl)borate) in dichloromethane with a glassy carbon working electrode at 25°C and scan rates of 50, 100, 200, 300 and 500 mV s^{-1}. Scans initiated in the direction of the arrow.**

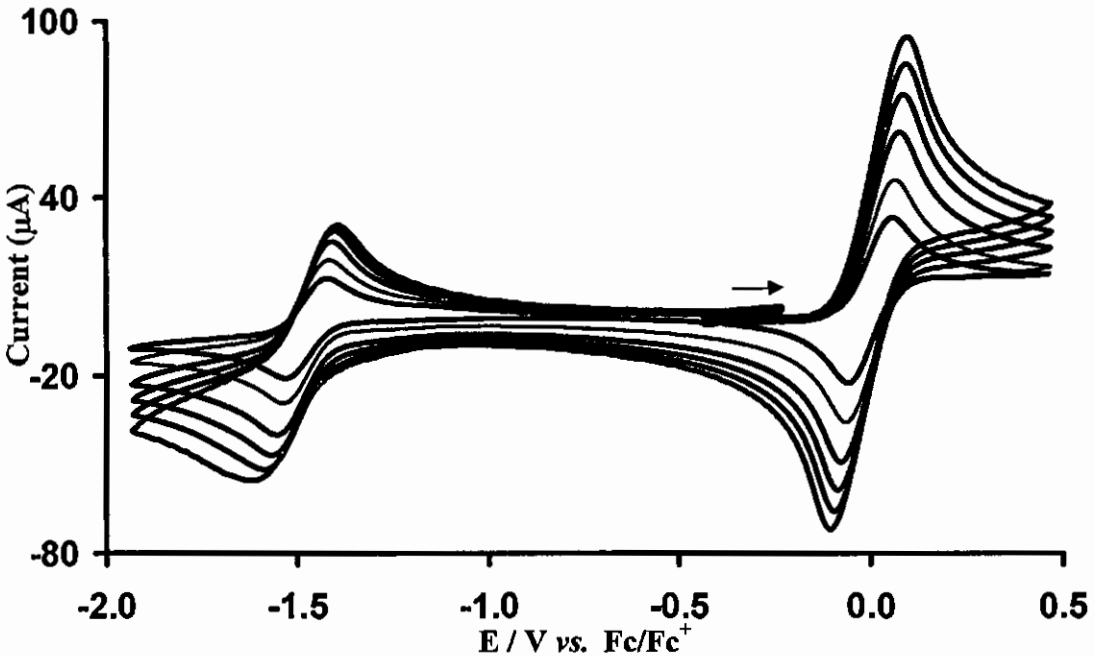

Figure 3. 26: **The cyclic voltammograms of 2.0 mmol dm^{-3} Ti(acac)$_2$biphen (supporting electrolyte is 0.1 mol dm^{-3} tetrabutylammonium tetrakis(pentafluorophenyl)borate) in dichloromethane with a glassy carbon working electrode at 25°C and scan rates of 50, 100, 200, 300, 400 and 500 mV s^{-1}. Scans initiated in the direction of the arrow.**

Table 3.11: The cyclic voltammetry data obtained from voltammograms (*vs.* Fc/Fc$^+$) of [Ti(acac)$_2$biphen] and free ferrocene measured in 0.1 mol dm^{-3} tetrabutylammonium tetrakis[pentafluorophenyl]borate/ CH_2Cl_2 with a glassy carbon working electrode at 25°C. Scan rates, E_{pc} (cathodic peak potential), ΔE_p (difference between the anodic and cathodic peak potentials), E^{01} (formal reduction potentials), and i_{pc}/i_{pa} (cathodic/anodic peak current relationship) are shown. The concentration of [Ti(tfba)$_2$biphen] was 2.0 mmol dm^{-3}. $E^{01} = (E_{pa} + E_{pc})/2$.

ν / mV s^{-1}	E_{pc} / mV	ΔE_p / mV	E^{01} / mV	i_{pc}/i_{pa}*
Fc at 50***	-74	144	0	1.0
12 at 50	-1546	147	-1477	1.0
12 at 100	-1551	170	-1478	0.9
12 at 200	-1567	191	-1482	0.9
12 at 300	-1582	213	-1486	0.9
12 at 400	-1599	249	-1492	0.9

*** i_{pa}/i_{pc} for ferrocene**
***** internal standard**

It can be seen from **Table 3.11**, that the [Ti(acac)$_2$biphen] displays a reduction as well as an oxidation peak with i_{pa}/i_{pc}` = 1, which represents a chemically reversible and electrochemical quasi-reversible process at a scan rate of 50 mV s^{-1} with ΔE_p = 147 mV. It is known that ferrocene exhibits an electrochemical reversible process and ΔE_p values for ferrocene as internal standard were found to be between 102 mV and 144 mV. The large ΔE_p is due to the slow electron transfer kinetics between the metal ions in solution and the electrode.

Table 3. 12: **The cyclic voltammetry data obtained from voltammograms (*vs.* Fc/Fc$^+$) of [Ti(ba)$_2$biphen] and free ferrocene measured in 0.1 mol dm^{-3} tetrabutylammonium tetrakis[pentafluorophenyl]borate/ CH_2Cl_2 with a glassy carbon working electrode at 25°C. Scan rates, E_{pc} (cathodic peak potential), ΔE_p (difference between the anodic and cathodic peak potentials), E^{01} (formal reduction potentials), and i_{pc}/i_{pa} (cathodic/anodic peak current relationship) are shown. The concentration of the [Ti(tfba)$_2$biphen] was 2.0 mmol dm^{-3}. $E^{01} = (E_{pa} + E_{pc})/2$.**

ν / mV s^{-1}	E_{pc} / mV	ΔE_p / mV	E^{01} / mV	i_{pc}/i_{pa}*
Fc at 50***	-63	124	0.0	1.0
11 at 50	-1567	183	-1475	1.1
11 at 100	-1585	214	-1478	1.0
11 at 200	-1616	261	-1486	0.9
11 at 300	-1641	300	-1491	0.7
11 at 400	-1662	338	-1493	0.6

* i_{pa}/i_{pc} **for ferrocene**
*** **internal standard**

Table 3. 13: **The cyclic voltammetry data obtained from voltammograms (*vs.* Fc/Fc$^+$) of [Ti(dbm)$_2$biphen] and free ferrocene measured in 0.1 mol dm^{-3} tetrabutylammonium tetrakis[pentafluorophenyl]borate/CH_2Cl_2 with a glassy carbon working electrode at 25°C. Scan rates, E_{pc} (cathodic peak potential), ΔE_p (difference between the anodic and cathodic peak potentials), E^{01} (formal reduction potentials), and i_{pc}/i_{pa} (cathodic/anodic peak current relationship) are shown. The concentration of the [Ti(tfba)$_2$biphen] was 2.0 mmol dm^{-3}. $E^{01} = (E_{pa} + E_{pc})/2$.**

ν / mV s^{-1}	E_{pc} / mV	ΔE_p / mV	E^{01} / mV	i_{pc}/i_{pa}*
Fc at 50***	-59	115	1.0	1.0
10 at 50	-1521	142	-1450	0.9
10 at 100	-1530	160	-1450	0.9
10 at 200	-1550	179	-1461	0.9
10 at 300	-1568	204	-1466	0.9
10 at 400	-1581	222	-1467	0.9

* i_{pa}/i_{pc} **for ferrocene**
*** **internal standard**

Table 3. 14: **The cyclic voltammetry data obtained from voltammograms (*vs.* Fc/Fc$^+$) of [Ti(tfba)$_2$biphen] and free ferrocene measured in 0.1 mol dm^{-3} tetrabutylammonium tetrakis[pentafluorophenyl]borate/ CH_2Cl_2 with a glassy carbon working electrode at 25°C. Scan rates, E_{pc} (cathodic peak potential), ΔE_p (difference between the anodic and cathodic peak potentials), E^{01} (formal reduction potentials), and i_{pc}/i_{pa} (cathodic/anodic peak current relationship) are shown. The concentration of the [Ti(tfba)$_2$biphen] was 2.0 mmol dm^{-3}. $E^{01} = (E_{pa} + E_{pc})/2$.**

ν / mV s^{-1}	E_{pc} / mV	ΔE_p / mV	E^{01} / mV[a]	i_{pc}/i_{pa}*
Fc at 50***	-51	102	0	0.9
13 at 50	-1205	119	-1146	0.5
13 at 100	-1213	131	-1148	0.5
13 at 200	-1234	155	-1157	0.4
13 at 300	-1252	163	-1171	0.4
13 at 400	-1258	185	-1165	0.3

* i_{pa}/i_{pc} **for ferrocene**
*** **internal standard**

3.5 Substitution Kinetics

The substitution of two Cl^- ions from $[Ti(acac)_2Cl_2]$, **7**, with 2,2'-biphenyldiolato^{-2} to give the product, $[Ti(acac)_2biphen]$, **12**, is reported in this section.

3.5.1 The Beer Lambert Law

The UV spectra of $[Ti(acac)_2Cl_2]$, **7**, and the product of substitution $[Ti(acac)_2biphen]$, **12**, from the reaction of $[Ti(acac)_2Cl_2]$ and 2,2'-biphenyldiol (biphen) in acetonitrile at 25°C are given in **Figure 3.27**. The linear relationship between the absorbance, A, and concentration of $[Ti(acac)_2Cl_2]$ and $[Ti(acac)_2biphen]$ at $\lambda_{experimental}$ = 340 nm (**Figure 3.27**) confirm the validity of the Beer Lambert law ($A = \varepsilon cl$, with ε = extinction coefficient and l = path length = 1 cm) for both titanium(IV) complexes.

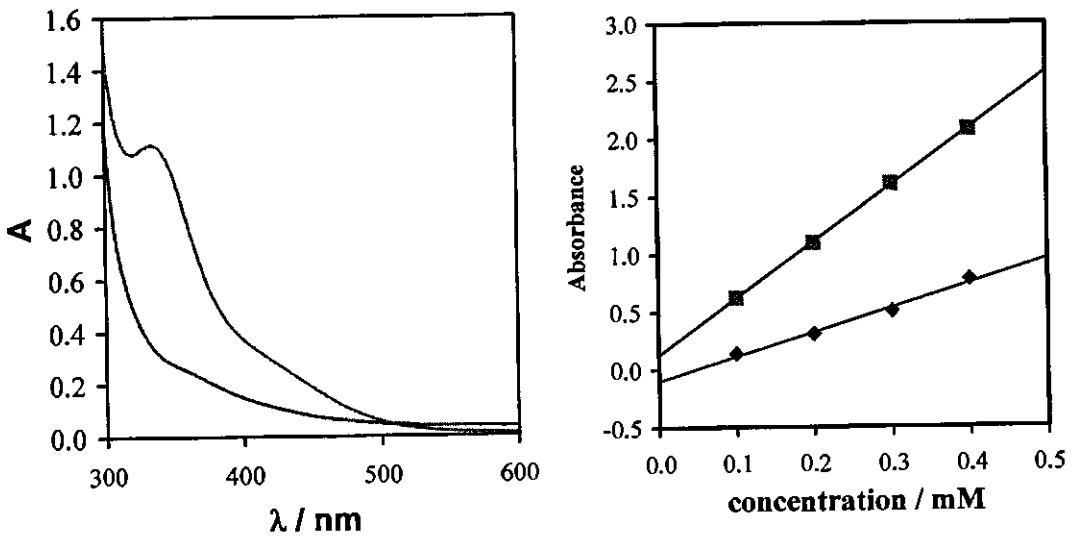

Figure 3.27: Left: UV spectra of 0.2 mmol dm^{-3} solutions of $[Ti(acac)_2Cl_2]$ (bottom graph) and $[Ti(acac)_2biphen]$ (top graph). Right: The linear relationship between absorbance and concentration of $[Ti(acac)_2Cl_2]$ (bottom graph) and $[Ti(acac)_2biphen]$ (top graph) complexes at λ = 340 nm confirms the validity of the Beer Lambert law, A = εcl, for (7) and (12).

3.5.2 Product Identification from the Substitution Reaction of $Ti(acac)_2Cl_2$ with H_2biphenol.

The substitution reaction of $[Ti(acac)_2Cl_2]$, 7, and 2,2'-biphenyldiol was followed by means of UV/vis spectroscopy. The synthesis of the product of the substitution reaction, $[Ti(acac)_2biphen]$, **12**, is described in paragraph 3.2.3. The product, **12**, was formed after refluxing $[Ti(acac)_2Cl_2]$ and 2,2'-biphenyldiol at 82°C for *ca.* 5 hours. To confirm that the same product, **12**, formed at experimental temperatures 15°C, 25°C and 36°C, at which the substitution kinetics was followed, the synthesis was repeated at room temperature and the formation of the product was also followed by ^1H NMR at 25°C.

3.5.2.1 Synthesis of the product of substitution at room temperature

Stoichiometric amounts of $[Ti(acac)_2Cl_2]$ (0.1010 g, 0.31 mmol) and 2,2'-biphenyldiol (0.0585 g, 0.31 mmol) were stirred at room temperature (RT) for 25 hours under a N_2 atmosphere, representing second-order conditions. The unreacted reactants were washed with methanol, the precipitant filtered and stored under argon atmosphere. A yield of 11 mg (8.2 %) was obtained. Heat and the excess of 2,2'-biphenyldiol is needed to drive the reaction to completion:

$$[Ti(acac)_2Cl_2] + 2,2'\text{-biphenyldiol} \rightleftharpoons [Ti(acac)_2biphen] + 2HCl$$

The ^1H NMR spectrum of the reaction product from this synthesis is identical to the ^1H NMR spectrum of the product synthesized under reflux. The reaction at RT confirms that the substitution of chlorine ligands with 2,2'-biphenyldiol in $[Ti(acac)_2Cl_2]$ takes place at RT.

3.5.2.2 The ^1H NMR monitored reaction between $[Ti(acac)_2Cl_2]$ and 2,2'-biphenyldiol

The reaction between $[Ti(acac)_2Cl_2]$ and 2,2'-biphenyldiol was followed qualitatively via NMR with the purpose of identifying the reaction product. A mixture of $[Ti(acac)_2Cl_2]$ and a slight excess of 2,2'-biphenyldiol was monitored on ^1H NMR for 3 days. The obtained ^1H NMR spectra in $CDCl_3$ shows a slow conversion to the product. Additionally, the ^1H NMR spectra show an extra peak at δ = 7.6 ppm (See Figure 3. 28). This peak might be a consequence of the presence of HCl produced by the reaction. No other product, *e.g.*

[Ti(biphen)$_2$] was observed. After 3 days $CDCl_3$ was removed by evaporation and the obtained precipitate washed with methanol. A clean ^1H NMR spectrum consistent with [Ti(acac)$_2$biphen] was obtained.

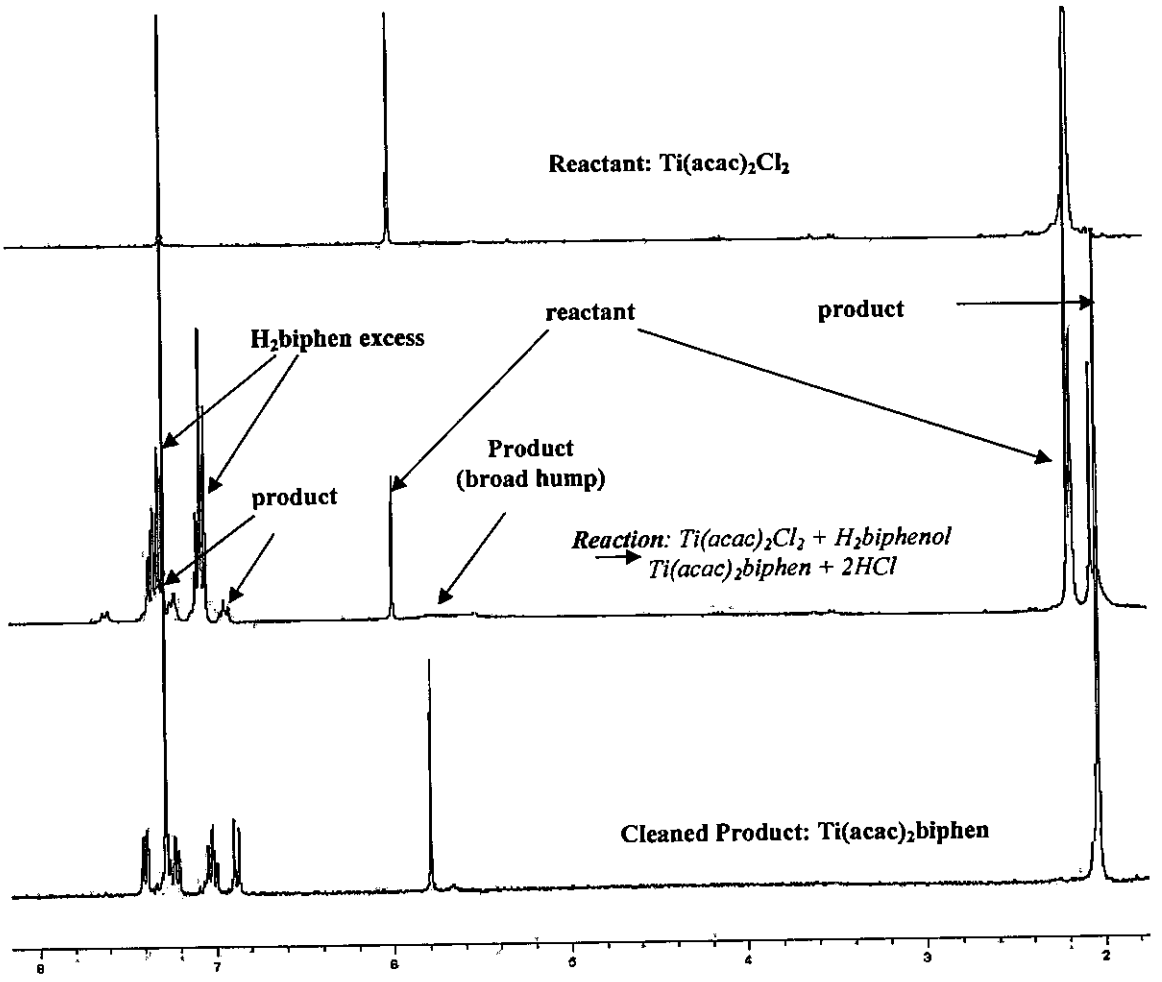

Figure 3. 28: **^1H NMR spectrum in $CDCl_3$ of a mixture of [Ti(acac)$_2$Cl$_2$] and 2,2'-biphenyldiol. The formation of the product, [Ti(acac)$_2$biphen], is indicated.**

3.5.2.3 UV/vis monitored reaction between [Ti(acac)$_2$Cl$_2$] and 2,2'-biphenyldiol

The UV/vis spectra of the reaction between [Ti(acac)$_2$Cl$_2$] and 2,2'-biphenyldiol are given in Figure 3. 29. The UV/vis spectra of the reactions were taken at equal time intervals until the reactions were complete. The final spectrum obtained looks similar to [Ti(acac)$_2$biphen]'s UV/vis spectrum (See **Figure 3.27**). As the reaction progressed, there was an increase in absorption of the [Ti(acac)$_2$Cl$_2$] spectrum, until it approaches spectra of [Ti(acac)$_2$biphen].

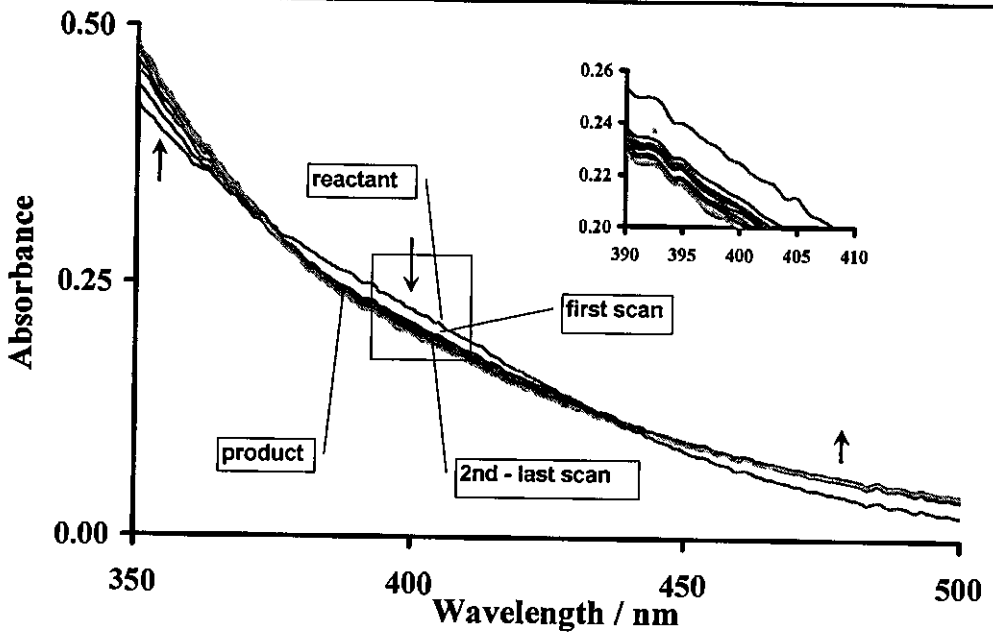

Figure 3. 29: **UV/vis spectra of a mixture of $[Ti(acac)_2Cl_2]$ and 2,2'-biphenyldiol in CH_3CN. The first spectrum of the reactant was taken 10 s after mixing. Hereafter spectra were obtained every 300 s. The formation of the product, $[Ti(acac)_2biphen]$, is indicated. The insert: the expansion for the reaction between 390 nm and 410 nm.**

The above-mentioned results are consistent with $[Ti(acac)_2biphen]$ as reaction product from the substitution reaction of Cl^- in $Ti(acac)_2Cl_2$ by the 2,2'-biphenyldiol ligand.

3.5.3 Substitution Kinetics of Ti(β-diketonato)$_2$Cl$_2$ with H$_2$biphenol.

In this section the substitution of the Cl^- ligand in the titanium(IV) complex, $[Ti(acac)_2Cl_2]$, with the 2,2'-biphenyldiol is reported. It is observed that 2,2'-biphenyldiol reacts with $[Ti(acac)_2Cl_2]$ with the replacement both Cl^- ligands, as illustrated in Scheme 3. 7.

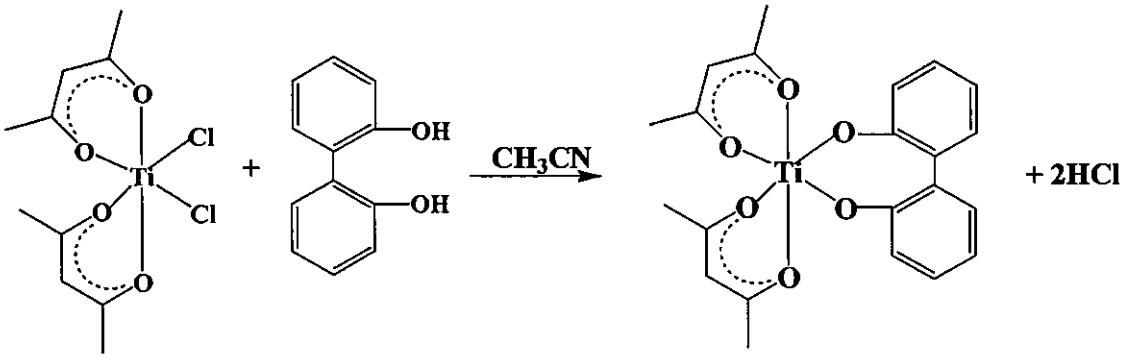

Scheme 3. 7: **Substitution of Cl⁻ in the octahedral titanium(IV) complex, $[Ti(acac)_2Cl_2]$, with 2,2'-biphenyldiol, to give $[Ti(acac)_2biphen]$.**

The above substitution reaction was studied by means of UV/vis techniques under pseudo first order conditions with the concentration of the incoming 2,2'-biphenyldiol ligand at least ten times higher than the concentration of the titanium complex. The reaction was followed at 340 nm. Figure 3. 30 illustrates typical absorbance *vs.* time data obtained. The temperature and 2,2'-biphenyldiol concentration dependence of the substitution reaction of Cl^- in $[Ti(acac)_2Cl_2]$ with 2,2'-biphenyldiol is given in Figure 3. 31.

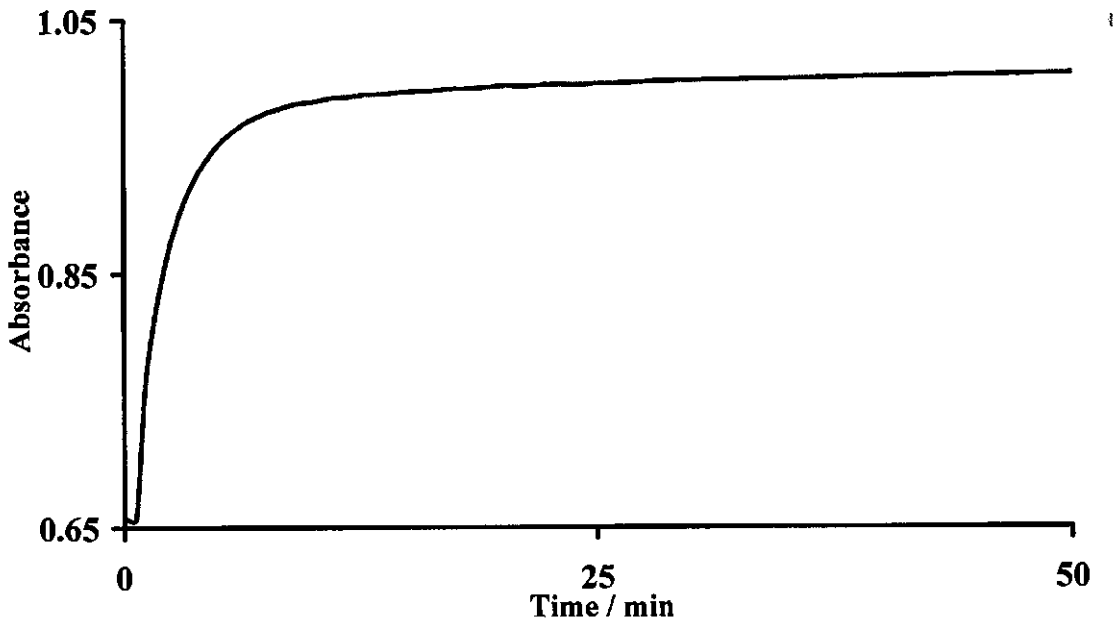

Figure 3. 30: **Absorbance *vs.* time data obtained for the UV/vis monitored substitution reaction in acetonitrile at 340 nm. $[Ti(acac)_2Cl_2]$ = 0.4 mmol dm^{-3}, $[H_2biphen]$ = 40 mmol dm^{-3}.**

Rate constants were calculated utilizing a suitable fitting program[30] which fitted kinetic data to the first-order equation[33], $[A]_t = [A]_0 e^{(-k_{obs} t)}$, where $[A]_t$ = absorbance of selected species at

time t. Upon realizing that [2,2'-biphenyldiol] >> [$Ti(acac)_2Cl_2$], it follows that these graphs satisfy the following equation[33], $k_{obs} = k_1[2,2'\text{-biphenyldiol}] + k_{-1}$, with k_1 = slope and k_{-1} = intercept of the graph of k_{obs} versus [2,2'-biphenyldiol] (See Figure 3. 31).

The enthalpy and entropy of activation, ΔH^* and ΔS^*, for the reaction were determined from the least-squares fits[30] of the reaction rate constants *vs.* temperature data according to the Eyring relationship[33], Equation 3. 4. The Equation 3. 4 can also be written in the linear form, as in Equation 3. 5.

$$k = \frac{k_B T}{h}\exp(\frac{-\Delta H^*}{RT})\exp(\frac{\Delta S^*}{R}) \qquad \text{Equation 3. 4}$$

$$\ln\frac{k}{T} = \frac{-\Delta H^*}{RT} + \frac{\Delta S^*}{R} + \ln\frac{k_B}{T} \qquad \text{Equation 3. 5}$$

k_B is the Boltzmann's constant, h = Planck's constant and R the universal gas constant. A plot of ln(k/T) *vs.* T^{-1} is linear, with a slope of $-\Delta H^*/R$, and an intercept of $\{\ln(k_B/h) + \Delta S^*/R\}$. This linear relationship is illustrated in the relevant temperature *vs.* concentration graphs, *e.g.* Figure 3. 31. The free energy of activation, ΔG^*, may be calculated from the equation, $\Delta G^* = \Delta H^* - T\Delta S^*$.[34] The activation parameters at 298 K are summarized in Table 3. 15.

The pseudo-first-order rate constants were determined for various H_2biphenol concentrations in acetonitrile at three different temperatures (15.0, 24.2 and 36.2 °C). The Eyring curve of $\ln(k_2/T)$ *vs* 1/T of the substitution reaction of [$Ti(acac)_2Cl_2$] with H_2biphenol (2,2'-biphenyldiol) in acetonitrile is given in Figure 3. 31 (right). The values of the second-order rate constants at the various temperatures and activation parameters are given in Table 3. 15.

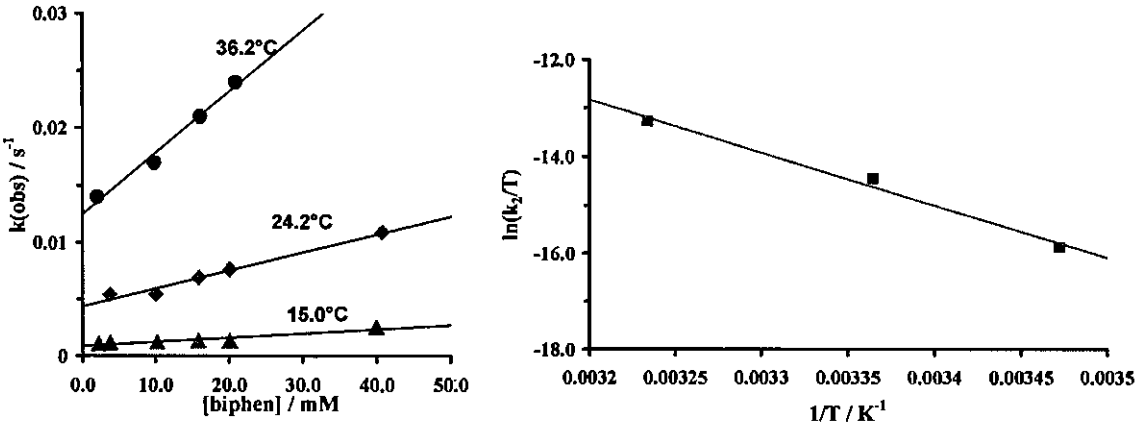

Figure 3. 31: **Left: Graph of k_{obs} *vs* [biphen] for the substitution reaction of $Ti(acac)_2Cl_2$ with H_2biphenol (2,2'-biphenyldiol) ligand at 15.0°C, 24.2°C and 36.2°C. The slope gives the second order rate constant for** Scheme 3. 8. **Right: the graph of $\ln(k_2/T)$ *vs* T^{-1} of 0.0004 mol dm^{-3} $[Ti(acac)_2Cl_2]$ with 2,2'-biphenyldiol.**

Table 3. 15: **The values of the second-order rate constant, k_2, at various temperatures and the activation parameters of the reaction of $[Ti(acac)_2Cl_2]$ with H_2biphenol in acetonitrile.**

Complex	T / °C	10^5 k_2 / dm^3 mol^{-1} s^{-1}	ΔH^* / kJ mol^{-1}	ΔS^* / J mol^{-1} K^{-1}	ΔG^* / kJ mol^{-1}
$Ti(acac)_2Cl_2$	15.0	3.67	90(10)	-10(30)	-93(1)
	24.2	15.8			
	36.2	53.4			

3.5.4 Proposed Mechanism for the Substitution Reaction

The small negative to positive (within experimental error) calculated ΔS^* value is consistent with a dissociative mechanism. This is expected, since titanium complexes with a coordination sphere of seven are unknown. From the UV/vis spectrum (Figure 3. 29), two reactions were observed:

1 A fast first reaction that could not be measured, but can be seen from the difference between the UV spectrum before and just after mixing of the two reactants.

2 A second slower reaction with rate constant given in Table 3. 15.

Scheme 3. 8 gives a schematic presentation of a proposed dissociative mechanism of the substitution reaction of $[Ti(acac)_2Cl_2]$ with 2,2'-biphenyldiol. The schematic representation shows two kinetically indistinguishable mechanisms. For the first mechanism the rate determining step may be the dissociation of the chlorine group from the titanium complex (step I). Step II will then be fast. This mechanism is, however, kinetically indistinguishable

I). Step II will then be fast. This mechanism is, however, kinetically indistinguishable from the one where step I is a fast equilibrium and step II is the rate determining step with rate constant, k_2. The rate constant of the first reaction could not be measured in this study.

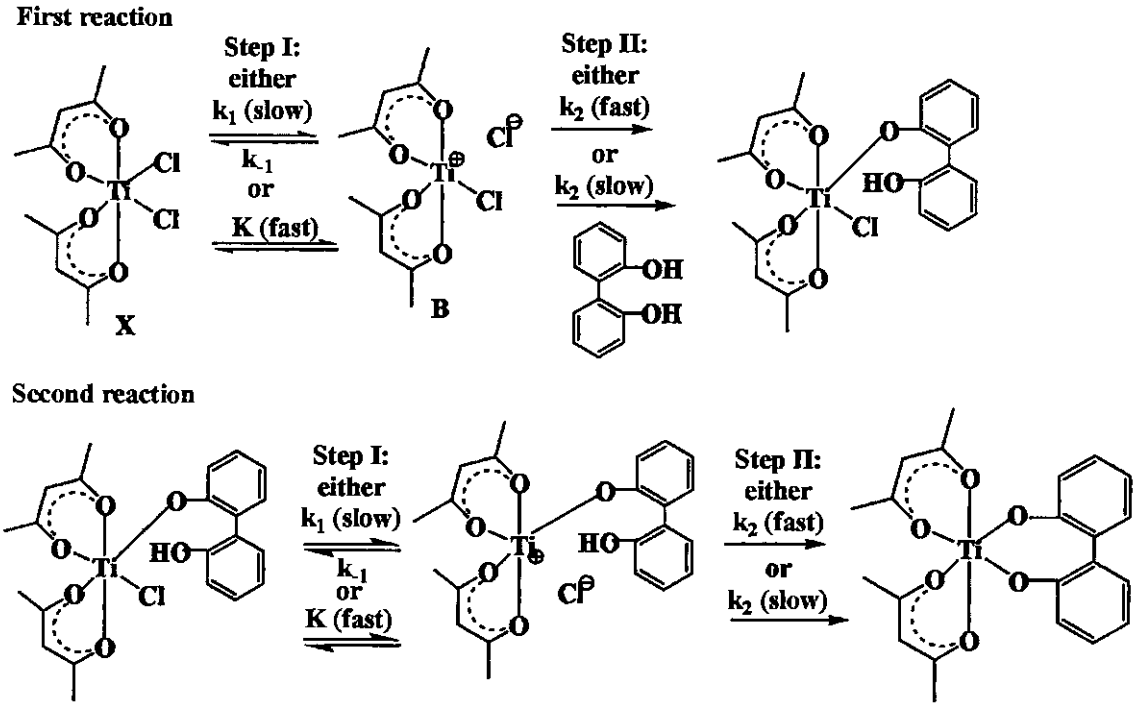

Scheme 3. 8: **Schematic representation of the proposed dissociative mechanism for the substitution reaction between $Ti(acac)_2Cl_2$ with H_2biphenol ligand.**

The reaction as in Scheme 3. 8 takes place in two consecutive reactions involving the substitution of one monodentate (Cl^-) ligand at a time. To derive the rate law for Scheme 3. 8, it is convenient to consider the following equivalent mechanisms where the compounds are substituted with symbols X, B, C and P:

$$X \underset{k_{-1}}{\overset{k_1}{\rightleftharpoons}} B + C \qquad B + Z \xrightarrow{k_2} P \qquad X + Z \longrightarrow C + P$$

Mechanism 1

$$X \overset{K}{\rightleftharpoons} B + C \qquad B + Z \xrightarrow{k_2} P \qquad X + Z \longrightarrow C + P$$

Mechanism 2

The derived rate law for Mechanism 1 is as follows:

$$\frac{d[P]}{dt} = k_2[B][C] \qquad (1)$$

$$\frac{d[B]}{dt} = k_1[X] - k_{-1}[B][C] - k_2[B][Z] = 0$$

$$\therefore [B] = \frac{k_1[X]}{k_{-1}[C] + k_2[Z]} \qquad (2)$$

Substitute equation 2 into equation 1:

$$\frac{d[P]}{dt} = \frac{k_2[Z]k_1[X]}{k_{-1}[C] + k_2[Z]} = \frac{k_1k_2[Z][X]}{k_{-1}[C] + k_2[Z]}$$

If $k_2[Z] << k_{-1}[C]$:

$$\frac{d[P]}{dt} = \frac{k_1k_2[Z][X]}{k_{-1}[C]} = k_A[X][Z]$$

With k_A the rate constant determined experimentally, $k_A = \frac{k_1k_2}{k_{-1}[C]}$ for the first reaction.

For the second reaction follow similarly that

$\frac{d[P]}{dt} = k_B[X][Z]$ with $k_B = \frac{k_1k_2}{k_{-1}[C]}$.

If $k_2[Z] >> k_{-1}[C]$:

$$\frac{d[P]}{dt} = \frac{k_1k_2[Z][X]}{k_2[Z]} = k_1[X]$$

This shows that the reaction is independent of Z. The reaction was found to be first order in Z. Therefore the kinetic results eliminate the second option, $k_2[Z] >> k_{-1}[C]$, from mechanism 1.

From the rate law for Mechanism 2 follows that:

$$K = \frac{[B][C]}{[X]} \text{ thus } [B] = \frac{K[X]}{[C]}$$

$$\frac{d[P]}{dt} = k_2[B][Z] = \frac{K k_2 [Z][X]}{[C]} = k_A[X][Z] \text{ for the first reaction}$$

or

$$\frac{d[P]}{dt} = k_B[X][Z] \text{ for the second reaction}$$

It follows that for both mechanisms:

First reaction: $\frac{d[P]}{dt} = k_A[X][Z]$ with $k_A = \frac{k_1k_2}{k_{-1}[C]}$.

Second reaction: $\frac{d[P]}{dt} = k_B[X][Z]$ with $k_B = \frac{k_1k_2}{k_{-1}[C]}$.

In the current study, k_A was too fast to determine. k_B was determined.

3.6 References

[1] du Plessis, W. C., Vosloo, T. G. and Swarts, J. C., *J. Chem. Soc., Dalton Trans.*, 2507 (1998).
[2] Kagarise, R. E., *J. Am. Chem. Soc.*, 77, 1377 (1955).
[3] Kemp, K. C., *Synthesis, electrochemical, kinetic and thermodynamic studies of new ruthenocene-containing beta-diketonato rhodium(I) complexes with biomedical applications,* M. Sc. Thesis, University of the Free State, R.S.A., 2004.
[4] Conradie, M. M., *Synthesis, kinetic and computational chemistry of thiophene-containing beta-diketonato complexes of rhodium(I) and rhodium(III),* M. Sc. Thesis, University of the Free State, R.S.A., 2007.
[5] Lowrey, A. H., D'Antonio, P. D. and Karle, J., *J. Am. Chem. Soc.*, **93**, 6399 (1971).
[6] Fay, R. C. and Lowry, *Inorg. Chem.*, **6**, 1512 (1967).
[7] Serpone, N. and Fay, R. C., *Inorg. Chem.*, **6**, 1835 (1967).
[8]. Kubaschewski, O., Evans, E. L., and Alcock, C. B., *Metallurgical Thermochemistry,* 4th Ed., Oxford, UK, 1967, Table A, p. 304.
[9] Keppler, B. K. and Heim, M. E., *Drugs of the Future*, **3**, 638 (1988).
[10] Smith, G. D., Caughlan, C. N. and Campbell, J. A., *Inorg. Chem.*; **11(12)**; 2989 (1972).
[11] Shapet'ko, N. N., Shigorin, D. N., Skoldinov, A. P., Ryabchikova, T. S. and Reshetova, L. N., *J. Struct. Chem.*, **6**, 138 (1965).
[12] Bradley, D. C. and Holloway, C. E., *J. Chem. Soc. A*, **87**, 1909 (1965).
[13] Doyle, G.; and Tobias, R .S., *Inorg. Chem.* 6, 1111 (1967).
[14] Bellamy, L. J. and Branch, R. F., *J. Chem. Soc.*, 4491 (1954).
[15] Holtzclaw, H. F. Jr. and Collman, J. P., *J. Am. Chem. Soc.*, **79**, 3318 (1957).
[16] Fenton, D. E. and Newman, R., *J. Chem. Soc., Dalton Trans.*, 655 (1974).
[17] Prasad, R. N., Agrawal, M. and Sharma, M., *J. Chil. Chem.* Soc., **48(1)** (2003).
[18] Keppler, B. K., Friesen, C., Moritz, H. G., Vongerichten, H. and Vogel, E., *Struct. Bonding.*, **78**, 97 (1991).
[19] Stary, J., *The Solvent Extraction of Metal Chelates*, MacMillan Company, New York (1964), p. 196 – 202.
[20] Rao, P. V., Rao, C. P., Wegelius, E. K., Kolehmainen, E. and Rissanen, K., *J. Chem. Soc., Dalton Trans.*, 4470 (1999).
[21] Serpone, N. and Fay, R. C., *Inorg. Chim. Acta.*, **57**, 211 (1982).
[22] Fay, R. C. and Piper, T. S., *J. Am. Chem. Soc.*, **84**, 2303 (1962).
[23] Smith, J. A. S. and Wilkins, E. J., *J. Chem. Soc., C.*, 1749 (1966).
[24] Fay, R. C. and Piper, T. S., *J. Am. Chem. Soc.*, **85**, 500 (1963).
[25] Hon, P. K., Belford, R. L. and Pfluger, C. E., *J. Chem. Phys.*, **43**, 1323 (1965); Hon, P. K., Pfluger, C. E. and Belford, R. L., *Inorg. Chem.*, **5**, 516 (1966).
[26] McConnell, H. M., *J. Chem. Phys.*, **27**, 226 (1957).
[27] Maron, S.H. and Lando, J.B., *Fundamentals of Physical Chemistry,* Macmillan Publishing Co. Inc., New York, 1974, p 376 – 383.
[28] Atkins, P.W., *Physical Chemistry*, 5th Ed., Oxford University Press, Oxford, 1994, p. 141 – 154, 288.
[29] du Plessis, W. C., Davis, W. L., Cronje, S. J. and Swarts, J. C., *Inorg. Chim. Acta.*, **314**, 97 (2001).
[30] MINSQ, Least squares parameter estimation, Version 3.12, MicroMath Scientific Software, Salt Lake, UT, 1990.
[31] du Plessis, W. C., Vosloo, T. G. and Swarts, J. C., *J. Chem. Soc., Dalton Trans.*, 2507 (1998).
[32]Martell, A.E., *Stability Constants of Metal-Ion Complexes,* The Chemical Society, London, Special Publication No. 25, 3rd Ed., part II, 1971, p. 365.
[33] Espenson, J. H., *Chemical Kinetics and Reaction Mechanisms*, 2nd Ed., McGraw-Hill, New York, p. 156.
[34] Atkins, P. W., *Physical Chemistry*, 5th Ed., Oxford University Press, Oxford, 1994, p. 939 – 950.

4 Experimental.

4.1 Introduction.

In this chapter all experimental procedures, reaction conditions and techniques are described. The reaction flasks were oven-dried and flame-dried and flushed with N_2 prior to the start of the experiment.

4.2 Materials.

Solid and liquid reagents (Merck, Aldrich) employed in preparations were used without further purification. Solvents were distilled prior to use and water was double distilled. Organic solvents were dried according to published methods.[1] Melting points (m.p.) were determined with DSC {Differential Scanning Calorimetry}, (for enthalpy changes, 0.5 – 1.0 mg samples) at heating and cooling rates of 10°C min^{-1} between 25 and 250°C using a TA Instruments DSC 10 thermal analyser fitted with a Du-Pond Instruments mechanical cooling accessory and a TA Instruments Thermal Analyst data processing unit.

4.2.1 Synthesis of β-diketones.

4.2.1.1 Synthesis of 1-phenyl-3-thenoyl-1,3-propanedione, [$H_5C_6COCH_2COC_4H_3S$].

The reaction was performed under Schlenk conditions. Acetophenone (1.2014 g, 10.0 mmol) was dissolved in THF (1 ml), transferred to the 3-neck flask with the aid of syringe, rinsed with THF (1 ml), and added to the solution. The solution was degassed for 15 minutes while stirring. Lithium diisopropylamide (7.33 ml of 1.8 M solution in heptane/tertahydrofuran/ethylbenzene, 11.0 mmol) was added slowly to the solution under N_2 atmosphere on ice-bath. The syringe was washed with THF (1 ml); and stirred for 15 minutes under N_2 atmosphere. Ethyl 2-thiophenecarboxylate (1.5622 g, 10 mmol) in THF (1 ml) was added to the reaction mixture

under a N_2 atmosphere, and then stirred overnight. Ether (30 ml) was added to the solution and precipitate was formed. The precipitate was filtered and washed with ether (2 x 40 ml). Ether (20 ml) and 0.2 M HCl (10 ml) were stirred with the precipitate. The product was extracted with ether (2 x 50 ml). The combined ether layers were washed with water, dried with anhydrous $MgSO_4$ and evaporated to dryness to give $H_5C_6COCH_2COC_4H_3S$. Yield 0.3065 g (13%). Melting point 79.32°C. ν (C=O)/cm^{-1} = 1559. NMR: δ_H (300 MHz, $CDCl_3$)/ppm: 6.70 (s, 1H, CH); 7.20 (t, 1H, C_4H_3S); 7.44 – 7.58 (m, 3H, C_6H_5); 7.64 – 7.69 (d, 1H, C_4H_3S); 7.81 – 7.84 (d, 1H, C_4H_3S); 7.92 – 7.98 (d, 2H, C_6H_5).

4.2.1.2 Synthesis of 1-phenyl-4-nitrophenyl-1,3-propanedione, $[H_5C_6COCH_2COC_6H_4NO_2]$:

The reaction was performed under Schlenk conditions. Acetophenone (1.2022 g, 10 mmol) was dissolved in THF (1 ml), transferred to the 3-neck flask with the aid of syringe, rinsed with THF (1 ml), and added to the solution. The solution was degassed for 15 minutes while stirring. Lithium diisopropylamide (7.33 ml of 1.8 M solution in heptane/tertahydrofuran/ethylbenzene, 11 mmol) was added slowly to the solution under N_2 atmosphere on ice-bath. The syringe was washed with THF (1 ml); and stirred for 15 minutes under N_2 atmosphere. Methyl 4-nitro benzoate (1.8115 g, 10.0 mmol) in THF (8 ml) was added to the reaction mixture under a N_2 atmosphere, and then stirred for overnight. Ether (30 ml) was added to the solution and precipitate was formed. The precipitate was filtered and washed with ether (2 x 40 ml). Ether (20 ml) and 0.2M HCl (10 ml) were stirred with the precipitate. The product was extracted with ether (2 x 50 ml). The combined ether layers were washed with water, dried with anhydrous $MgSO_4$ and evaporated to dryness. Recrystallization from acetone-water mixture afforded $H_5C_6COCH_2COC_6H_4NO_2$. Yield 0.4120 g (15.36%). Melting point 140.86°C. NMR: δ_H (300 MHz, $CDCl_3$)/ppm: 6.91 (s, 1H, CH); 7.47 – 7.64 (m, 3H, C_6H_5); 7.98 – 8.08 (d, 2H, C_6H_5); 8.11 – 8.18 (d, 2H, $C_6H_5NO_2$); 8.28 – 8.38 (d, 2H, $C_6H_5NO_2$).

4.2.2 Synthesis of Ti(β-diketonato)$_2$Cl$_2$ complexes.

4.2.2.1 Synthesis of dichlorobis(2,4-pentanedionato-κ^2O,O') titanium(IV), $[TiCl_2(acac)_2]$.[2]

To the stirred solution of acetylacetone (1.6092 g, 16.1 mmol) in dichloromethane (35 ml), a solution of titanium(IV) tetrachloride (1.5227 g, 8.03 mmol) in dichloromethane (5 ml) was added dropwise. The reaction mixture was stirred and purged with a slow stream of N_2 for 20 minutes. The solution was boiled down to about 30 ml, hexane (35 ml) was added slowly, left standing for overnight to crystallize, filtered, dried and stored under N_2 atmosphere. Yield: 2.1741 g (85.3%). Melting point 192.99°C, literature.[2] 190-193°. ν (C=O)/cm^{-1} = 1517. NMR: δ_H (300 MHz, $CDCl_3$)/ppm: 2.14 – 2.26 (s, 12H, 4 x CH_3); 5.98 – 6.03 (s, 2H, 2 x CH).

4.2.2.2 Synthesis of dichlorobis(1-phenyl-1,3-butanedionato-κ^2O,O') titanium(IV), [$TiCl_2(ba)_2$].[3]

To the stirred solution of benzoylacetone (0.1865 g, 1.15 mmol) in chloroform (15 ml), the solution of titanium(IV) tetrachloride (0.1090 g, 0.575 mmol) in chloroform (10 ml) was added dropwise. The reaction mixture was refluxed for 2 hours under slow stream of N_2, and filtered hot to remove unreacted material. To the filtrate, hexane (25 ml) was added slowly, allowed to crystallise overnight in a freezer, filtered, dried and stored under N_2 atmosphere. Yield: 195.5 mg (77.1%). Melting point 238.12°C, literature.[3] 209-210°. ν (C=O)/cm^{-1} = 1597. NMR: δ_H (300 MHz, $CDCl_3$)/ppm: 2.28 – 2.45 (s, 6H, 2 x CH_3); 6.61 – 6.72 (s, 2H, 2 x CH); 7.39 – 7.66 (m, 6H, 2 x 3H, C_6H_5); 7.84 – 8.18 (m, 4H, 2 x 2H, C_6H_5). (The reaction can also be prepared using toluene.)

4.2.2.3 Synthesis of dichlorobis(1,3-diphenyl-1,3-propanedionato-κ^2O,O') titanium(IV), [$TiCl_2(dbm)_2$].[3]

To the stirred solution of dibenzoylmethane (0.1502 g, 0.670 mmol) in toluene (10 ml) was slowly added titanium(IV) chloride (0.0816 g, 0.430 mmol) in toluene (15 ml). The reaction mixture was refluxed for 2 hours with a stream of N_2 passing through the solution to evolve hydrogen chloride gas. The reaction mixture was filtered hot and hexane (30 ml) was added slowly to the filtrate. The mixture was placed in a freezer for overnight to crystallise, filtered,

dried and stored under N_2 atmosphere. Yield: 0.1475 g (60.65%). Melting point 144.69°C, literature.[3] 262.5-263.5°. ν (C=O)/cm^{-1} = 1593. NMR: δ_H (300 MHz, $CDCl_3$)/ppm: 7.31 – 7.38 (s, 2H, 2 x CH); 7.40 – 7.71 (m, 12H, 4 x 3H, C_6H_5); 7.84 – 8.18 (m, 8H, 4 x 2H, C_6H_5). (The reaction can also be prepared in chloform.)

4.2.2.4 Synthesis of dichlorobis(1-phenyl-3-thenoylpropanedionato-κ^2O,O')titanium(IV), [Ti(thba)$_2$Cl$_2$].

To the stirred solution of 1-phenyl-3-thenoylpropanedione (0.0967 mg, 0.670 mmol) in toluene (10 ml) the titanium(IV) tetrachloride (0.0398 g, 0.210 mmol) in toluene (15 ml) was added slowly. The reaction mixture was refluxed for 2 hours with a stream of N_2 passing through the solution to evolve hydrogen chloride gas. The reaction mixture was filtered hot, and hexane (30 ml) was added slowly to the filtrate. The mixture was placed in a freezer for overnight to crystallise, filtered, dried and stored under N_2 atmosphere. Yield: 0.0801 g (60.65%) Yield: 0.0801 g (66.09%). ν (C=O)/cm^{-1} = 1523. NMR: δ_H (300 MHz, $CDCl_3$)/ppm (at 55°C): 6.68 – 6.72 (s, 2H, 2 x CH); 7.16 – 7.22 (m, 2H, 2 x CH, C_4H_3S); 7.46 – 7.56 (m, 6H, 2 x 3H, C_6H_5); 7.63 – 7.67 (d, 2H, 2 x CH, C_4H_3S); 7.81 – 7.84 (d, 2H, 2 x CH, C_4H_3S); 7.94 – 7.99 (d, 4H, 2 x 2H, C_6H_5).

4.2.2.5 Synthesis of dichlorobis(4,4,4-trifluoro-1-phenyl-1,3-butanedionato-κ^2O,O') titanium(IV), [Ti(tfba)$_2$Cl$_2$].

To the stirred solution of 4,4,4-trifluoro-1-phenyl-1,3-butanedione (0.2502 g, 1.16 mmol) in toluene (15 ml) the solution of titanium(IV) chloride (0.1106 g, 0.580 mmol) in toluene (15 ml) was slowly added. The reaction mixture was refluxed for 2 hours with a stream of N_2 passing through the solution to evolve hydrogen chloride gas. The reaction mixture was filtered hot, and hexane (30 ml) was added slowly to the filtrate. The mixture was placed in a freezer for overnight to crystallise, filtered, dried and stored under N_2 atmosphere. Yield: 0.0509 g (15.99%). ν (C=O)/cm^{-1} = 1590. NMR: δ_H (300 MHz, $CDCl_3$)/ppm: 6.84 (s, 2H, 2 x CH); 7.39 – 7.70 (m, 6H, 3 x 2H, C_6H_5).

4.2.3 Synthesis of (2,2'-Biphenyldiolato)bis(β-diketonato) titanium(IV) complexes.

4.2.3.1 Synthesis of (2,2'-Biphenyldiolato)bis(2,4-pentadionato-κ^2O,O') titanium(IV), [Ti($OC_6H_4C_6H_4O$)($acac)_2$].

To stirred solution of 2,2'-biphenyldiol (0.2174 g, 1.167 mmol) in CH_3CN (15 ml), a solution of $Ti(acac)_2Cl_2$ (0.3700 g, 1.167 mmol) in CH_3CN (15 ml) was added dropwise at room temperature to give orange red solution and refluxed for 4.6 hours. The reaction mixture was cooled to room temperature and filtered. The precipitate was washed in MeOH to dissolve unreacted biphenol, filtered, dried and stored under N_2 atmosphere. Yield: 0.3893 g (77.5%). Melting point >250°C. ν (C=O)/cm^{-1} = 1589. NMR: δ_H (300 MHz, $CDCl_3$)/ppm: 2.01 – 2.09 (s, 12H, 4 x CH_3); 5.78 – 5.83 (s, 2H, 2 x CH); 6.83 – 6.93 (d, 2H, 2 x CH); 6.96 – 7.05 (t, 2H, 2 x CH); 7.18 – 7.25 (t, 2H, 2 x CH, aromaticH); 7.36 – 7.42 (d, 2H, 2 x CH, aromaticH);

4.2.3.2 Synthesis of (2,2'-Biphenyldiolato)bis(1-phenyl-1,3-butanedionato-κ^2O,O') titanium(IV), [Ti($OC_6H_4C_6H_4O$)($ba)_2$].

To a stirred solution of 2,2'-biphenyldiol (0.0314 g, 0.170 mmol) in CH_3CN (15 ml), a solution of $Ti(ba)_2Cl_2$ (0.0750 g, 0.170 mmol) in CH_3CN (15 ml) was added dropwise at room temperature to give red solution and refluxed for 4.6 hours. The reaction mixture was cooled to room temperature, solvent evaporated to dryness. The crude product was washed in MeOH to dissolve unreacted biphenol, filtered, dried and stored under N_2 atmosphere. Yield: 0.0191 g (20.4%). Melting point >250°C ν (C=O)/cm^{-1} = 1584. NMR: δ_H (600 MHz, $CDCl_3$)/ppm: 2.20 (s, 6H, 2 x CH_3); 6.48 (s, 2H, 2 x CH); 7.01 – 7.11 (m, 4H, 4 x CH, aromaticH); 7.30 – 7.35 (t, 2H, 2 x CH, aromaticH); 7.36 – 7.41 (t, 4H, 4 x CH, aromaticH); 7.43 – 7.48 (d, 2H, 2 x CH, aromaticH); 7.48 – 7.53 (t, 2H, 2 x CH, aromaticH); 7.78 – 7.85 (d, 4H, 2 x 2H, C_6H_5).

4.2.3.3 Synthesis of (2,2'-Biphenyldiolato)bis(1,3-diphenyl-1,3-propanedionato-κ^2O,O')titanium(IV), [Ti($OC_6H_4C_6H_4O$)(dbm)$_2$].

To a stirred solution of 2,2'-biphenyldiol (0.0509 g, 0.273 mmol) in CH_3CN (15 ml), $Ti(dbm)_2Cl_2$ (0.1545 g, 0.273 mmol) in CH_3CN (15 ml) was added dropwise at room temperature to give brown red solution and refluxed for 4.6 hours. The reaction mixture was cooled to room temperature, and the solvent evaporated to dryness. The crude product was washed in MeOH to dissolve unreacted biphenol, filtered, dried and stored under N_2 atmosphere. Yield: 0.0228 g (12.3%). Melting point 244.93°C. ν (C=O)/cm^{-1} = 1589. NMR: δ_H (300 MHz, $CDCl_3$)/ppm: 7.08 – 7.16 (m, 4H, 4 x CH); 7.18 – 7.22 (s, 2H, 2 x CH); 7.33 – 7.57 (m, 16H, 16 x CH, aromaticH); 7.86 – 8.05 (d, 8H, 4 x 2H, C_6H_5).

4.2.3.4 Synthesis of (2,2'-Biphenyldiolato)bis(4,4,4-trifluoro-1-phenyl-1,3-butanedionato-κ^2O,O')titanium(IV), [Ti($OC_6H_4C_6H_4O$)(tfba)$_2$].

To a stirred solution of 2,2'-biphenyldiol (0.0276 g, 0.148 mmol) and sodium acetate (12.2 mg, 0.145 mmol) in CH_3CN (15 ml), a solution of $Ti(tfba)_2Cl_2$ (0.0815 g, 0.150 mmol) in CH_3CN (15 ml) was added dropwise at room temperature to give red solution and refluxed for 4.6 hours. The reaction mixture was cooled to room temperature, solvent evaporated to dryness to remove volatile products. The crude product was washed in MeOH to dissolve unreacted biphenol, filtered, dried and stored under N_2 atmosphere. Yield: 0.0241 g (24.6%). Melting point >250°C. ν (C=O)/cm^{-1} = 1610. NMR: δ_H (600 MHz, $CDCl_3$)/ppm: 6.90 (s, 2H, 2 x CH); 7.04 – 7.09 (t, 2H, 2 x CH, aromaticH); 7.14 – 7.20 (t, 2H, 2 x CH, aromaticH); 7.35 – 7.40 (t, 2H, 2 x CH, aromaticH); 7.46 – 7.54 (6H, 2 x 3H, C_6H_5); 7.62 – 7.68 (t, 2H, 2 x CH, aromaticH); 7.88 – 7.95 (d, 4H, 2 x 2H, C_6H_5).

4.2.3.5 Synthesis of (2,2'-Biphenyldiolato)bis(1-phenyl-3-thenoylpropanedionato-κ^2O,O')titanium(IV), [Ti($OC_6H_4C_6H_4O$)(thba)$_2$].

To a stirred solution of 2,2'-biphenyldiol (0.0162 g, 0.087 mmol) and sodium acetate (0.0088 g, 0.105 mmol) in CH_3CN (15 ml), a solution of $Ti(thba)_2Cl_2$ (0.0620 g, 0.087 mmol) in warm CH_3CN (15 ml) was added dropwise at room temperature to give deep red solution and refluxed for 4.6 hours. The reaction mixture was cooled to room temperature, solvent evaporated to dryness to remove unreacted volatile reactants. The crude product was washed in MeOH to dissolve unreacted biphenol, filtered, dried and stored under N_2 atmosphere. Yield: 0.0234 g (35.0%). Melting point >250°C. ν (C=O)/cm^{-1} = 1658. NMR: δ_H (300 MHz, $CDCl_3$)/ppm: 7.08 – 7.16 (m, 4H, 4 x CH); 7.18 – 7.22 (s, 2H, 2 x CH); 7.33 – 7.57 (m, 16H, 16 x CH, aromaticH); 7.86 – 8.05 (d, 8H, 4 x 2H, aromaticH).

4.2.3.6 Tetrabutylammonium tetrakis[pentafluorophenyl]borate.

Lithium tetrakis[pentafluorophenyl]borate (25 g, 0.046 mol) was dissolved in 20 ml methanol (AR). Tetrabutylammonium bromide (12.75 g, 0.039 mol) dissolved in 10 ml methanol (AR) was added drop wise at room temperature over 15 min to the lithium solution [a precipitate forms]. The solution (closed with septum) was left at 0°C for 30 min, and then overnight at -25°C. An off-white precipitate from a brown liquid was obtained by filtration and washed with 10 ml cold (-25°C) methanol (AR). The solid was dissolved in excess (30 ml) dry, distilled CH_2Cl_2. A few spatulas $MgSO_4$ was added and covered with a septum, the mixture was stirred for 2h at room temperature. The $MgSO_4$ was filtered off and washed with CH_2Cl_2. The CH_2Cl_2 was evaporated and crude product was obtained as a white solid (21.7g, 0.024 mol, 60%). Further purification by recrystallization was achieved as follows: To a solution of product (9 g, 0.01 mol) in 11 ml CH_2Cl_2 was added 55 ml ether drop wise, while stirring, over 20 min at room temperature. The covered (closed with a septum) solution was cooled at 0°C for an hour and then overnight at -25°C. The precipitate was filtered off and washed with 30 ml hexanes (distilled). The solid was air dried for 2h and recrystallization was repeated for a second time. Yield 20.7 g (58%). Melting point = 159-161°C. δ_H (300MHz, $CDCl_3$)/ppm: 0.98 (t; 12H; 4 x CH_3); 1.36 (q, 8H; 4 x CH_2); 1.56 (q, 8H; 4 x CH_2); 3.03 (t, 8H; 4 x CH_2), Spectrum 13.

4.3 Spectroscopic measurements.

^{1}H NMR measurements at 294 K (21°C) were recorded on a Bruker Advance DPX 300 MHz NMR spectrometer. Variable temperature ^{1}H NMR was recorded on a Bruker 600 MHz NMR. The chemical shifts were reported relative to $SiMe_4$ at 0.00 ppm. IR spectra were recorded on a Digilab FTS 2000 Fourier transform spectrometer utilizing a He-Ne laser at 632.6 nm. UV spectra were recorded in a Cary 50 Probe UV/Visible spectrophotometer. pH readings were obtained using an Orion model SA 720, equipped with a glass electrode. The pH meter was calibrated using buffers at pH 7.00 and 10.00. The temperature was controlled using a water bath to within 21.0°C ± 0.1 °C.

4.4 Electrochemistry.

Measurements on ca. 2.0 mmol dm^{-3} solutions of the complexes in dry air free dichloromethane containing 0.10 mmol dm^{-3} tetrabutylammonium tetrakis(pentafluorophenyl)borate as supporting electrolyte were conducted under a blanket of purified argon at 25°C utilizing a BAS 100 B/W electrochemical workstation interfaced with a personal computer. A three electrode cell, which utilized a Pt auxiliary electrode, a glassy carbon working electrode (surface area 0.0707 cm^2) (pre-treated by polishing on a Beuhler microcloth first with 1 micron and then with ¼ micron diamond paste), and an in-house constructed Ag/AgCl reference electrode are employed. All temperatures were kept constant to within 0.1°C. Successive experiments under the same experimental conditions. All formal reduction and oxidation potentials were reproducible within 5 mV. Experimentally, potentials were measured against the Ag/AgCl reference electrode. Results presented are referenced against ferrocene as an internal standard.

4.5 pK_a-determinations.

The pK_a' values were determined in a solvent system of water: acetonitrile (9:1 by volume) and an ionic strength of 0.1 mol dm^{-3} $NaClO_4 \cdot H_2O$. UV-spectra (0.2 mmol dm^{-3}) β-diketone at acidic pH and of the deprotonated β-diketonato at basic pH was obtained. From these spectra an analytical wavelength where the charge in absorbance between the β-diketone and β-diketonato forms is greatest, was chosen at which the pK_a' could be determined. The titration of 100 ml β-

diketone solution were performed with 0.1 mol dm^{-3} and 1 mol dm^{-3} NaOH or with 0.1 mol dm^{-3} and 1 mol dm^{-3} $HClO_4$ depending on whether an acidic or a basic titration was performed. An effort was made to ensure that the increase in volume during the titration was no more than 5%. The absorbance changes with pH changes were measured on a Cary 50 Probe UV/Visible spectrophotometer, pH measurements were made with an Orion model SA 720 pH meter, equipped with a glass electrode. The pH meter was calibrated using buffers at pH 7.00 and 10.00. The pK_a' values where obtained by a least square fit (program MINSQ[4]) of the absorption/pH data to:

$$A_T = \frac{A_{HA}10^{-pH} + A_A 10^{-pK_a}}{10^{-pH} + 10^{-pK_a}}$$

with A_T = total absorbance, A_{HA} the absorbance of the β-diketone in the protonated form and A_A the absorbance of the β-diketone in the deprotonated (basic) form.

4.6 Kinetic measurements.

4.6.1 Isomerisation kinetics.

In the solid state, after long enough time has elapsed, β-diketones existed mainly as the enol isomer. Therefore, upon dissolving aged samples of β-diketones in $CDCl_3$, the slow formation of the keto isomer until the solution equilibrium position was reached, could be monitored by ^1H NMR utilising a Bruker Advance DPX 300 NMR spectrometer.

$$\text{keto} \underset{k_{-1}}{\overset{k_1}{\rightleftharpoons}} \text{enol}$$

The CH/CH_2 signal pair of the enol/keto forms of the β-diketone was identified and the % keto-isomer was calculated from the relationship (I = integral value):

$$\%\ \text{keto isomer} = \frac{I \text{ of keto signal}}{[(I \text{ of keto signal}) + (I \text{ of enol signal})]} \times 100$$

The first order rate constant $k_{obs} = k_1 + k_{-1}$ was obtained from the slope of ln[(%keto isomer at t = 0)/(%keto isomer at time t)] against time. The equilibrium constant K_c was obtained from the relationship:

$$K_c = \frac{(\%\ \text{enol isomer})}{(\%\ \text{keto isomer})}$$

k_1 and k_{-1} could be determined by simultaneous solution of $k_{obs} = k_1 + k_{-1}$ and $K_c = k_1/k_{-1}$.

4.6.2 Substitution kinetics.

The validity of the Beer-Lambert law ($A = \varepsilon c \ell$ with A = UV/Vis absorbance, ε = molar extinction coefficient, c = concentration and ℓ = path length = 1 cm) was confirmed for all complexes within the experimental concentration range of 0.004 mol dm^{-3} to 0.08 mol dm^{-3}. All substitution reactions were performed in freshly distilled acetonitrile under pseudo first order conditions, where the incoming ligand's concentration, H_2biphen, was 10 to 200 times in excess over the titanium complex concentration. The concentration of the titanium complex in the reaction = 0.4 mM. Pseudo first order rate constants, k_{obs}, were determined by monitoring the appearance of the [Ti(β-diketonato)$_2$(biphen)] product at the indicated wavelengths, λ_{exp}, (Table 3.13) on a Cary 50 Probe UV/Visible spectrophotometer.

4.6.3 Activation parameters

The activation parameters ΔH* (activation enthalpy), ΔS* (activation entropy) and ΔG* (free energy of activation) for the substitution reactions were determined from the least square fits of the reaction rate constants *vs.* temperature data according to the Arrhenium equation:

$$k = \left(\frac{RT}{Nh}\right) e^{(-\Delta H^*/RT)} e^{(\Delta S^*/R)}$$

or rewritten in a linear form:

$$\ln\left(\frac{k}{T}\right) = \left(\frac{-\Delta H^*}{RT}\right) + \left(\frac{\Delta S}{R}\right) + \ln\left(\frac{R}{Nh}\right)$$

with h = Planck constant = 6.625 x 10^{-34} J s, N = Avogadro's constant = 6.023 x 10^{23} mol^{-1}, R = Universal gas constant = 8.314 J mol^{-1} K^{-1}. The activation free energy was calculated from:

$$\Delta G^* = \Delta H^* - T\Delta S^*$$

4.7 References

[1] B.S. Furniss, A.J. Hannaford, P.W.G. Smith and A.R. Tatchell, *Vogel's Textbook of Practical Organic Chemistry*, 4th Edition, Longman, New York, p 264-318.
[2] Fay, R. C. and Lowry, R. N., *Inorg. Chem.*, **6**, 1512 (1967).
[3] Serpone, N. and Fay, R. C. *Inorg. Chem.*, **6**, 1835 (1967).
[4] L. Helm, MINSQ, Non-linear parameter estimation and model development, least squares parameter optimisation V3.12, MicroMath Scientific Software, Salt Lake City, UT, 1990.

5 Summary, Conclusions and Future Perspectives.

In this study, 2 phenyl containing β-diketones (1 of which is new), 5 octahedral β-diketonato titanium(IV) complexes of the type Ti(β-diketonato)$_2$Cl$_2$ (2 of which are new) and 5 new Ti(β-diketonato)$_2$(biphen) complexes were synthesised in multistep reactions. These compounds are shown in Figure 5. 1. These complexes were all characterised spectroscopically with IR, UV/VIS and ^{1}H NMR. Their physical properties were investigated with electrochemical, thermodynamic and kinetic techniques.

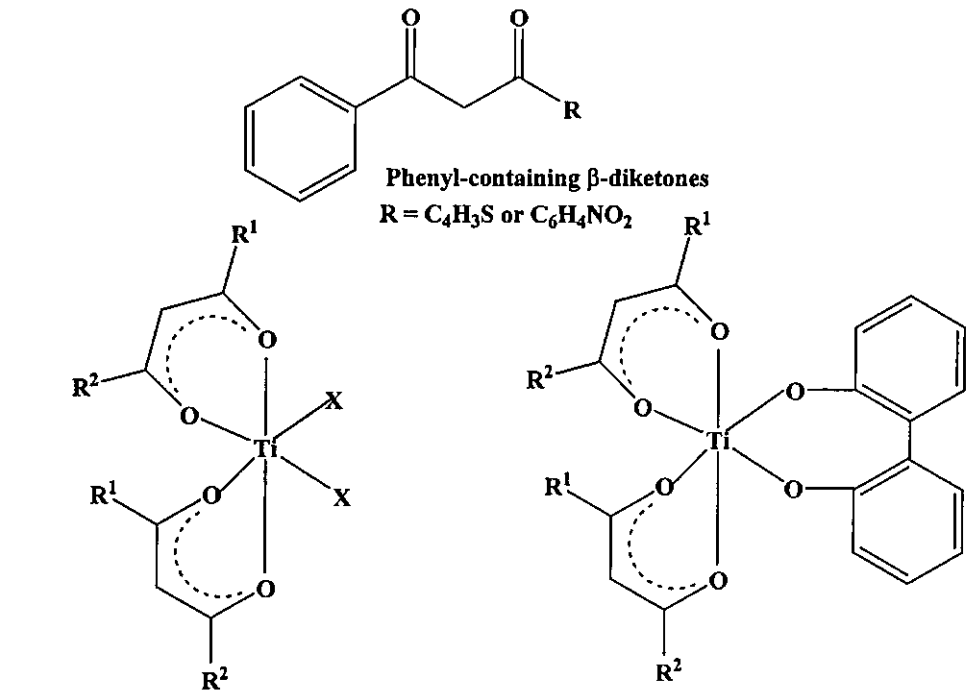

Figure 5. 1: **Structures of the complexes synthesized in this study.**

The pK_a' values for the β-diketones with R = $C_6H_4NO_2$ (8.02(7)) and C_4H_3S (9.21(5)) were determined spectroscopically in water containing 10% acetonitrile. The keto-enol isomerisation of the β-diketone $PhCOCH_2COCH_3$ was studied in $CDCl_3$ by ^{1}H NMR spectroscopy. The rate of conversion from enol to keto is 10 times faster than keto to enol.

The hydrolytic stability of Ti(β-diketonato)$_2$Cl$_2$ in acetonitrile treated with 6.25 % water increases in the order Ti(tfba)$_2$Cl$_2$ < Ti(acac)$_2$Cl$_2$ < Ti(ba)$_2$Cl$_2$ < Ti(dbm)$_2$Cl$_2$ << Ti(ba)$_2$(OEt)$_2$ (budoditane currently in phase II clinical trials for cancerostatic activity[1]) studied under similar conditions.[2]

Variable temparature ^{1}H NMR spectral studies of the octahedral Ti(β-diketonato)$_2$biphen complexes with β-diketonato = ba, thba and tfba established that these compounds all exist as a mixture of *cis* isomers in rapid exchange with each other in solution of $CDCl_3$.

The substitution of two Cl^- ions from [Ti(acac)$_2$Cl$_2$], with 2,2'-biphenyldiolato^{-2} showed a small second order rate constant $k_2 = 3.67 \times 10^{-5}$ dm^3 mol^{-1} s^{-1}. The small negative value of ΔS^* (-10 J mol^{-1} K^{-1}) is indicative of a dissociative mechanism.

Electrochemical studies in dichloromethane utilising cyclic voltammetry of both [Ti(β-diketonato)$_2$Cl$_2$] and [Ti(β-diketonato)$_2$(biphen)] complexes revealed a chemical reversible Ti^{4+}/Ti^{3+} couple. Electrochemically quasi-reversible behaviour was observed: the difference between oxidation and reduction potential, ΔE_p, varied between 114 and 146 mV for [Ti(β-diketonato)$_2$Cl$_2$]; between 123 and 146 mV for [Ti(β-diketonato)$_2$(biphen)] with β-diketonato = acac, dbm, tfba and irreversible with ΔE_p of 183 mV for Ti(PhCOCHCOCH$_3$)$_2$(biphen). The formal reduction potential of the Ti^{4+}/Ti^{3+} couple increases with the increase in group electronegativity of the R^1 and R^2 groups of the β-diketonato ligand $(R^1COCHCOR^2)^-$.

Future study possibilities from this are vast. In this study, a series of phenyl-containing bis-β-diketonato and biphen-titanium(IV) complexes were synthesised, tested for hydrolysis and subjected to electrochemistry and substitution kinetics. Applications of these complexes in this study in terms of catalysis and medical applications (anticancer activity) should be addressed. Similar studies could be extended towards Zr, Hf, Nb, Mo and V complexes. Quantification of trends within a group (Ti, Zr and Hf) or a certain row (Ti and V; Zr, Mo and Nb complexes) of the periodic table can be made. This would include polymerisation catalysis similar to Ziegler-Natta types of catalysts.[3]

A series of new titanium-containing β-diketones can possibly be made. The phenyl-containing β-diketones can be extended to other R-groups such as furyl, pyridine, H, bromo-phenyl, *etc.* and to be complexed to titanium(IV). The β-diketones can also be attached as an axial ligand to phthalocyaninato titanium complexes. The dihalobis(β-diketonato)titanium(IV) complexes from this study can be complexed to the other bi-negative hydroxy-containing ligands such as catechol, 1,1'-Methylenebis(2-naphthol) and tested as catalysts and potential anti-cancer applications.

---

[1] M. Guo and P.J. Sadler, *J. Chem. Soc., Dalton Trans.*, 2000, 7; J.R. Boyles, M.C. Baird, B.G. Campling and N. Jain, *J. Inorg. Biochem.*, 2001, **84**, 159.

[2] Keppler, B. K. and Heim, M. E., *Drugs of the Future*, **3**, 638 (1988).

[3] Cotton, F. A., Wilkinson, G. and Gaus, P. L., *Basic Inorganic Chemistry*, John Wiley and Sons, New York, 1995, pp. 719-720.

Appendix

^{1}H NMR Spectra

β-diketones

Spectrum 1: 1-phenyl-3-thenoyl-1,3-propanedione, [$H_5C_6COCH_2COC_4H_3S$].

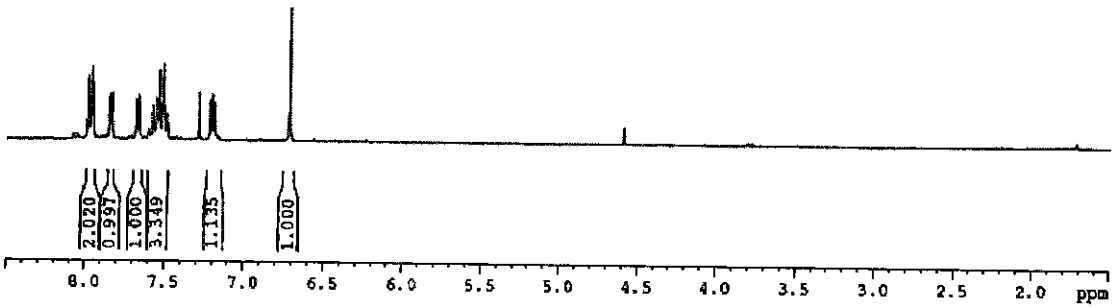

Spectrum 2: 1-phenyl-4-nitrophenyl-1,3-propanedione, [$H_5C_6COCH_2COC_6H_4NO_2$].

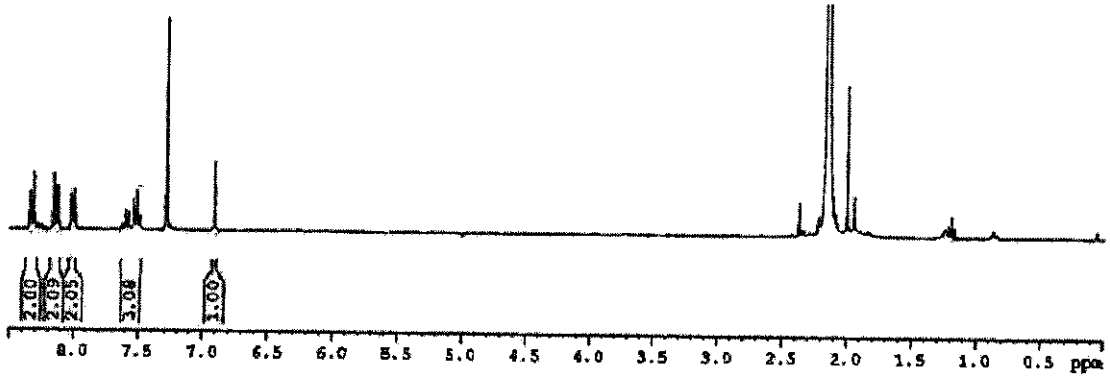

Titanium(IV) complexes

Spectrum 3: dichlorobis(2,4-pentanedionato-κ^2O,O')titanium(IV), [$TiCl_2(acac)_2$]

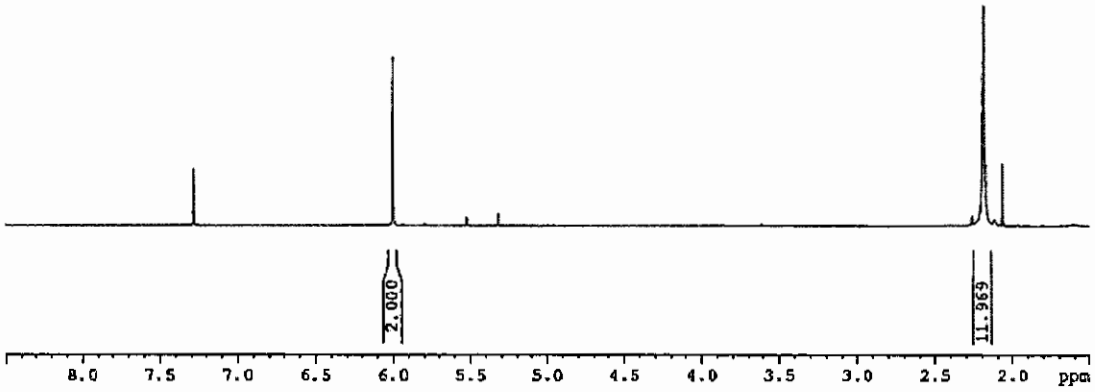

Spectrum 4: dichlorobis(1-phenyl-1,3-butanedionato-κ^2O,O')titanium(IV), [$TiCl_2(ba)_2$]

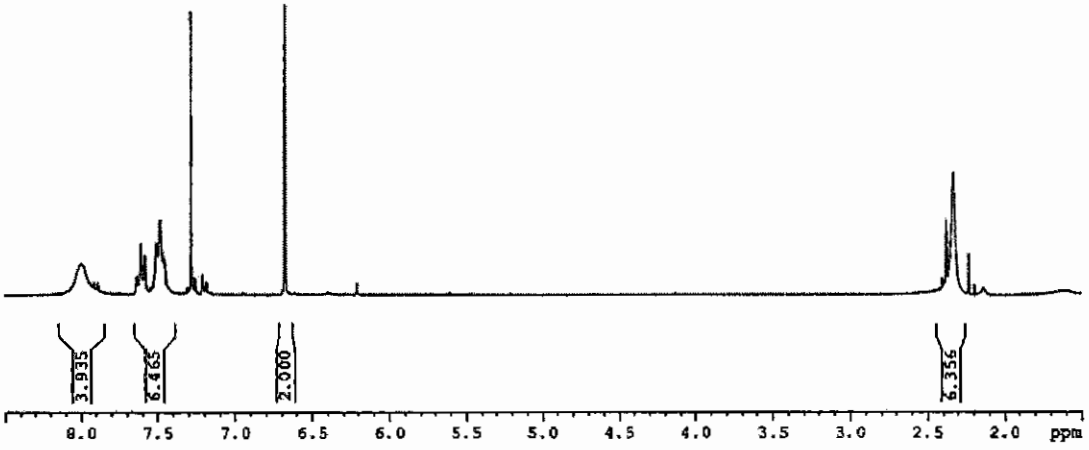

Spectrum 5: dichlorobis(1,3-diphenyl-1,3-propanedionato-κ^2O,O')titanium(IV), [$TiCl_2(dbm)_2$]

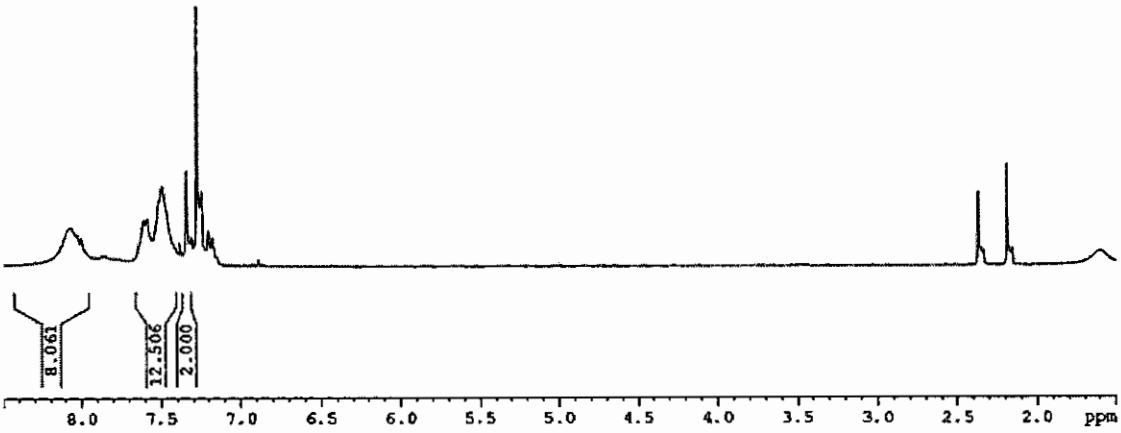

Spectrum 6: dichlorobis(1-phenyl-3-thenoylpropanedionato-κ^2O,O')titanium(IV), [Ti(thba)$_2$Cl$_2$]

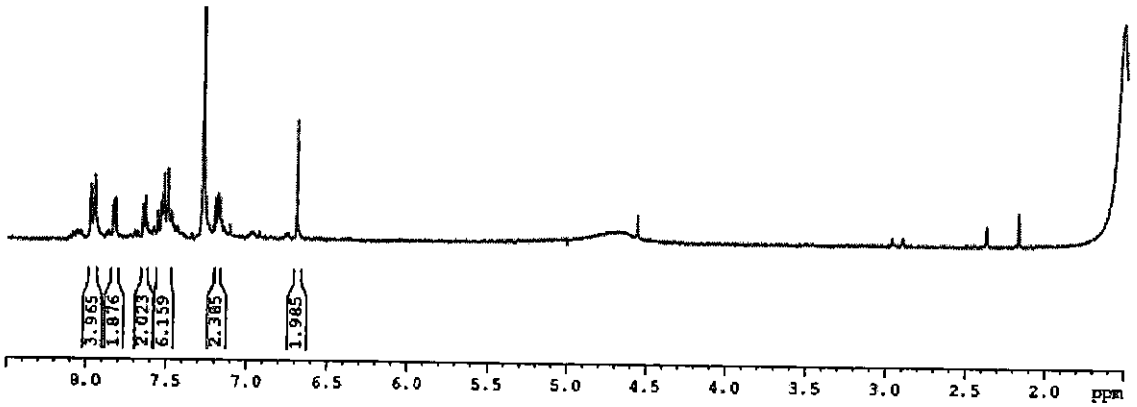

Spectrum 7: dichlorobis(4,4,4-trifluoro-1-phenyl-1,3-butanedionato-κ^2O,O')titanium(IV), [Ti(tfba)$_2$Cl$_2$]

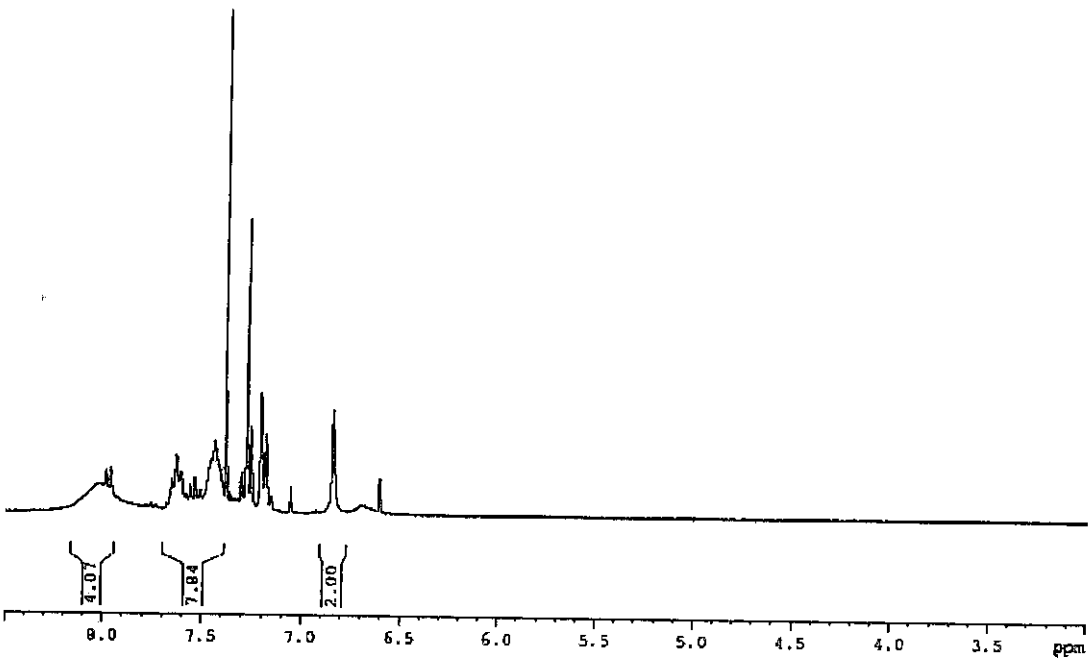

Spectrum 8: (2,2'-Biphenyldiolato)bis(2,4-pentadionato-κ^2O,O')titanium(IV), [Ti($OC_6H_4C_6H_4O$)$(acac)_2$].

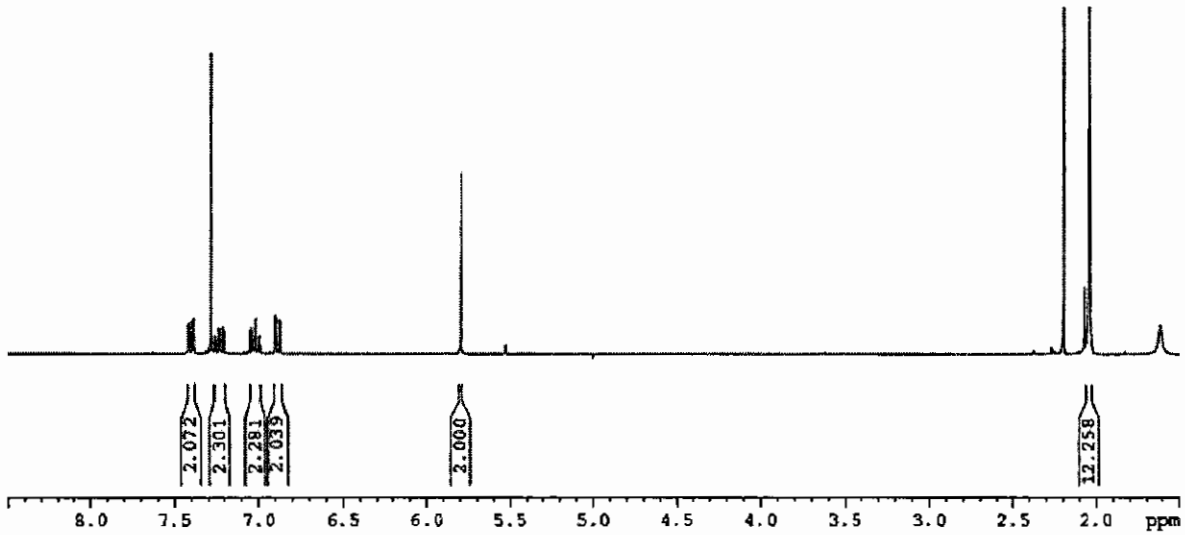

Spectrum 9: (2,2'-Biphenyldiolato)bis(1-phenyl-1,3-butanedionato-κ^2O,O')titanium(IV), [Ti($OC_6H_4C_6H_4O$)$(ba)_2$].

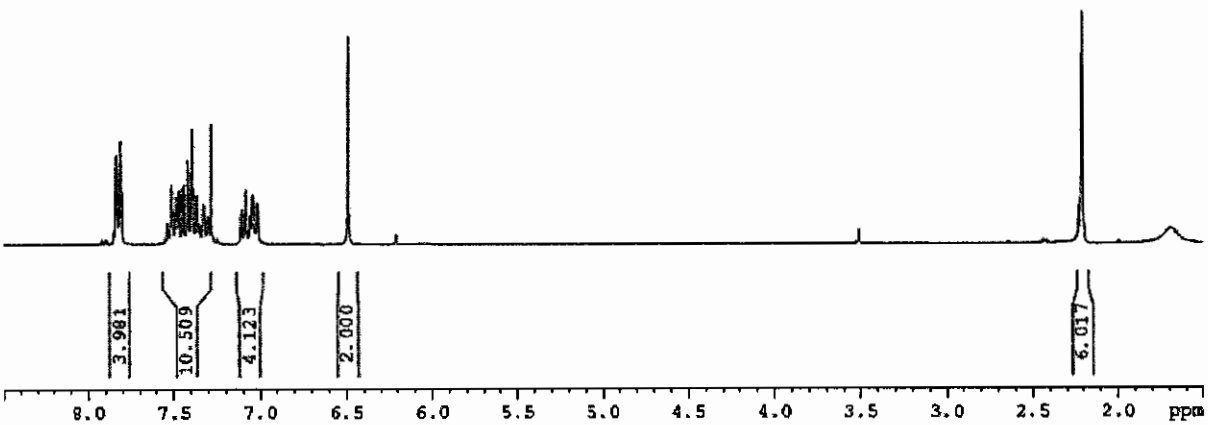

Spectrum 10: (2,2'-Biphenyldiolato)bis(1,3-diphenyl-1,3-propanedionato-κ^2O,O') titanium(IV), [Ti($OC_6H_4C_6H_4O$)($dbm)_2$].

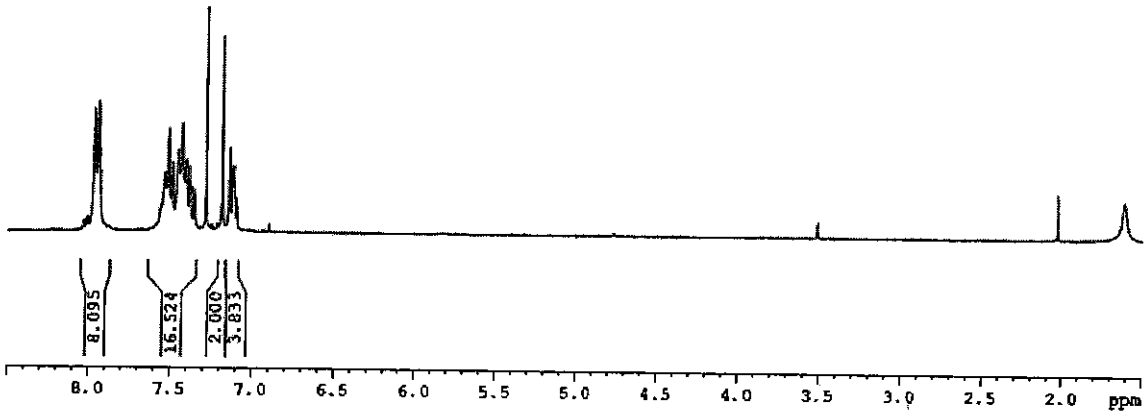

Spectrum 11: (2,2'-Biphenyldiolato)bis(4,4,4-trifluoro-1-phenyl-1,3-butanedionato-κ^2O,O')titanium(IV), [Ti($OC_6H_4C_6H_4O$)($tfba)_2$].

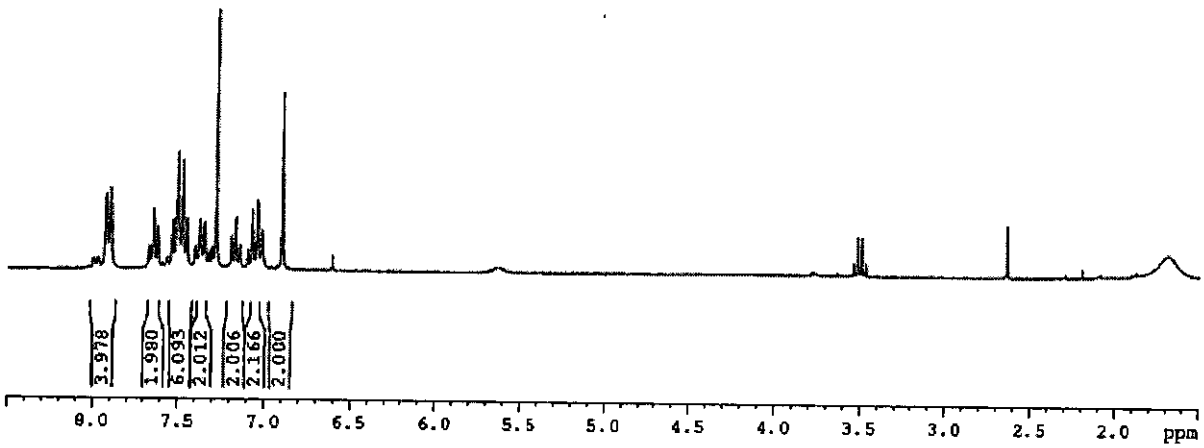

Spectrum 12: (2,2'-Biphenyldiolato)bis(1-phenyl-3-thenoylpropanedionato-κ^2O,O') titanium(IV), [Ti($OC_6H_4C_6H_4O$)(thba)$_2$].

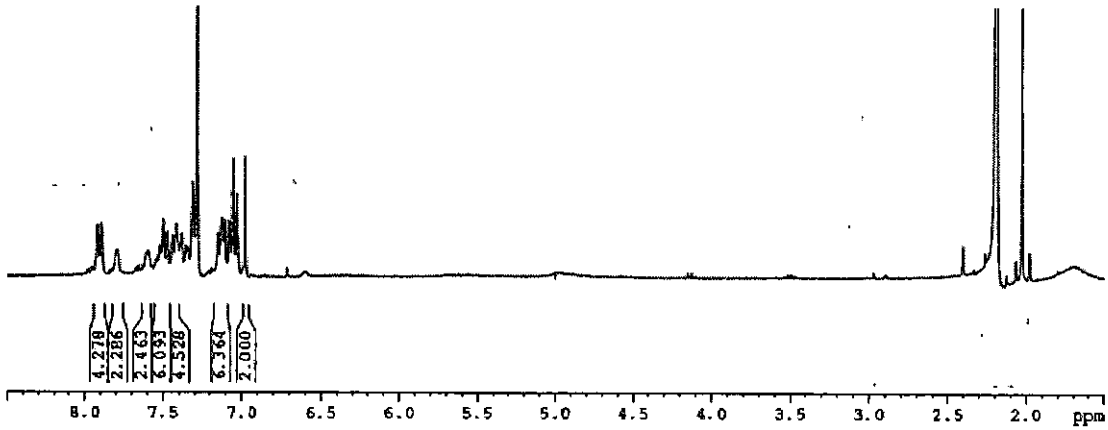

Spectrum 13: Tetrabutylammonium tetrakis[pentafluorophenyl]borate.

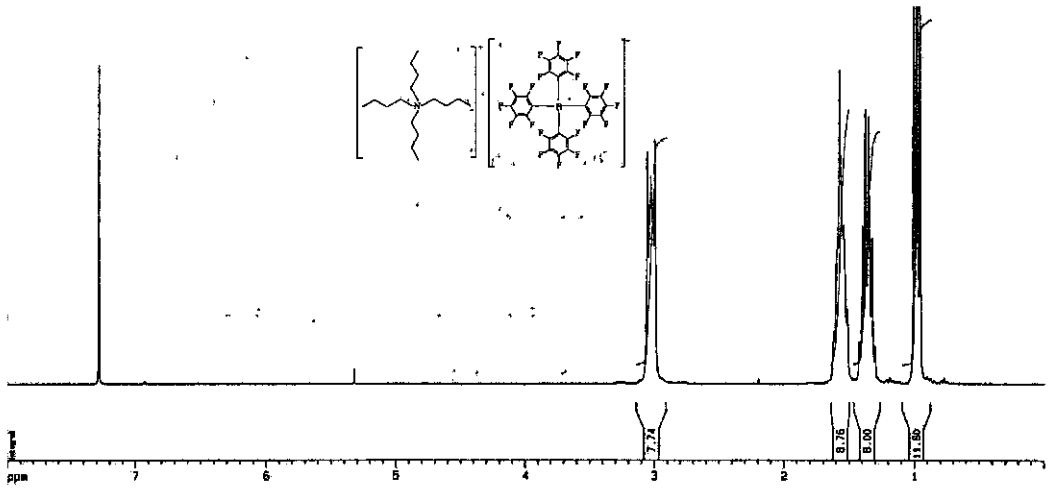

Abstract

In this study, phenyl-containing β-diketones, phenyl-containing and biphen-containing titanium(IV) complexes were synthesised. Seven of these compounds are new and five are previously reported complexes.

The keto-enol isomerisation kinetics of β-diketone $PhCOCH_2COCH_3$ has been studied by ^1H NMR spectroscopy in $CDCl_3$.

The temperature study of the isomer distribution biphen-containing titanium(IV) $Ti(ba)_2$biphen complex has been studied by ^1H NMR spectroscopy in $CDCl_3$.

Electrochemical studies were conducted in dichloromethane in the presence of $[NBu_4][B(C_6F_5)_4]$ non-coordinating supporting electrolyte. Electrochemical studies in dichloromethane utilising cyclic voltammetry of both [Ti(β-diketonato)$_2Cl_2$] and [Ti(β-diketonato)$_2$(biphen)] complexes revealed a chemical reversible Ti^{4+}/Ti^{3+} couple. Electrochemically quasi-reversible behaviour was observed: for [Ti(β-diketonato)$_2Cl_2$] and for [Ti(β-diketonato)$_2$(biphen)] with β-diketonato = acac, dbm, tfba and irreversible for $Ti(PhCOCHCOCH_3)_2$(biphen).

The substitution reaction of two Cl^- ions with 2,2'-biphenyldiolato^{-2} from the $[Ti(acac)_2Cl_2]$ is reported. The substitution reaction reveals a small negative value of entropy which suggests a dissociative mechanism.

Key words: Titanium, β-diketones, temperature study, electrochemistry.

Opsomming

In hierdie studie is fenielbevattende β-diketone, asook fenielbevattende en bifeenbevattende titaan(IV) komplekse gesintetiseer. Sewe van hierdie verbindings was tot nog toe totaal onbekend.

Die keto-enol isomerisasie kinetika van die β-diketoon $PhCOCH_2COCH_3$ is met behulp van ^1H KMR spektroskopie in $CDCl_3$ ondersoek bestudeer.

Die gedrag van die bifeenbevattende titaan(IV) $Ti(ba)_2$bifeen kompleks is met behulp van ^1H NMR spektroskopie in $CDCl_3$ bestudeer.

Elektrochemiese studies is in dichlorometaan in die tweenwoordigheid van $[NBu_4][B(C_6F_5)_4]$ as nie-koordinerende ondersteuningselektroliet uitgevoer. Alle titaanbevattende komplekse vertoon chemiese en elektrochemiese omkeerbaarheid vir die Ti^{4+}/Ti^{3+} koppels. [Ti(β-diketonato)$_2Cl_2$] en vir [Ti(β-diketonato)$_2$(bifeen)] met β-diketonato = acac, dbm, tfba het elektrochemiese kwasi-omkeerbaarheid vertoon, en $Ti(PhCOCHCOCH_3)_2$(bifeen) elektrochemiese onomkeerbaarheid.

Die substitusie reaksie van twee chloride-ione met 2,2'-bifenieldiolato^{-2} vanaf die [Ti(acac)$_2Cl_2$] kompleks is gerapporteer. Die substitusiereaksie vertoon 'n klein negatiewe entropiewaarde wat 'n dissosiatiewe meganisme voorstel.

Sleutelwoorde: Titaan, β-diketone, temperatuurstudie, elektrochemie.

I, declare that the dissertation hereby submitted by me for the Magister Scientiae degree at the University of the Free State is my own independent work and has not previously been submitted by me at another university/faculty. I further more cede copyright of the dissertation in favour of the University of the Free State.

Signed .....

Date 29/03/07